EW Physics at LHC

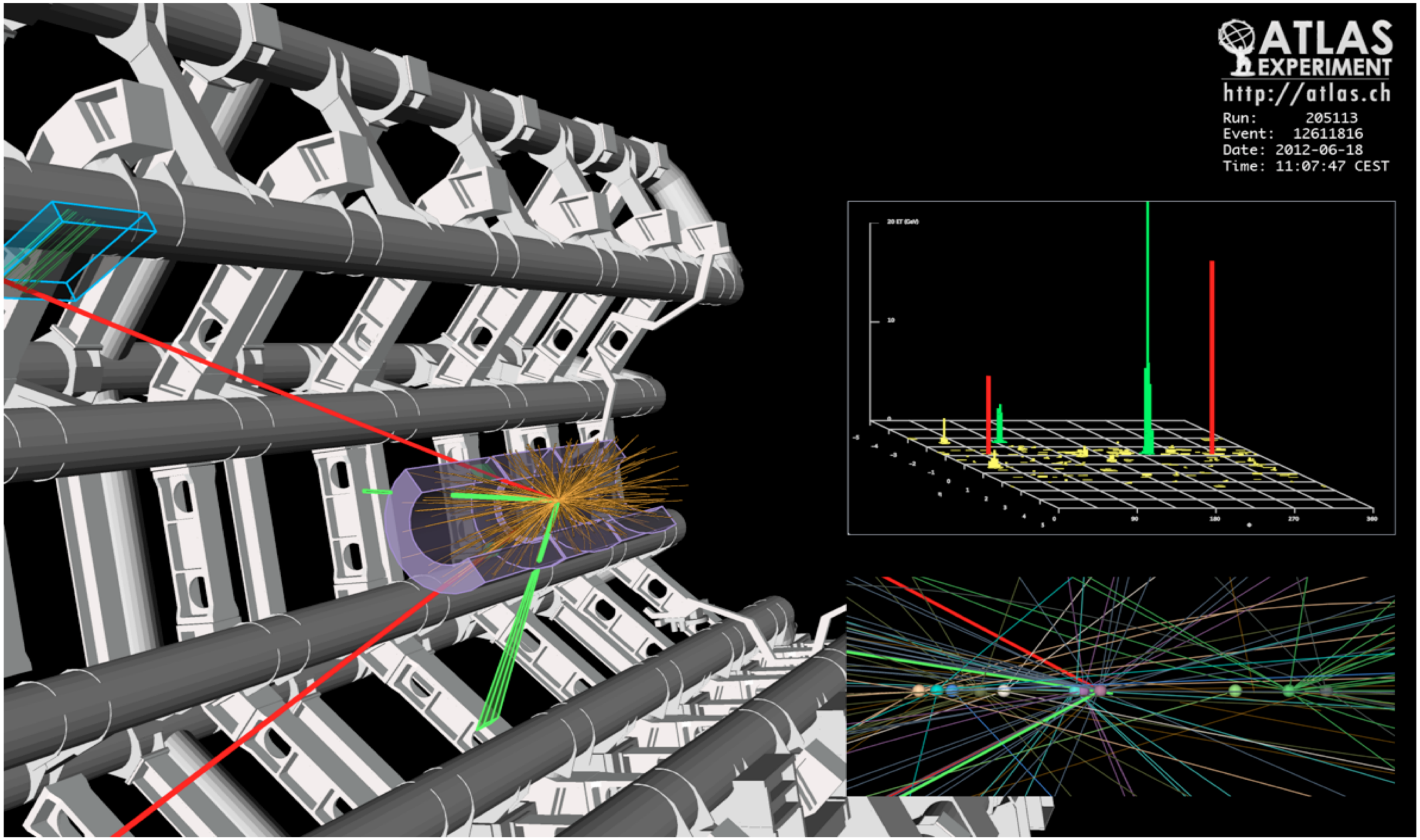

Event display of a 2e2mu candidate. EventNumber: 12611816 RunNumber: 205113 **m_4l=123.9 GeV**. m_12=87.9 GeV, m_34=19.6 GeV. e_1: pt=18.7 GeV, eta=-2.45, phi=1.68,. e_2: pt=75.96 GeV, eta=-1.16, phi=-2.13. mu_3: pt=19.6 GeV, eta=-1.14, phi=-0.87. mu_4: pt=7.9 GeV, eta=-1.13, phi=0.94

Contents

- Standard Candles
- W discovery & mass measurement (how precise?)
- W mass measurement at LHC
- W & Z cross sections. Ratios
- Di-bosons
- TGC & QTGC

Standard Candles

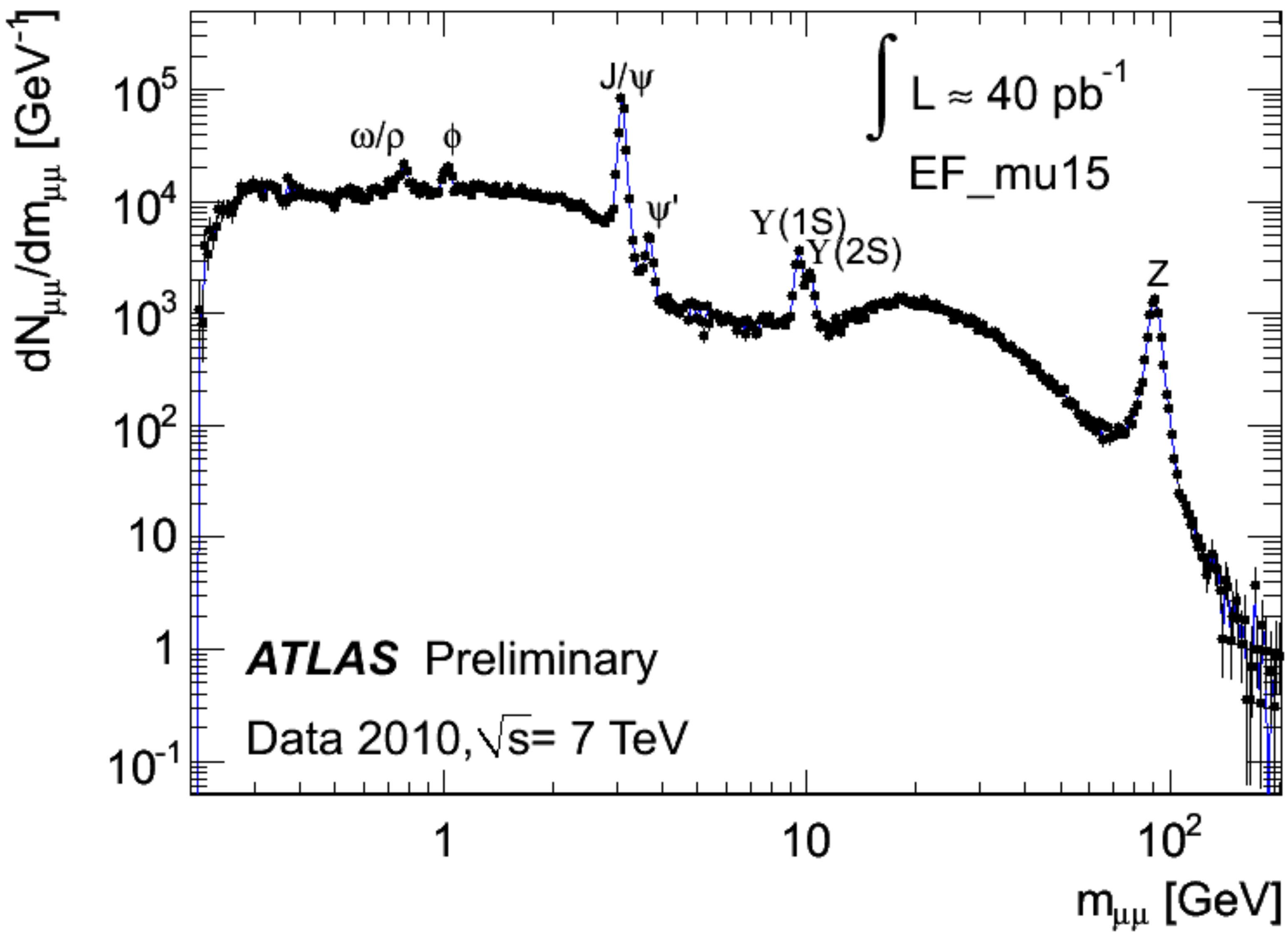

Constraints between m_W & m_{top}

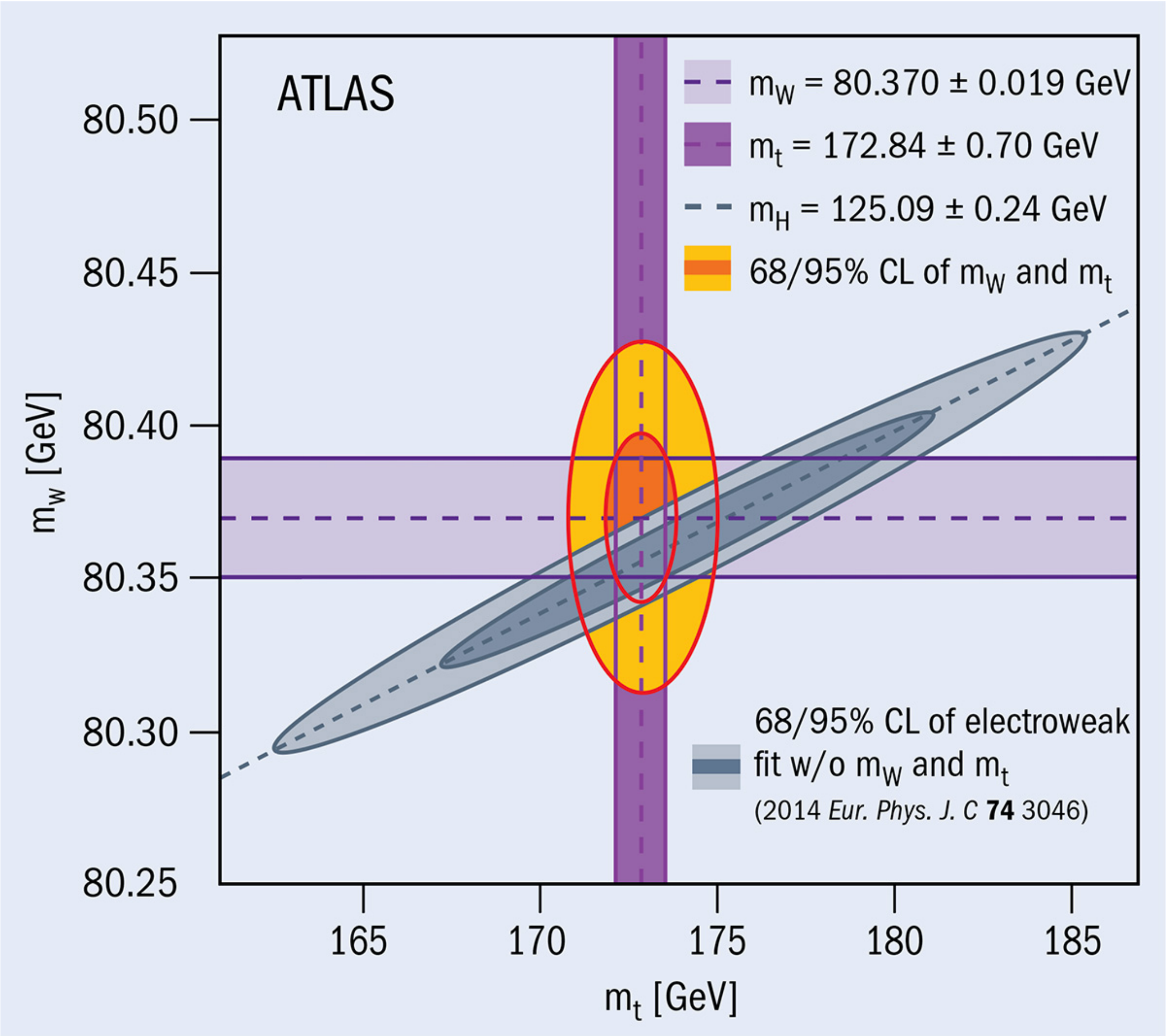

W & Z masses in SM

m_W and m_Z are constrained in the SM by

$$m_W^2\left(1-\frac{m_W^2}{m_Z^2}\right)=\frac{\pi\alpha}{\sqrt{2}G_F}(1+\Delta r),$$

Where

- GF is the Fermi constant.
- α is the coupling constant
- Δr includes higher order corrections and is sensitive to top quark mass and, logarithmically, to the mass of the Higgs.
- Δr receives contributions from additional particles and interactions? → the comparison of the measured and predicted values of m_W is a strong probe of the effects induced by physics beyond the SM.

W & Z masses in SM

$$m_W^2 \left(1 - \frac{m_W^2}{m_Z^2}\right) = \frac{\pi\alpha}{\sqrt{2}G_F}(1 + \Delta r),$$

The current Particle Data Group world average of m_W = 80385±15 MeV is dominated by the CDF and D0 measurements performed at $\sqrt{s}$ = 1:96 TeV.

Given the precisely measured values of , G_F and m_Z , and taking recent top-quark and Higgs-boson mass measurements, the SM prediction of m_W is m_W = 80358±8 MeV and m_W = 80362±8 MeV (different calculations).

The SM prediction uncertainty of 8 MeV represents therefore a target for the precision of future measurements of m_W.

W & Z decays

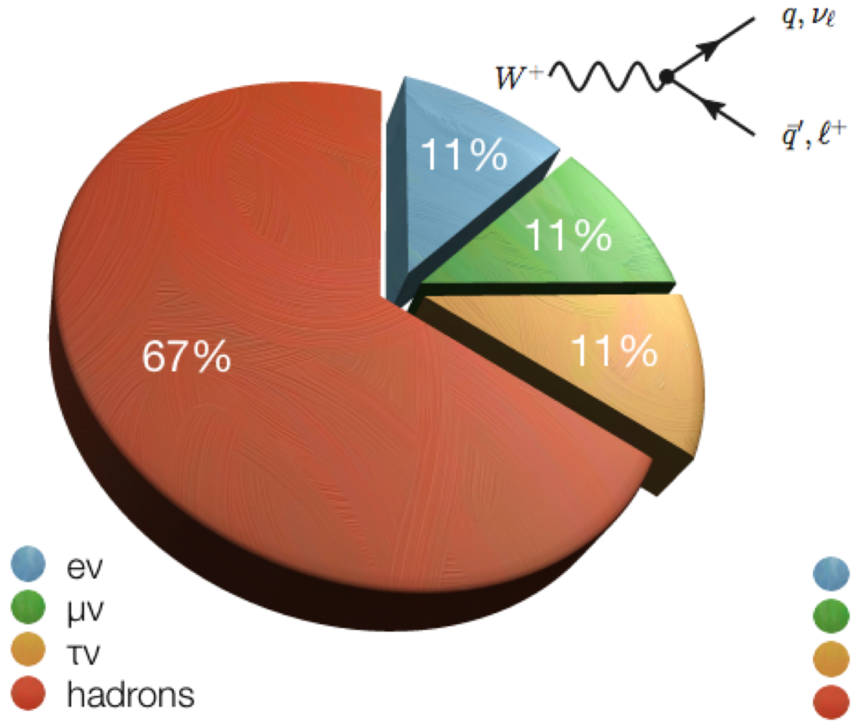

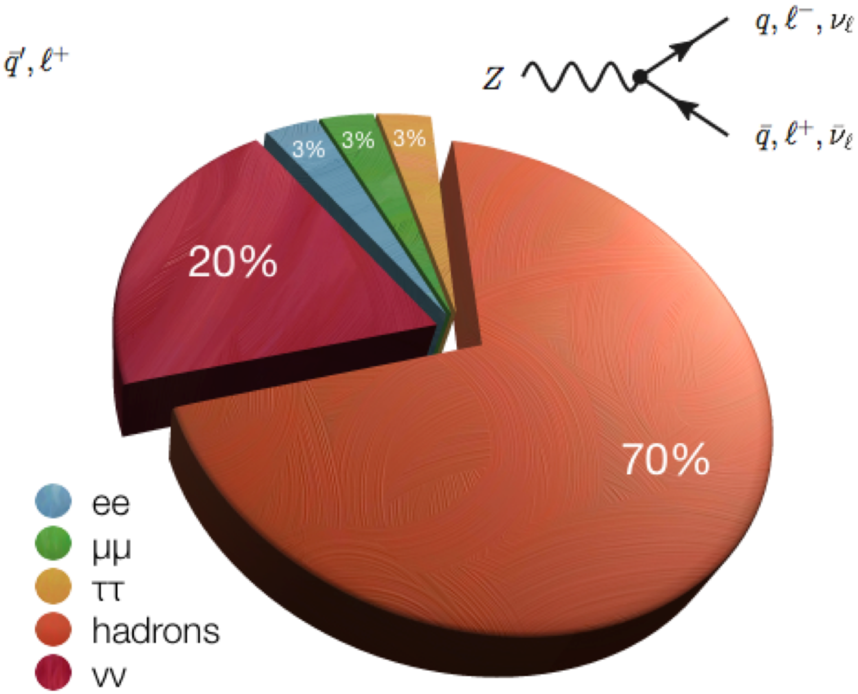

- Leptonic decays (e/μ): very clean, but small branching fractions.
- Hadronic decays: two-jet final states; large QCD dijet background.
- Tau decays (to ~few hadrons): somewhere in between…difficult

The Story of an Inelastic Lepton-Nucleon Scattering

First stage:

~ elastic scattering of the virtual particle (boson) with one quark of the N carrying a fraction "x" of the N

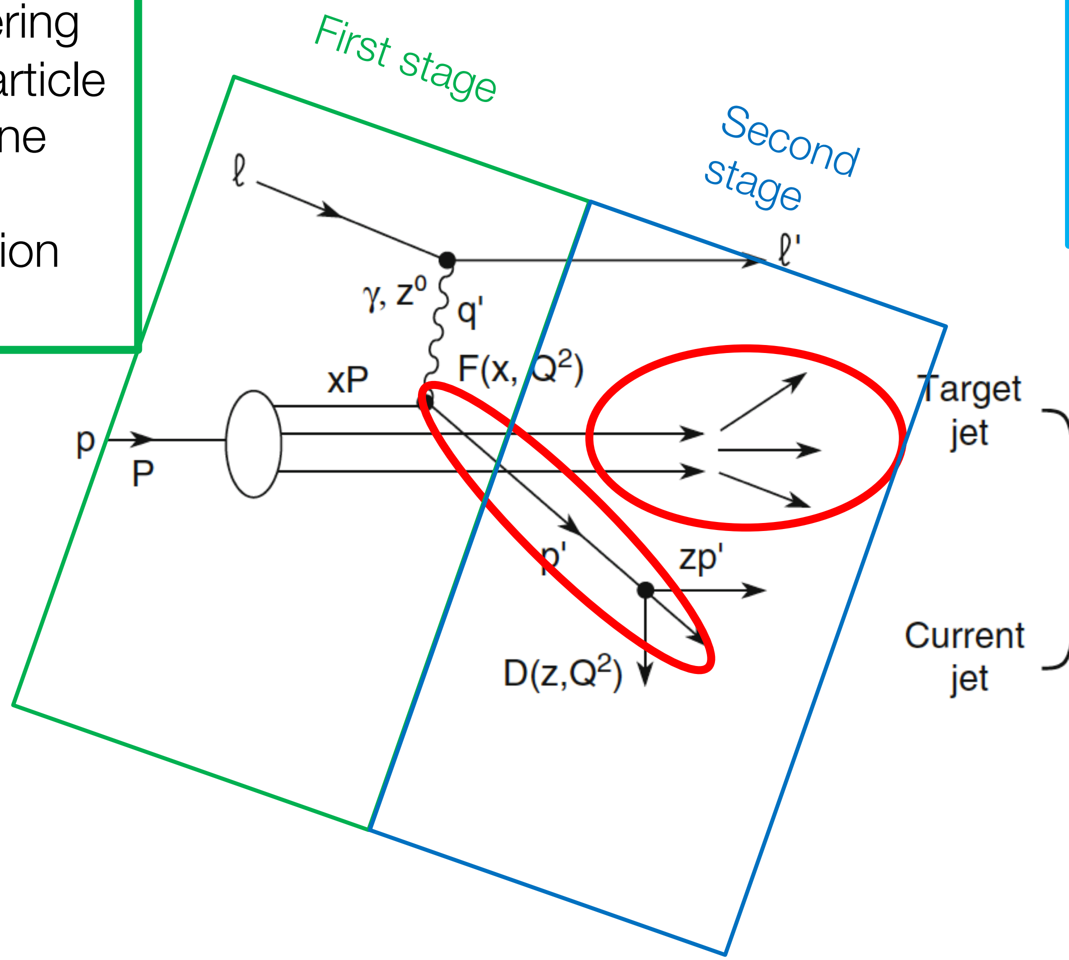

Second stage:

Fragmentation → quarks cannot exist 'alone' → 'dress' into two jets

Target jet ~ in the same direction of the incoming lepton

Current jet ~ at large angle with respect to the direction of the incoming lepton

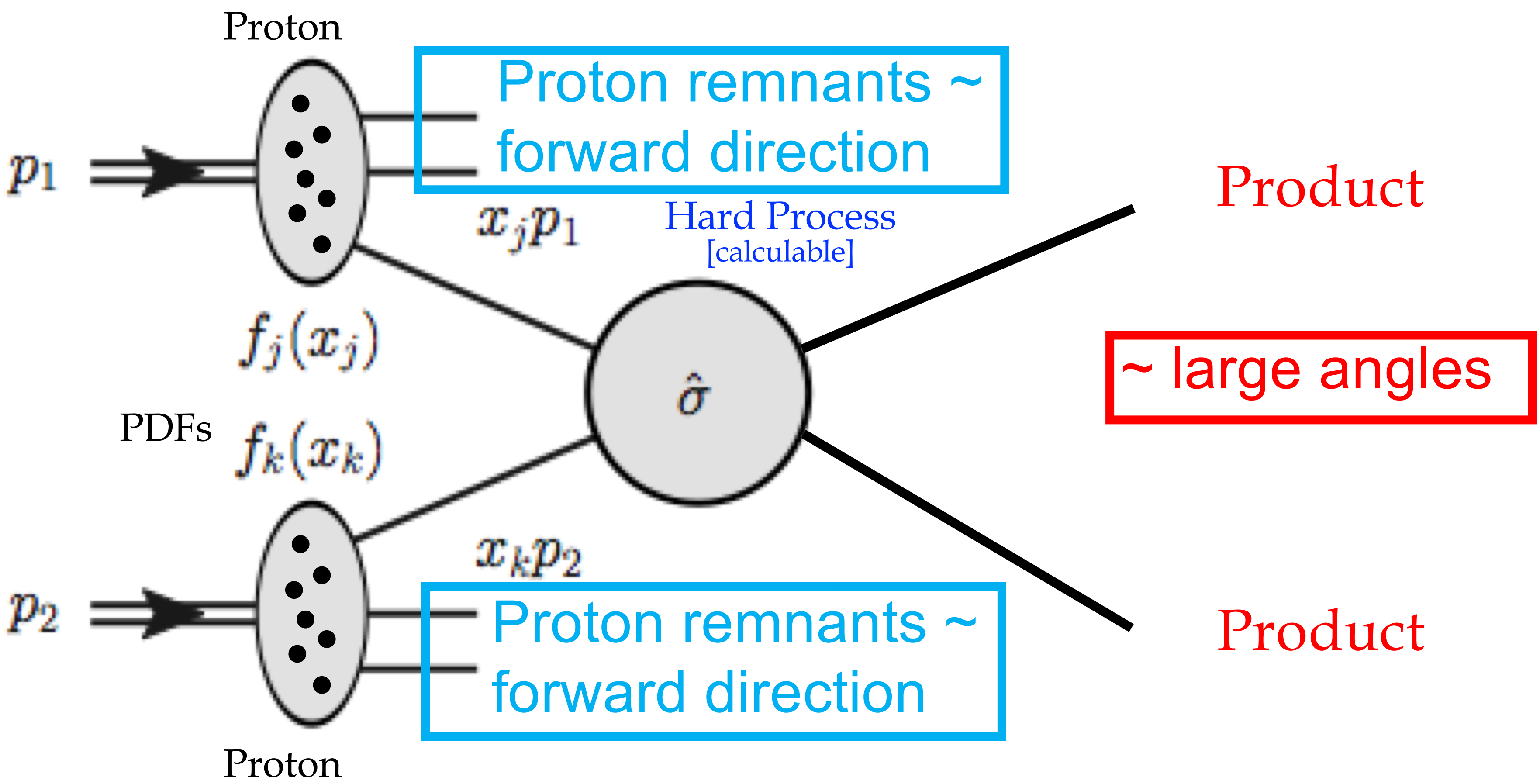
Proton
Proton remnants ~ forward direction
p_1
$x_j p_1$
Hard Process
[calculable]
Product
$f_j(x_j)$
~ large angles
PDFs
$f_k(x_k)$
$\hat{\sigma}$
$x_k p_2$
p_2
Proton remnants ~ forward direction
Product
Proton

Hadron Collider Signatures

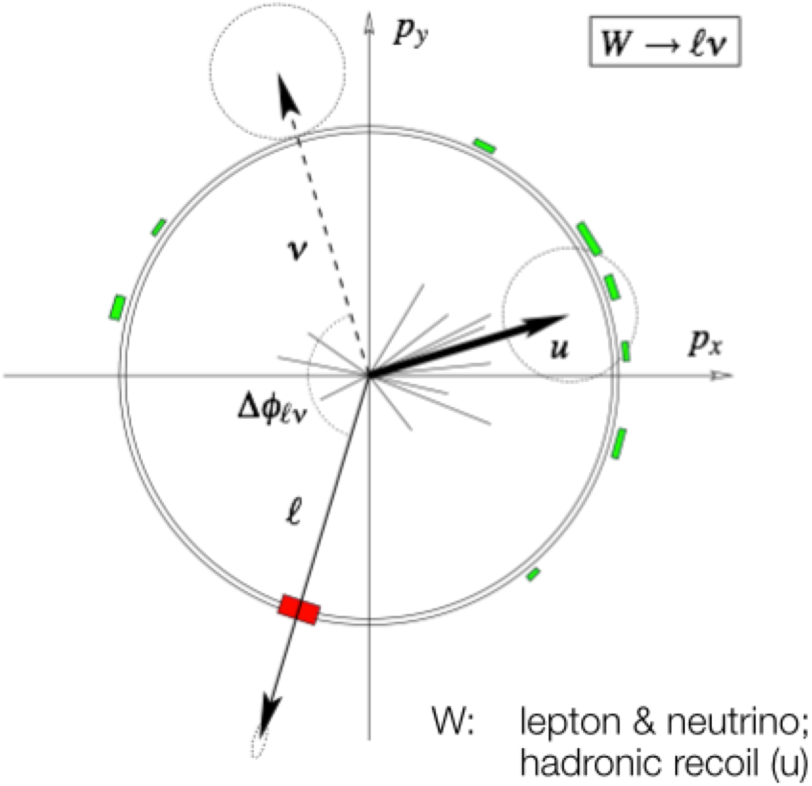

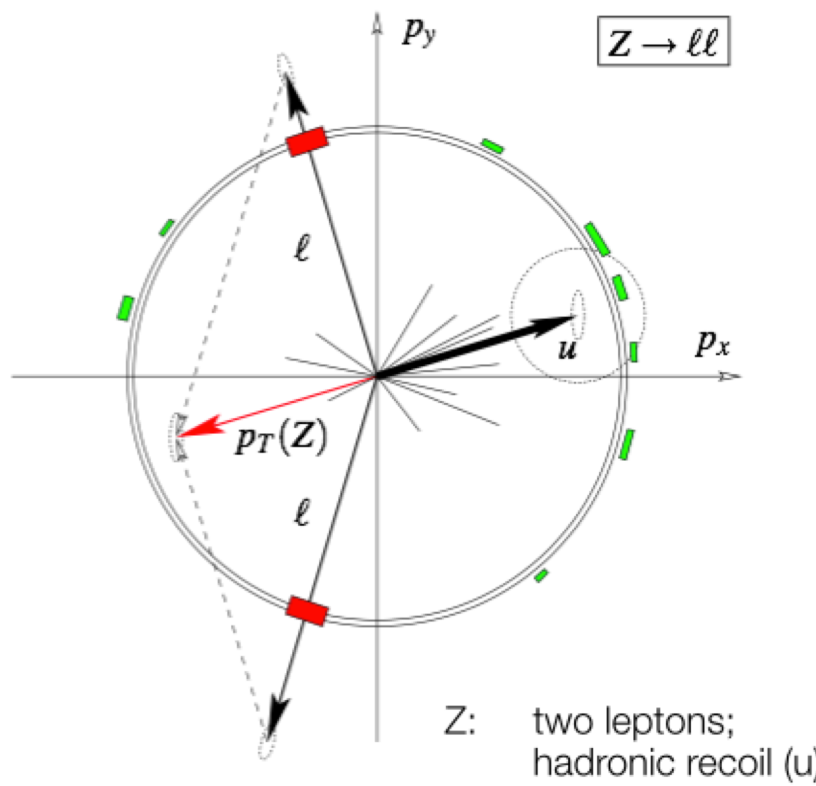

Additional hadronic activity ➛ recoil, not as clean as e^+e^-
Precision measurements: only leptonic decays

W/Z Production at pp machines (LHC)

Need quarks & anti-quarks!

Single W/Z production:

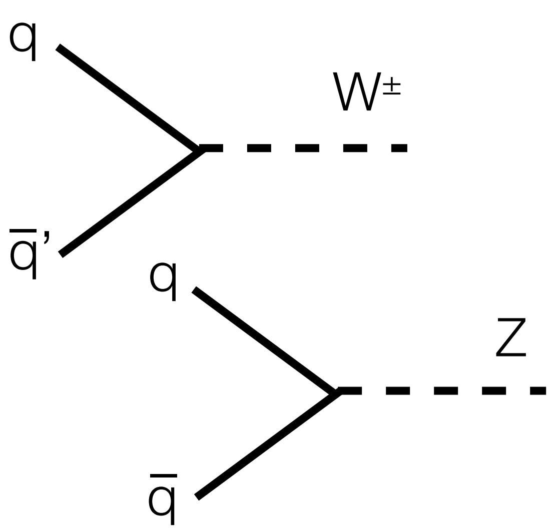

W production:

$$u\bar{d} \rightarrow W^+$$
$$d\bar{u} \rightarrow W^-$$

Z production:

$$d\bar{d} \rightarrow Z$$
$$d\bar{d} \rightarrow Z$$

p = uud

- At LHC energies these processes take place at low values of Bjorken-x
- Only sea quarks are involved
- At EW scales sea is driven by the gluon i.e. x-sections dominated by gluon uncertainty

Comparison w/ Tevatron:

- $p\bar{p}$-collider, i.e. valence anti-quarks available ...
- W/Z production at higher x ...

➡ Constraints on sea and gluon distributions

W^+/W^--Cross Section Ratio ...

proton = 2u + 1d

W+/W− rapidity distributions

Define:

W production:

$$u\bar{d} \rightarrow W^+$$
$$d\bar{u} \rightarrow W^-$$

$$R_{\mp} = \frac{\sigma_{W^-}}{\sigma_{W^+}}$$

$$R_{\mp} \approx \frac{d\bar{u}}{u\bar{d}} \approx \frac{d}{u}$$ [assuming $\bar{d}/\bar{u}$ =1]

Differential
:

$$R_{\mp}(y_W) = \frac{d\sigma/dy_W(W^-)}{d\sigma/dy_W(W^-)}$$
$$\approx \frac{d(x_1)\bar{u}(x_2)}{u(x_1)\bar{d}(x_2)} \approx \frac{d(x_1)}{u(x_1)}$$

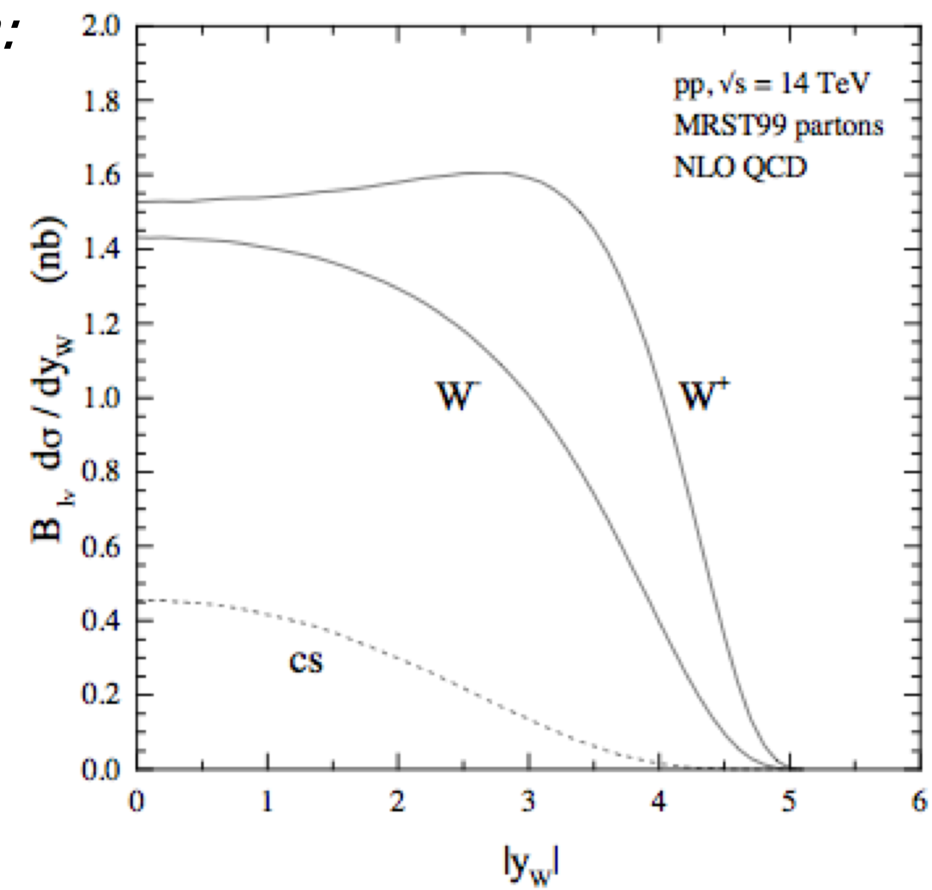

Z & W cross sections vs √s

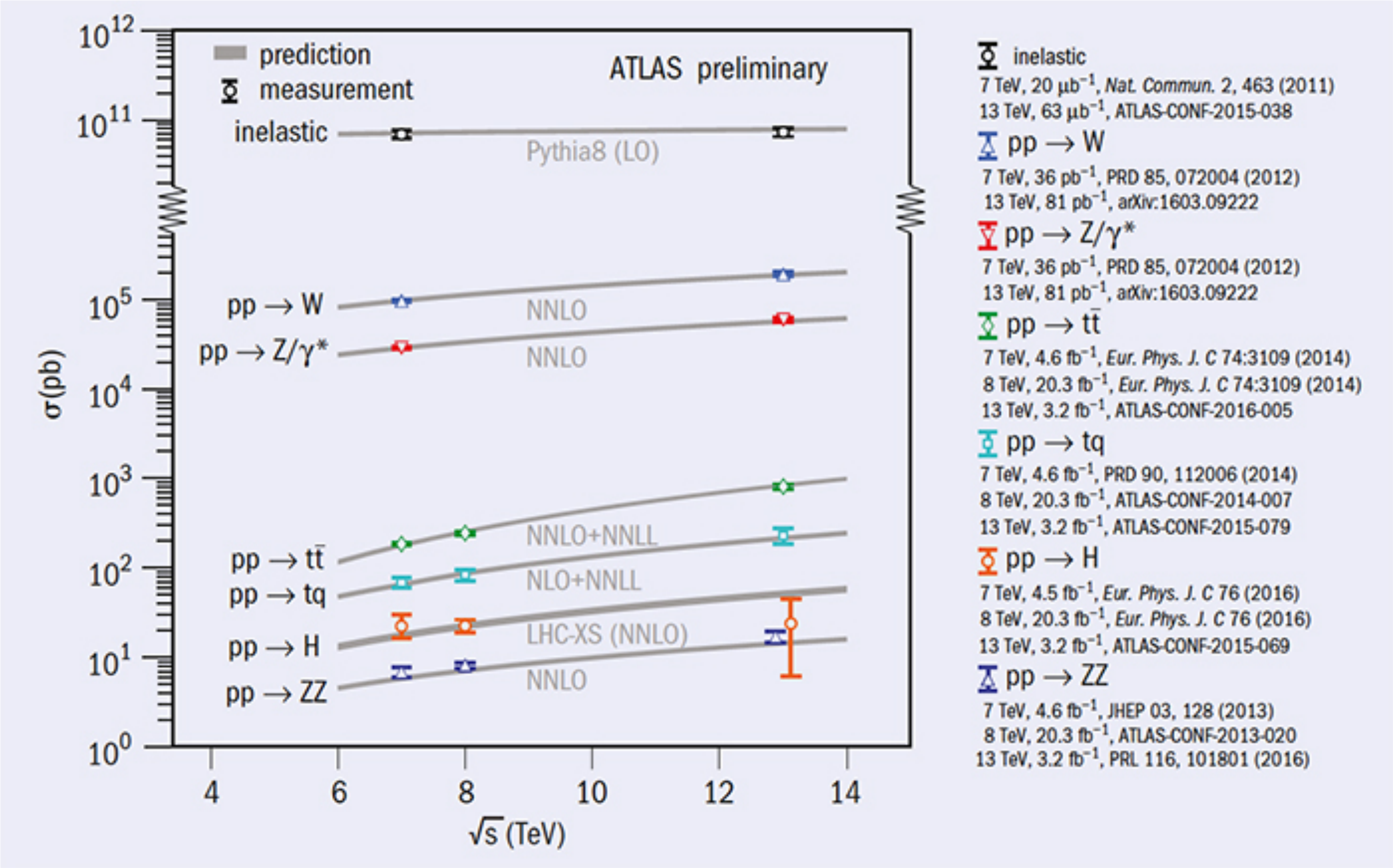

Differential Cross Section

NNLO cross sections:
scale uncertainties very small
… MC generators…
W asymmetry vs rapidity:
[sensitivity to PDFs]

$$A_W(y) = \frac{d\sigma(W^+)/dy - d\sigma(W^-)/dy}{d\sigma(W^+)/dy + d\sigma(W^-)/dy}$$

Proton-Proton Collider:

symmetry around y=0 ...

PDFs: u(x) > d(x) for large x ...
more W^+ at positive rapidity

d/u ratio < 1 ...

always more W^+ than W^-

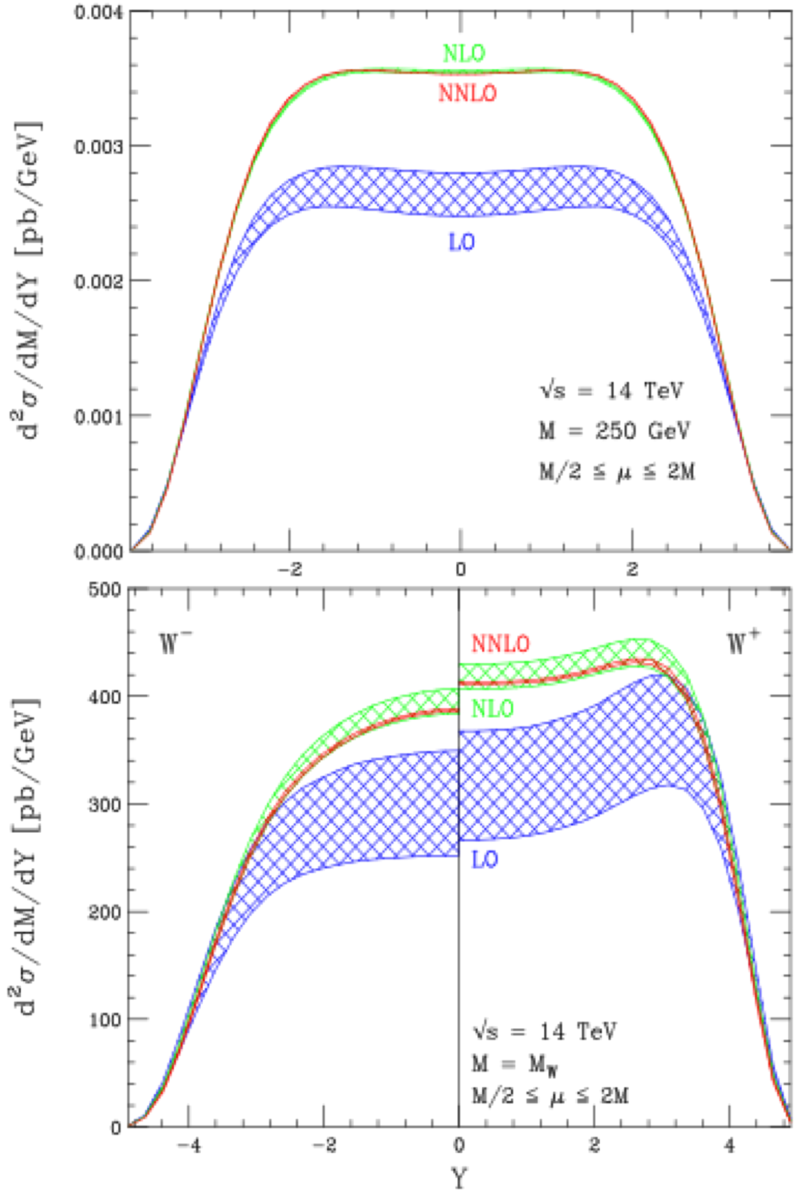

[C. Anastasiou et al., PRD 69 (2004) 094008]

PDF Uncertainty on W-Production ...

W± rapidity distribution

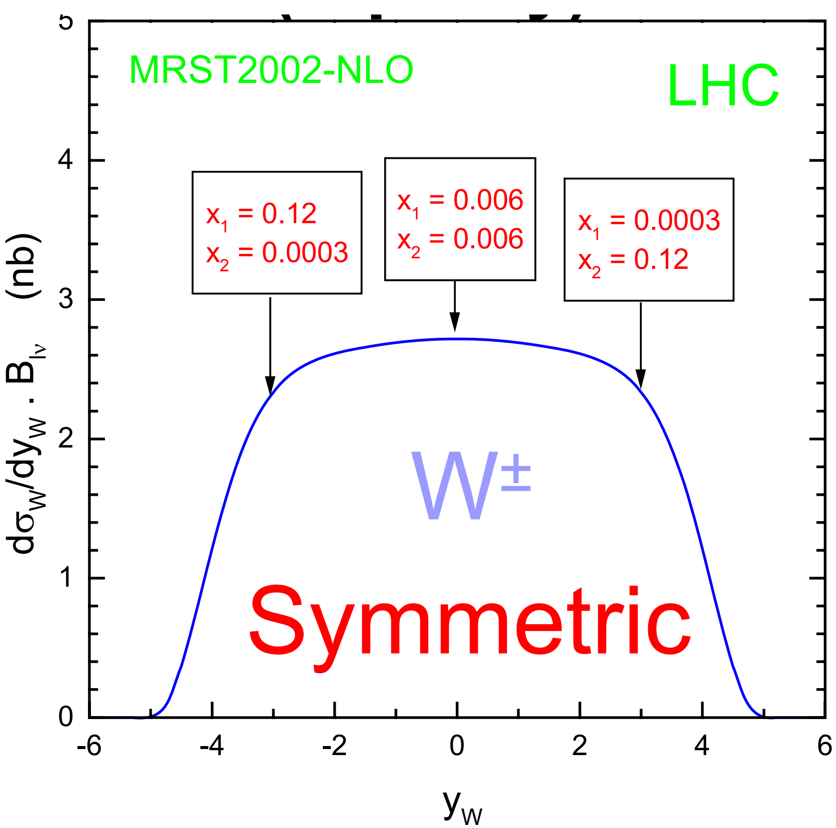

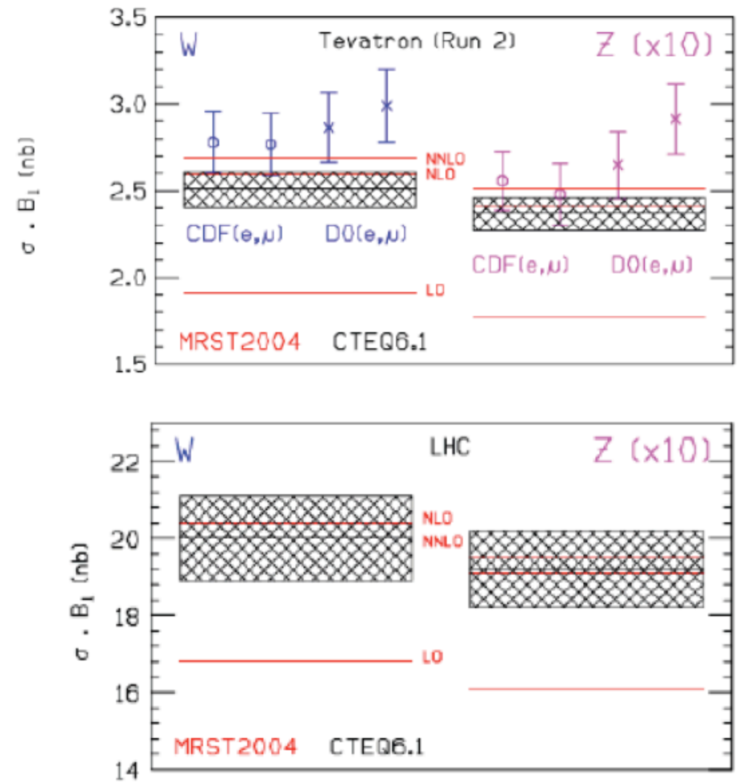

W± total cross section

4% MRST02 uncertainty

Theoretical uncertainty dominated by PDFs

Extra input from LHC measurements

Effect on PDFs of LHC W data

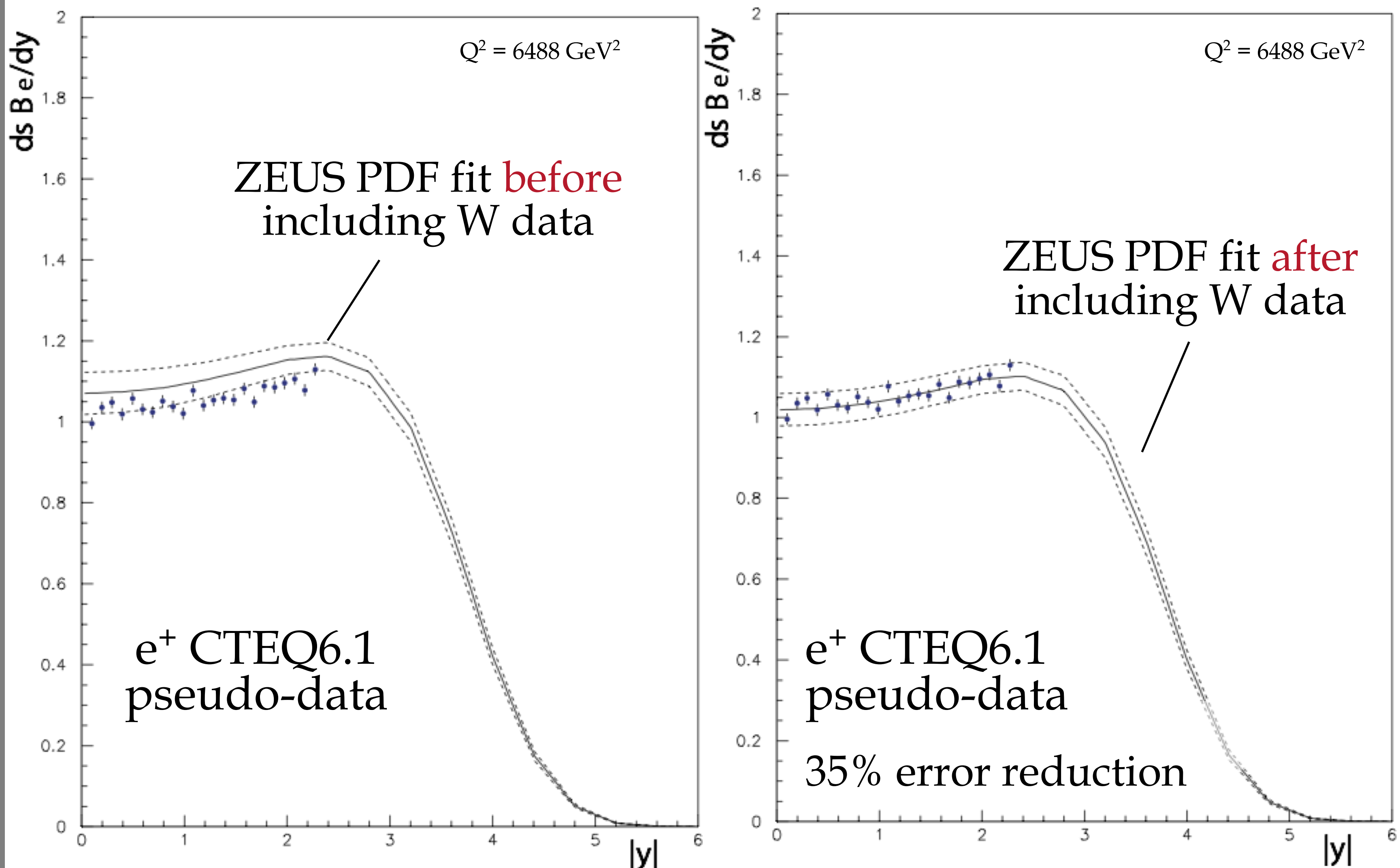

[Tricoli et al., arXiv:hep-ex/0509002v1]

W/Z discovery at the SPS

Discovery at hadron collider: CERN SppS 1982/3

Proton-antiproton collider at 540 GeV [dominant production process: quark-antiquark annihilation]

Two multipurpose experiments: UA1, UA2

Signature: decay in leptons [clean, QCD background suppressed]

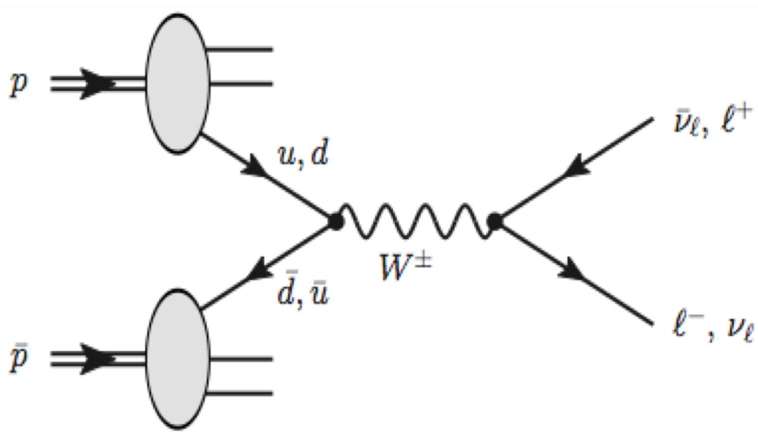

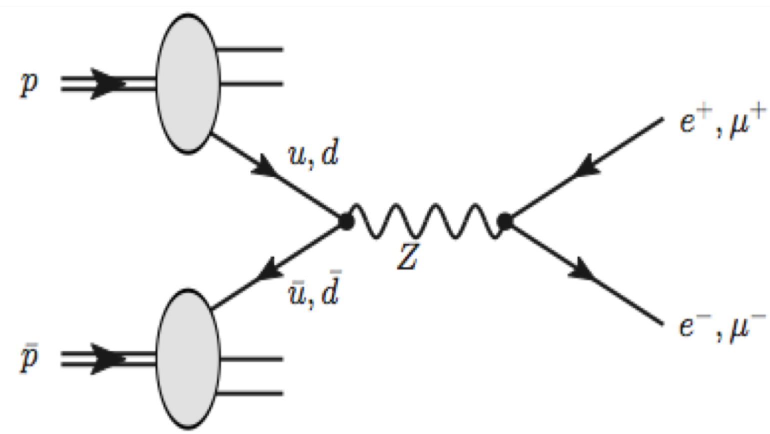

Z Signature at the SPS

1.3 Event signature: $p\bar{p} \rightarrow Z \rightarrow f\bar{f} + X$

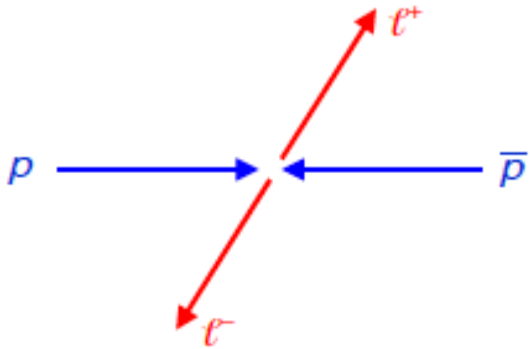

High-energy lepton pair:

$$m_{\ell\ell}^2 = (p_{\ell^+} + p_{\ell^-})^2 = M_Z^2$$

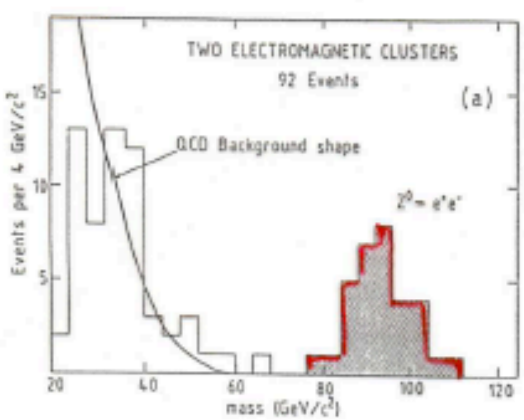

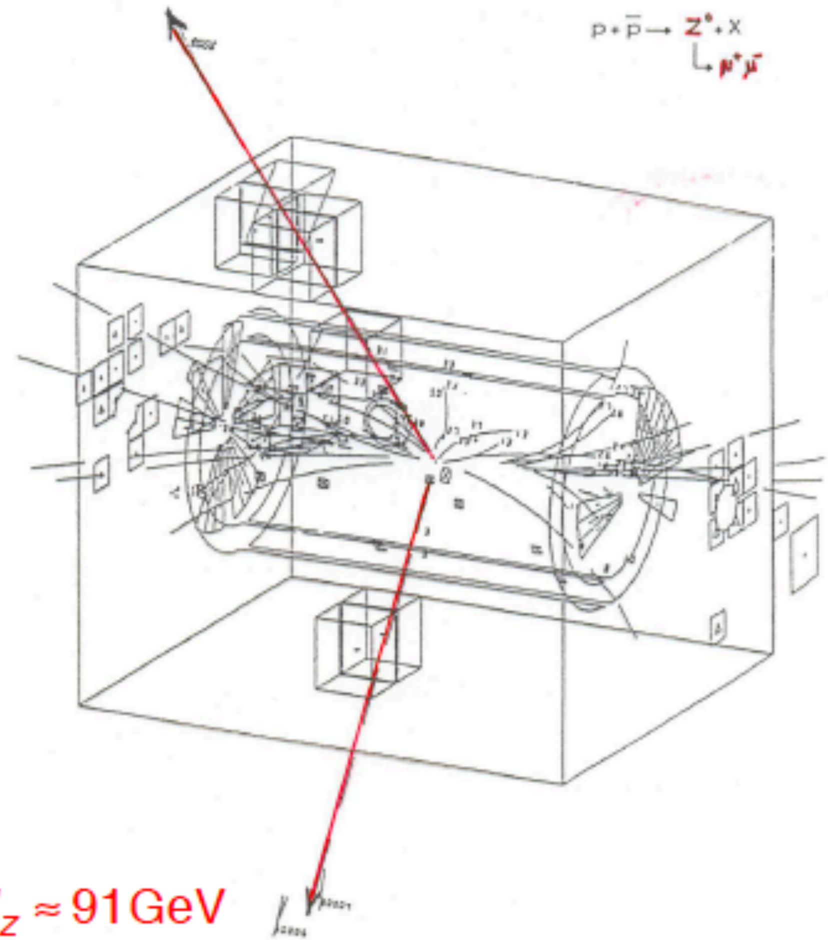

$M_Z \approx 91\,\mathrm{GeV}$

Z Candidates at UA2

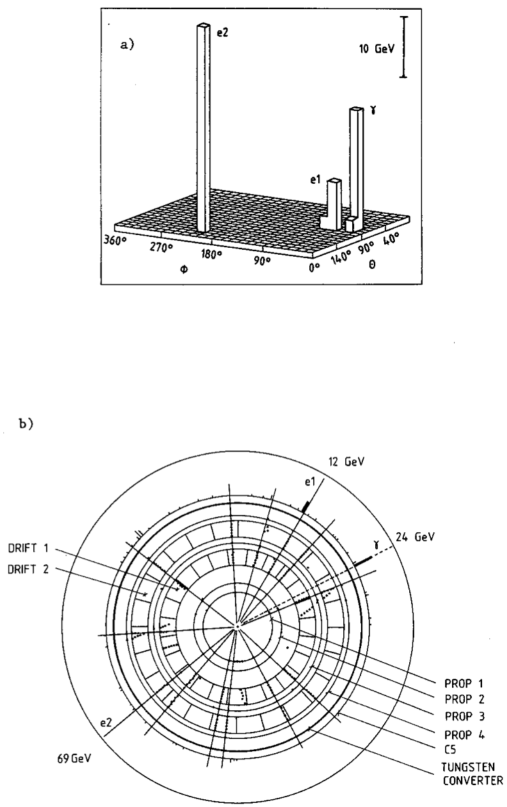

Figure 4

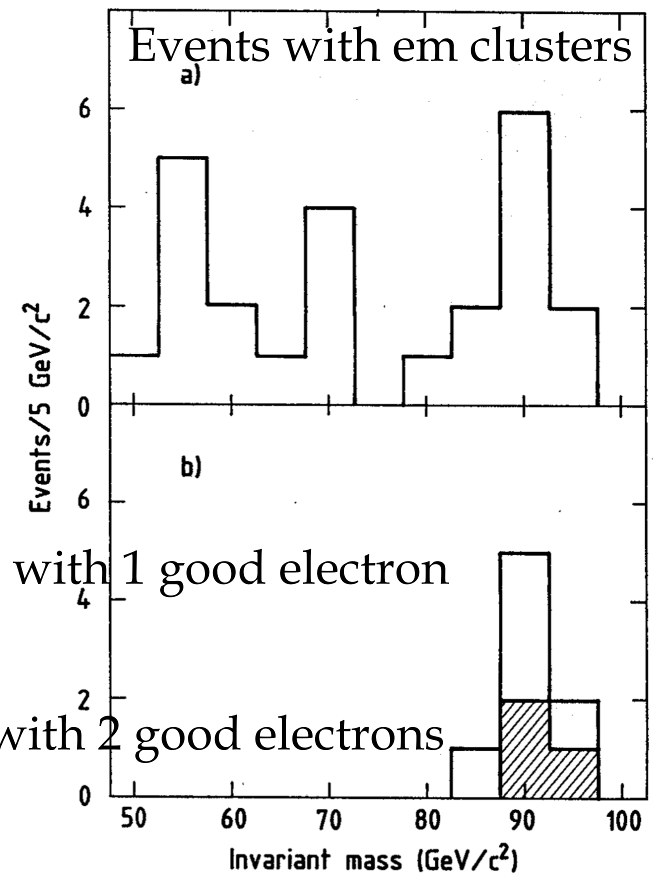

Invariant Mass of Electron Pairs
[P. Bagnaia et al., Phys. Lett. B129 (1983) 130]

UA1 Mass Distribution of Z candidates

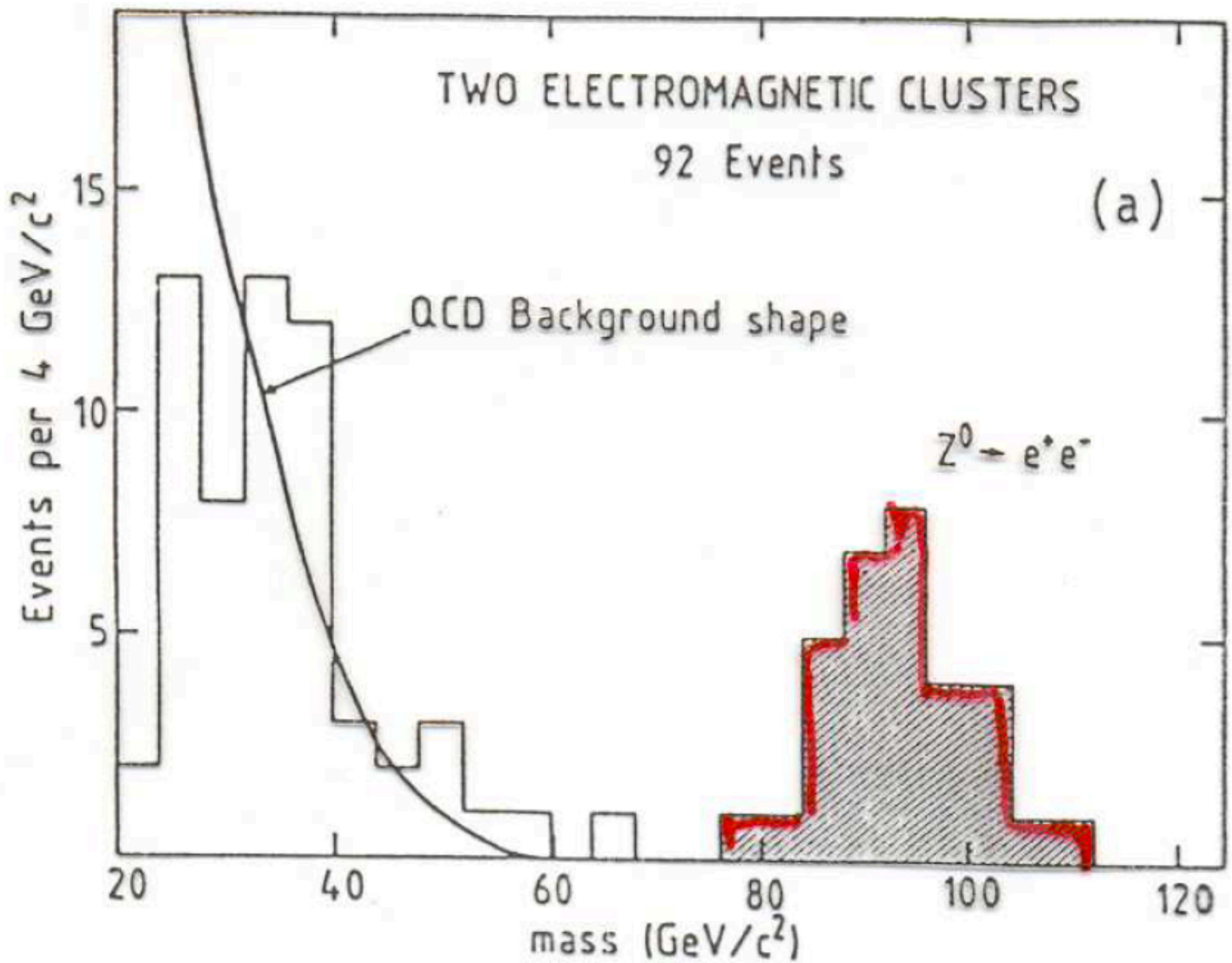

m_W measurement strategy→m_T

The mass of the W boson is determined from fits to

- the transverse momentum of the charged lepton, p_T

$$\vec{p}_{\mathrm{T}}^{\,\mathrm{miss}} = -\left(\vec{p}_{\mathrm{T}}^{\,\ell} + \vec{u}_{\mathrm{T}}\right)$$

For W bosons at rest, the transverse-momentum distributions of the W decay leptons have a Jacobian edge at a value of $m_W/2$

- to the transverse mass of the W boson, m_T.

$$m_{\mathrm{T}} = \sqrt{2 p_{\mathrm{T}}^{\ell} p_{\mathrm{T}}^{\mathrm{miss}} (1 - \cos\Delta\phi)},$$

- For W bosons at rest, the distribution of the transverse mass has an endpoint at the value of m_W, where m_W is the invariant mass of the charged-lepton and neutrino system, appearing in the Breit-Wigner distribution.

$$\frac{d\sigma}{dm} \propto \frac{m^2}{(m^2 - m_V^2)^2 + m^4 \Gamma_V^2 / m_V^2},$$

The Jacobian Edge

The expected final state distributions, referred to as templates, are simulated for several values of m_W including signal and background contributions..

The cross section can be expressed as

$$\frac{d\sigma}{d(\cos\hat{\theta})} = \sigma_0(\hat{s})(1+\cos^2\hat{\theta})$$

where s is the center of mass energy of the colliding quarks and where θ is the polar angle of the electron with respect to the proton beamline. The function $\theta_0(\widehat{s})$ is proportional to a Breit-Wigner distribution.

We define the quantity $E = \sqrt{\hat{s}}$ and $E_T = \sqrt{\hat{s}} * \sin(\theta)$. This quantity is useful because it is invariant under longitudinal boosts. In the W rest frame we can write the differential cross section in E_T as

$$\begin{aligned} \frac{d\sigma}{dE_T} &= \frac{2}{\sqrt{\hat{s}}}\frac{d\sigma}{d(\sin\hat{\theta})} \\ &= \frac{2}{\sqrt{\hat{s}}}\frac{d\sigma}{d(\cos\hat{\theta})}\left|\frac{d(\cos\hat{\theta})}{d(\sin\hat{\theta})}\right| \\ &= \frac{2}{\sqrt{\hat{s}}}\sigma_0(\hat{s})(1+\cos^2\hat{\theta})|\tan\hat{\theta}| \\ &= \sigma_0(\hat{s})\frac{4E_T}{\hat{s}}(2-4E_T^2/\hat{s})\frac{1}{\sqrt{1-4E_T^2/\hat{s}}} \end{aligned}$$

The Jacobian Edge

$$
\begin{aligned}
\frac{d\sigma}{dE_T} &= \frac{2}{\sqrt{\hat{s}}}\frac{d\sigma}{d(\sin\hat{\theta})} \\
&= \frac{2}{\sqrt{\hat{s}}}\frac{d\sigma}{d(\cos\hat{\theta})}\left|\frac{d(\cos\hat{\theta})}{d(\sin\hat{\theta})}\right| \\
&= \frac{2}{\sqrt{\hat{s}}}\sigma_0(\hat{s})(1+\cos^2\hat{\theta})|\tan\hat{\theta}| \\
&= \sigma_0(\hat{s})\frac{4E_T}{\hat{s}}(2-4E_T^2/\hat{s})\frac{1}{\sqrt{1-4E_T^2/\hat{s}}}
\end{aligned}
$$

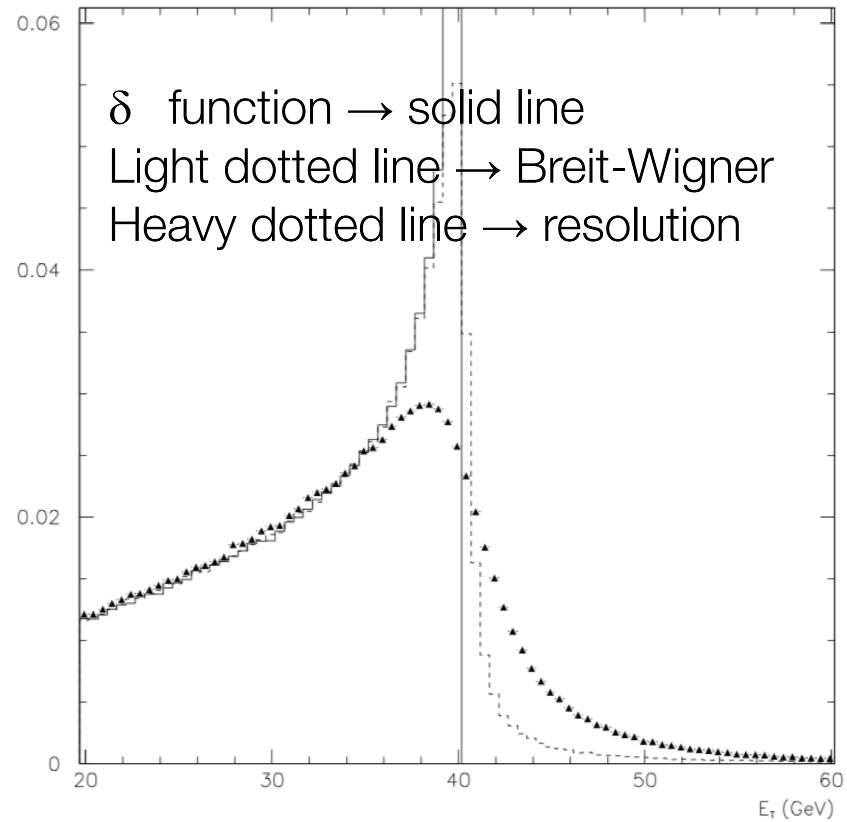

For $E_T = \sqrt{\hat{s}}/2$ we have a singularity! However σ_0 has the shape of a Breit-Wigner thus all these values are smeared and the discontinuity is recovered

m_W: generate many MC samples with different values of m_W and find which one fits best the data

W Signature at the SPS

1.4 Event signature: $p\bar{p} \rightarrow W \rightarrow \ell \bar{\nu}_\ell + X$ $W^- \rightarrow e\bar{\nu}$

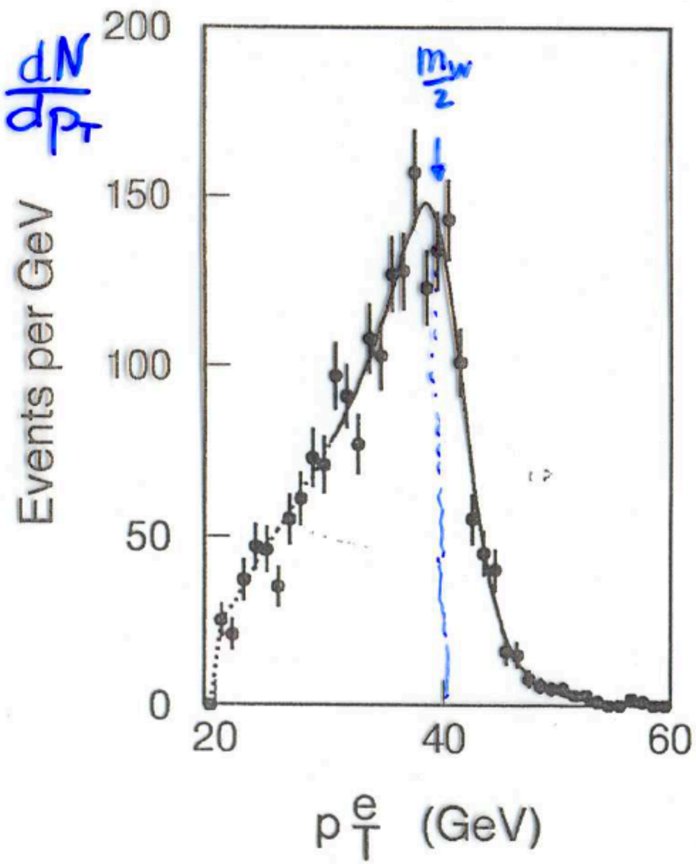

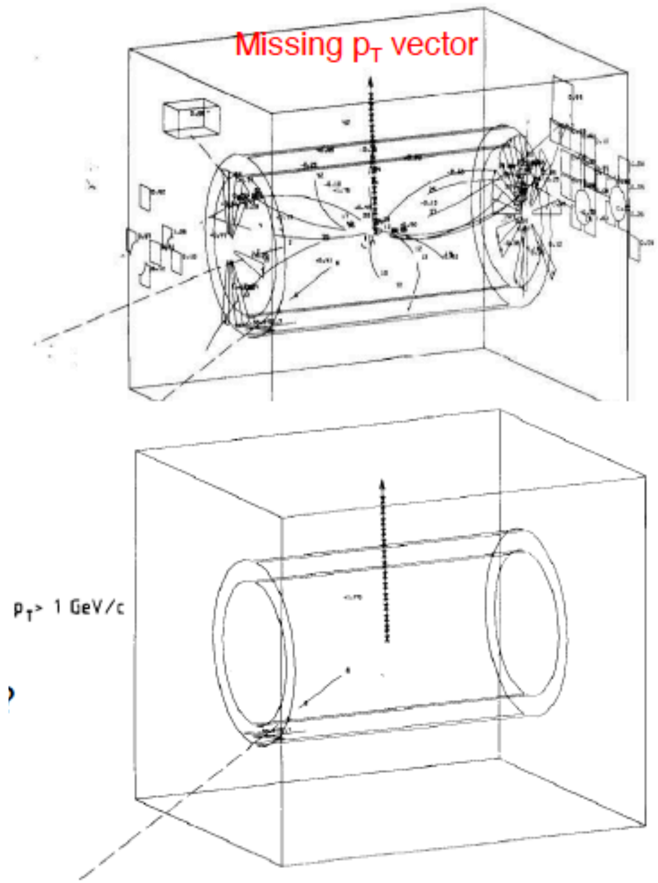

Fig. 16b. The same as picture (a), except that now only particles with p_T>1 GeV/c and calorimeters with E_T>1 GeV are shown.

W/Z at Tevatron

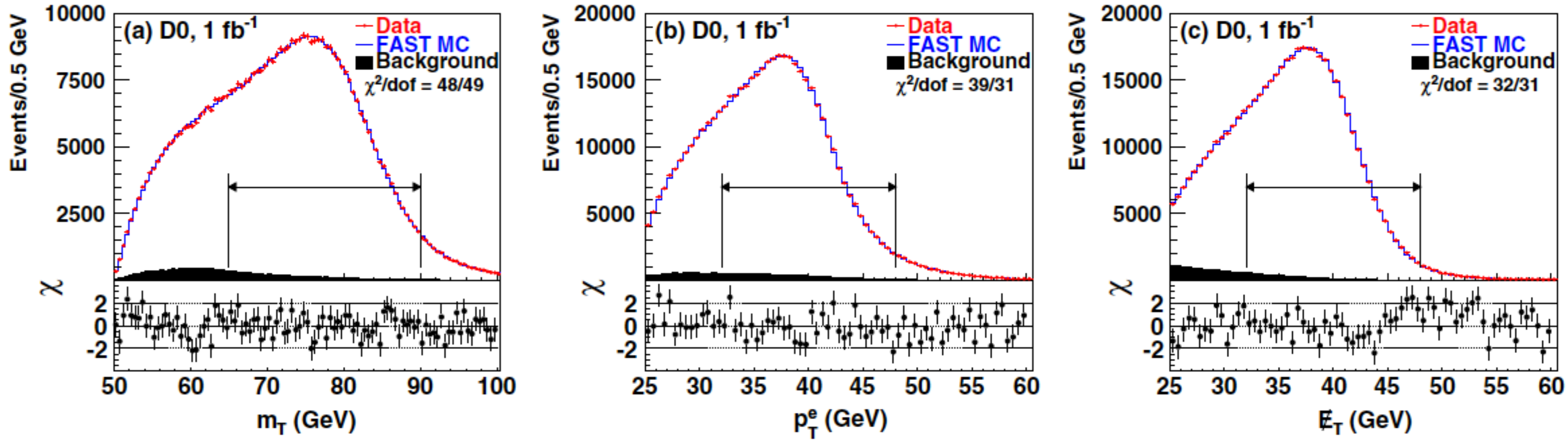

Tevatron: pp-collider [$\sqrt{s}$ = 1.8 TeV and 1.96 TeV]

W/Z cross sections;
asymmetries ...

Most precise W mass measurement to date

Diboson production, i.e. WW, WZ, ZZ

W/Z + jet production … [major background for top physics]

[V. M. Abazov et al., Phys. Rev. Lett. 103 (2009) 141801]

Isolation of High pT Leptons

Starting point for many hadron collider analyses:
isolated high-p_T leptons ➛ discriminate against QCD jets ...

QCD jets can be mis-reconstructed as leptons (“fake leptons”)

QCD jets may contain real leptons e.g. from semileptonic B decays [B ➛ lνX]

➛ soft and surrounded by other particles

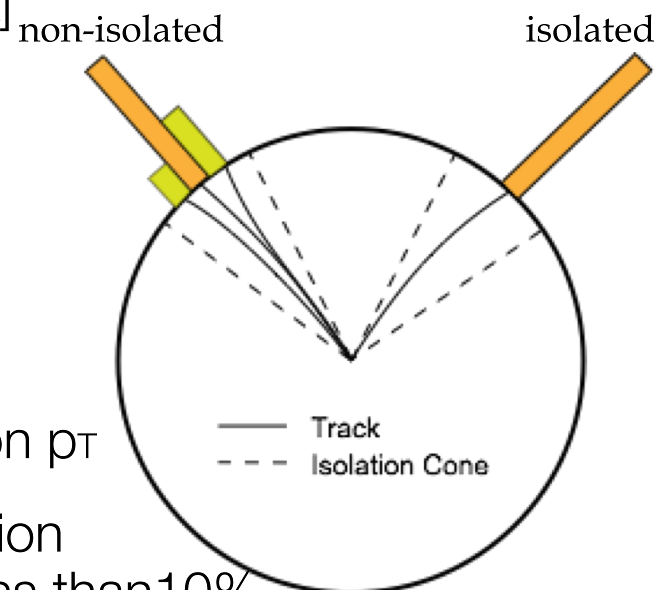

“Tight” lepton selection ...

Require e/μ with p_T > (at least) 20 GeV
Track isolation, e.g. ∑ p_T of other tracks in cone of ΔR=0.1 less than 10% of lepton p_T

Calorimeter isolation, e.g. energy deposition from other particles in cone of ΔR=0.2 less than10%

W± Signal & Control Regions

Signal Region (SR) contains events we want to select, Control Regions are close to SR but ortogonal. Need to have no correlation between SR&CR.

SR: Lepton quality & trigger match & E_T^{miss} > 25 GeV & m_T > 50 GeV & lepton isolation & Overlap Removal (OR)

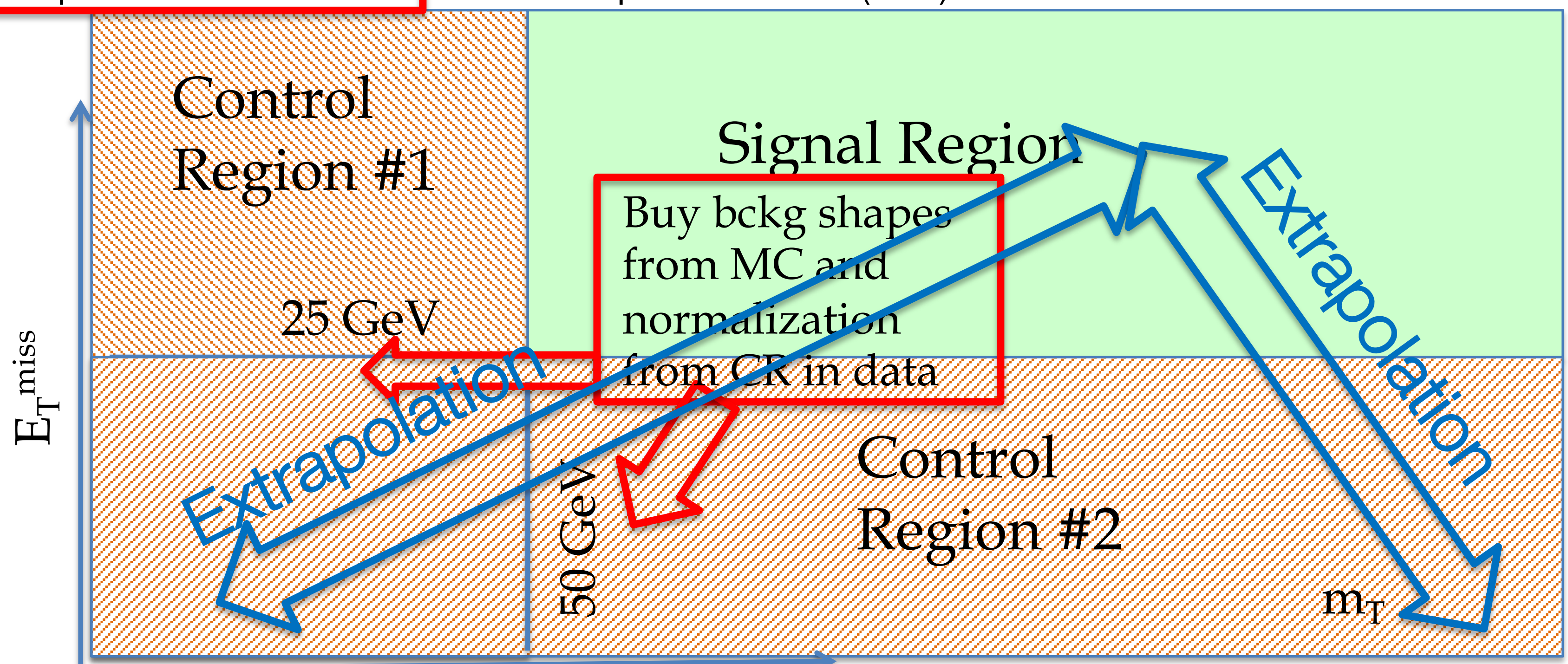

Background from heavy flavours decays and (for electrons) photon conversions determined using a "data-driven" technique.

Extrapolating from CR to SR

Multijet events vs the isolation variable for the W → eν (left) and W → μν (right) analysis for

- m_T (circles) and p_T^ℓ (squares) isolation with calorimeter-based isolation and
- m_T (triangles) and p_T^ℓ (stars) with track-based isolation.

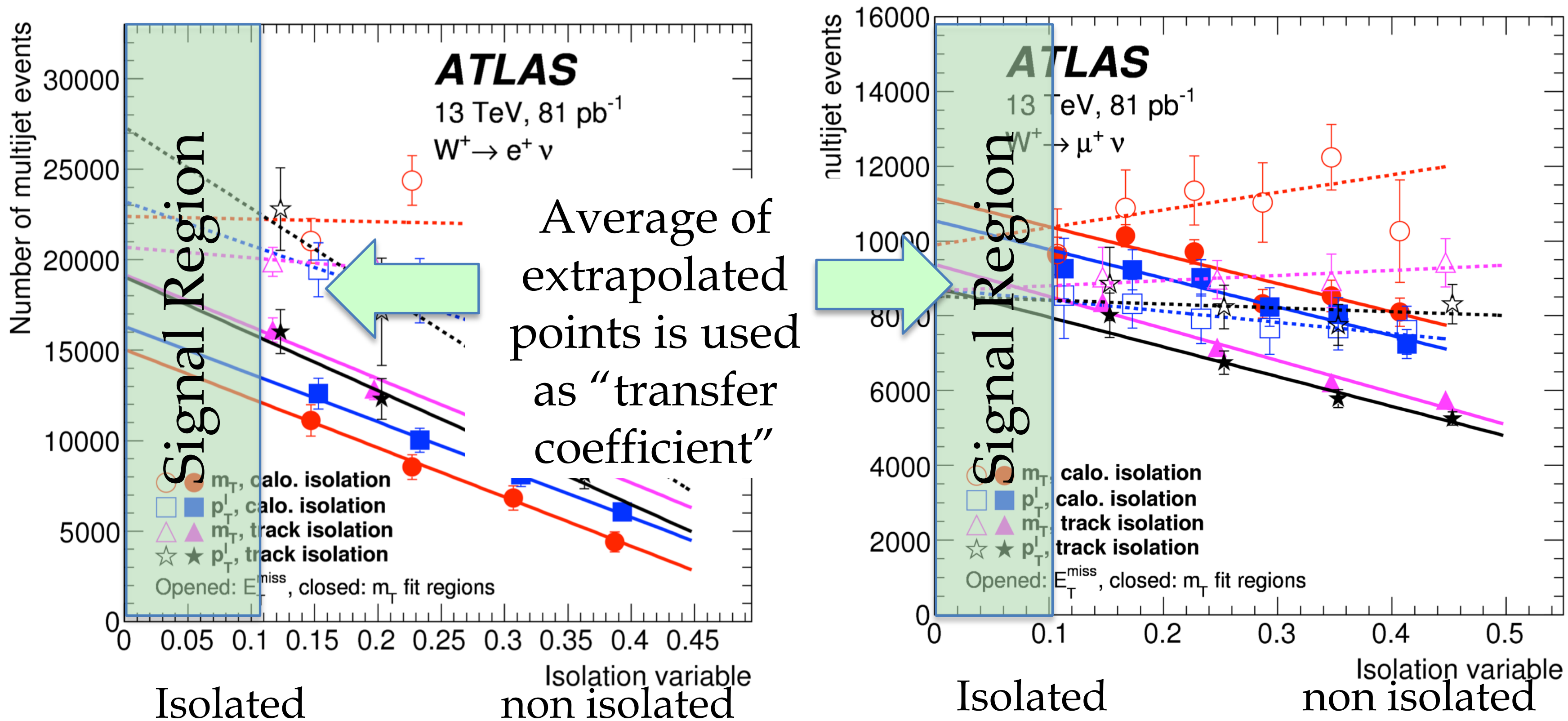

m_W measurement strategy - 1

The templates are

- compared to the observed distribution by means of a χ^2 compatibility test.
- The χ^2 values as a function of m_W are interpolated → the minimum value of χ^2 gives m_W

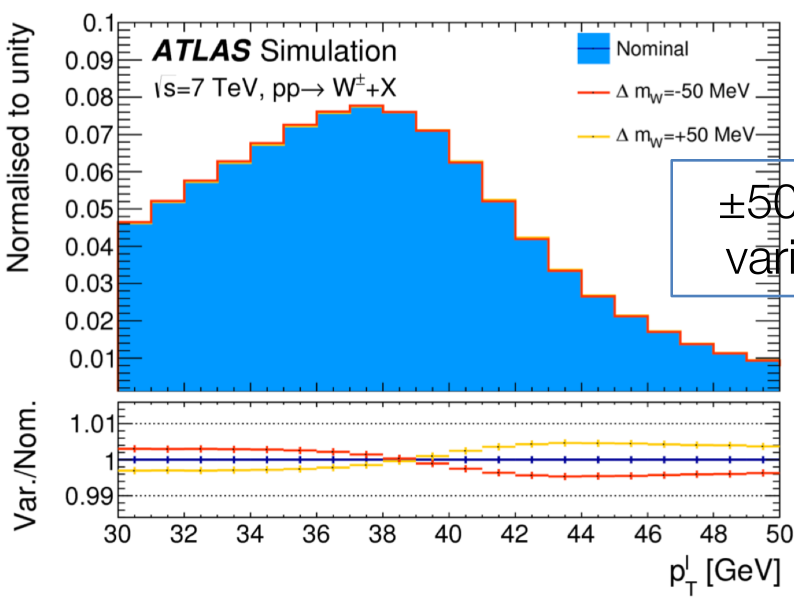

±50 MeV variation

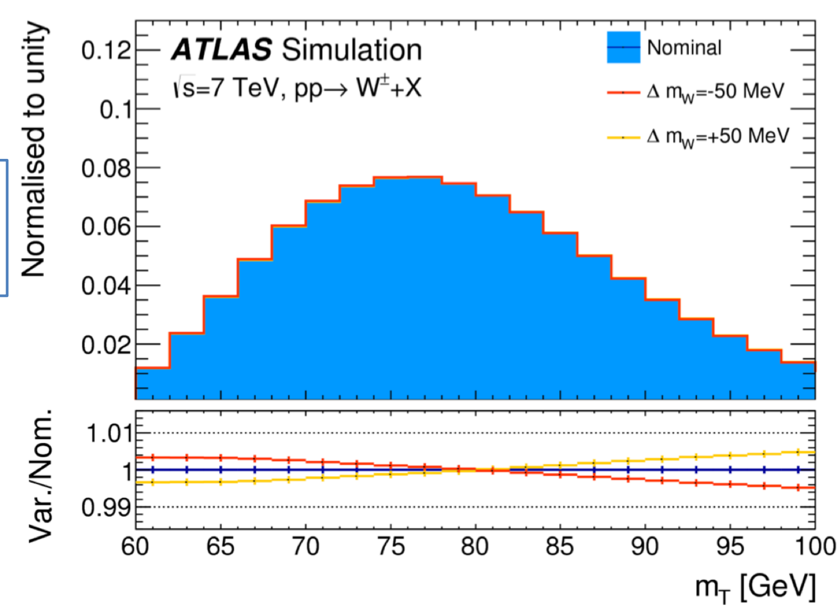

p_T^l has a Jacobian edge at $m_W/2$

m_T has a Jacobian edge at m_W

m_W measurement strategy - 2

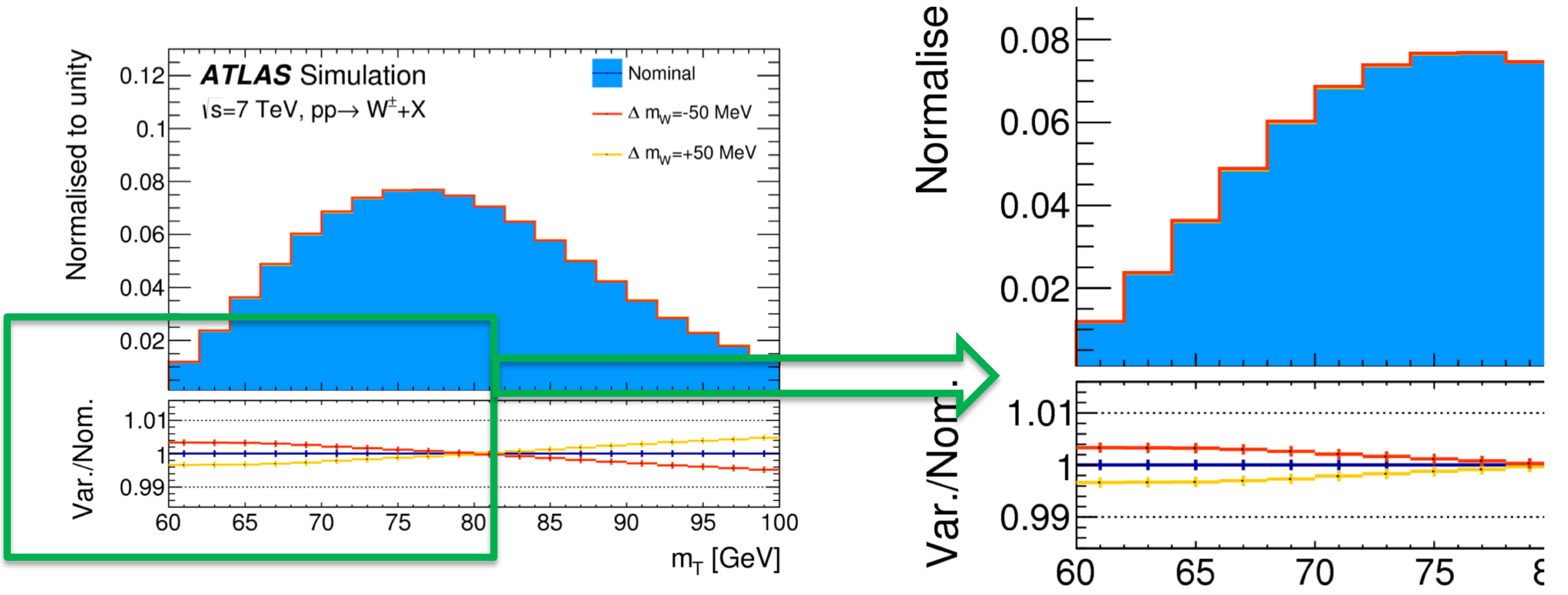

m_T has a Jacobian edge at m_W

The generation of large samples of simulated events in small steps of m_W would require an unsustainable amount of computing power → Predictions for different values of m_W are obtained from a single simulated reference sample, by reweighting the W-boson invariant mass distribution according to the Breit-Wigner parameterisation. The W-boson width is scaled accordingly, following the SM relation Γ_W / m^3_W.

m_W measurement → MC & Data

Templates are computed separately

- for + and - charged W bosons, &in several bins of η in the electron and muon decay channel including signal and background contributions

→ a few tens m_W templates with values of m_W in steps of 1 to 10 MeV within a range of 400 MeV, centred around the reference value used in the Monte Carlo signal samples.

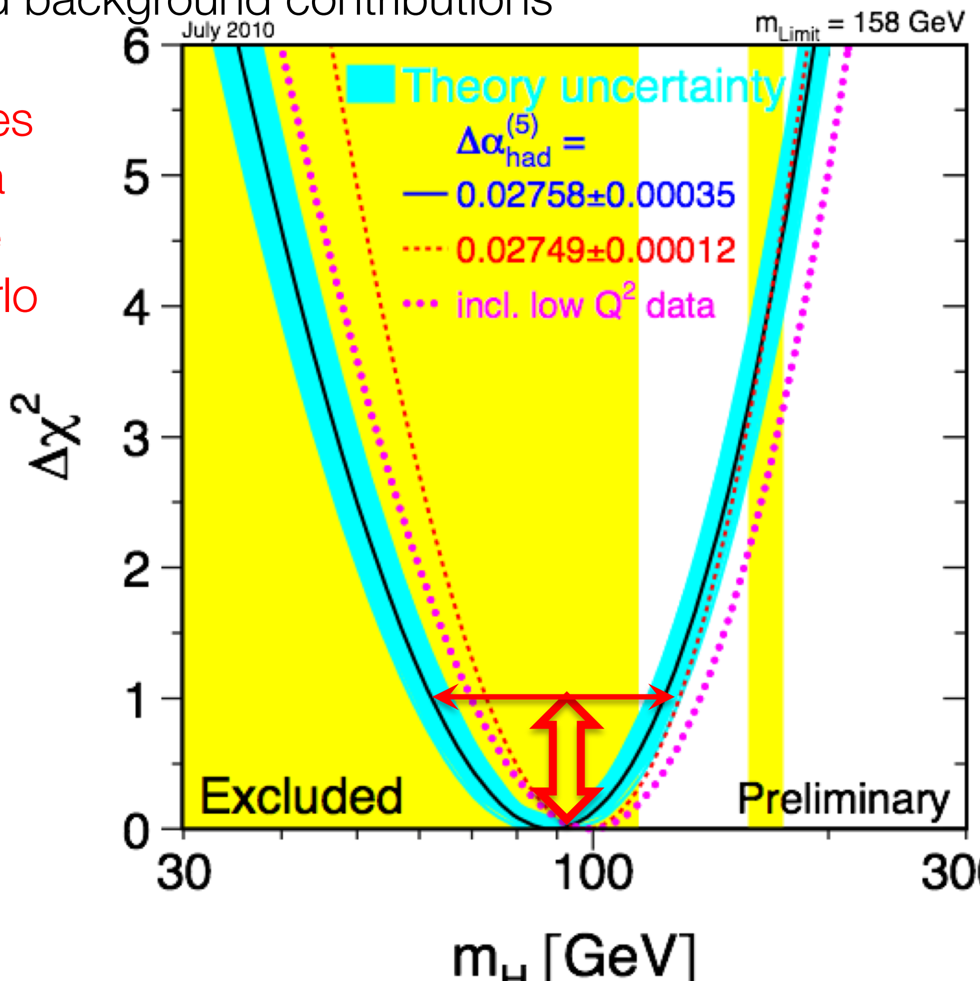

The statistical uncertainty = half width of the X^2 function at the value corresponding to one unit above the minimum.
Systematic uncertainties:

- physics-modelling corrections,
- detector-calibration corrections,
- and background subtraction

Experimental aspects

1. **The Z to ll event samples are used to calibrate the detector response.** Lepton momentum corrections are derived exploiting the precisely measured value of the Z-boson mass, m_Z , and the recoil response is calibrated using the expected momentum balance with p^T_{ll}. Identification and reconstruction efficiency corrections are determined from Z-boson events using the tag-and-probe method. The dependence of these corrections on p^T_l is important for the measurement of m_W, as it affects the shape of the template distributions.
2. The determination of m_Z from the lepton-pair invariant mass provides a first closure test of the lepton energy calibration.
3. **The detector response corrections and the physics modelling are verified in Z-boson events** by performing measurements of the Z-boson mass with the same method used to determine the W-boson mass, and comparing the results to the LEP combined value of m_Z , which is used as input for the lepton calibration.
4. The p^{miss}_T and m_T variables are defined in Z-boson events treating one of the reconstructed decay leptons as a neutrino. The extraction of m_Z from the m_T distribution provides a test of the recoil calibration. The combination of the extraction of m_Z from the m_{ll}, p^l_T and m_T distributions provides a closure test of the measurement procedure. The accuracy of this validation procedure is limited by the size of the Z-boson sample, which is approximately ten times smaller than the W-boson sample.

Tuning the reconstruction

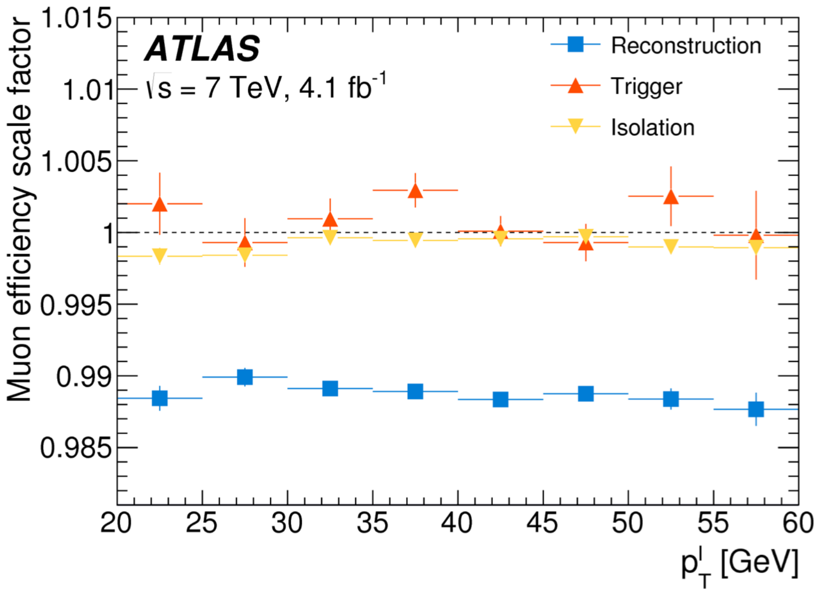

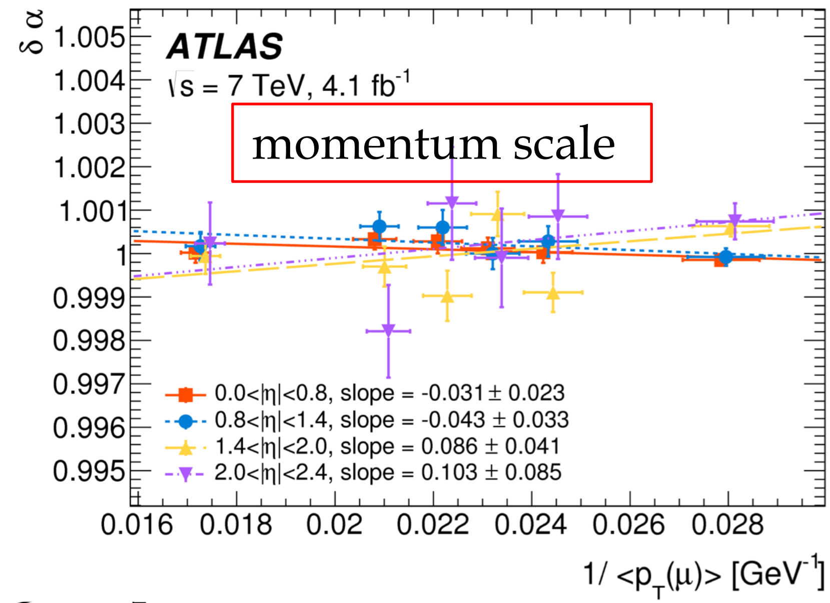

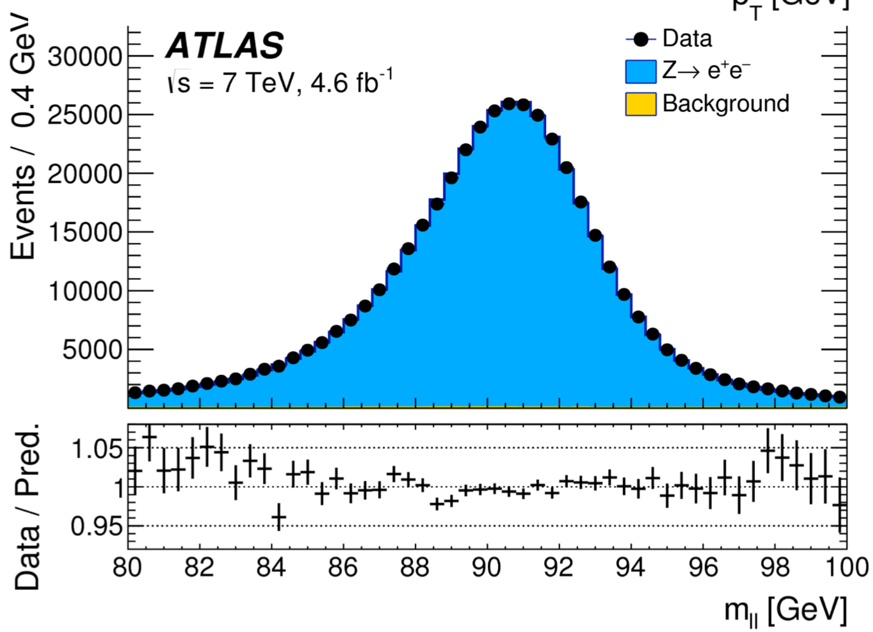

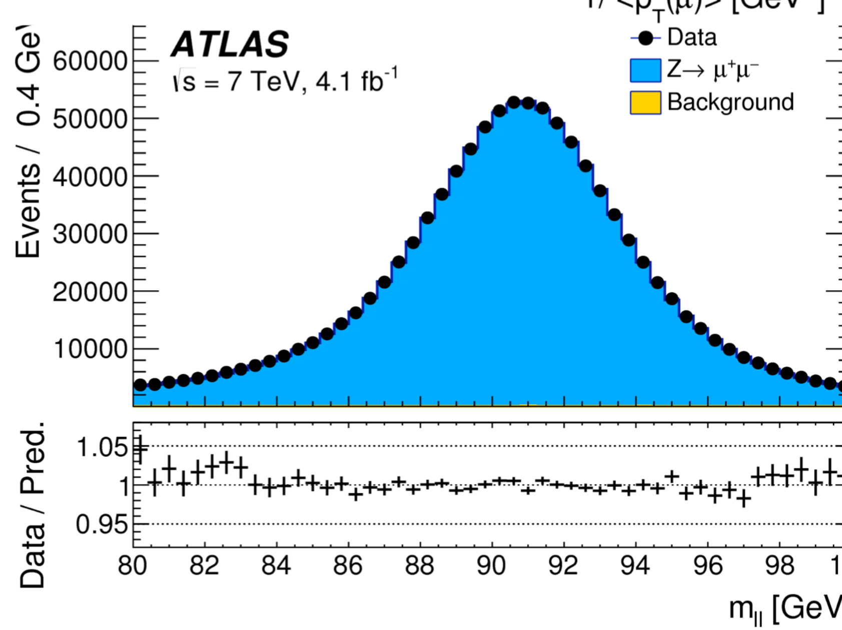

Variables used for m_W analysis

electrons

muons

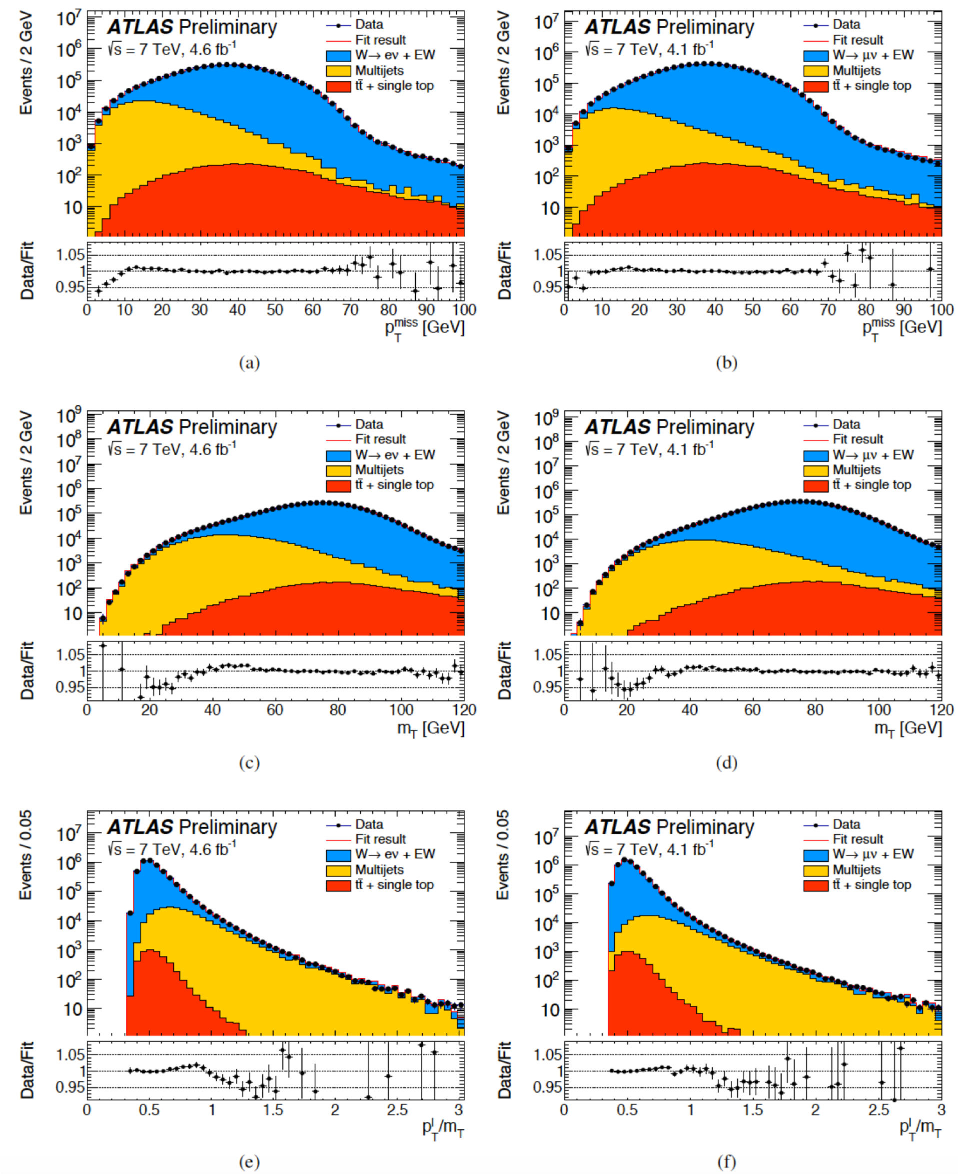

(a) (b)

(c) (d)

(e) (f)

m_T distributions from the W →lν

Measurement of W± and Z-boson production cross sections in pp collisions at √s = 13 TeV with the ATLAS detector, *Phys. Lett. B 759 (2016) 601*

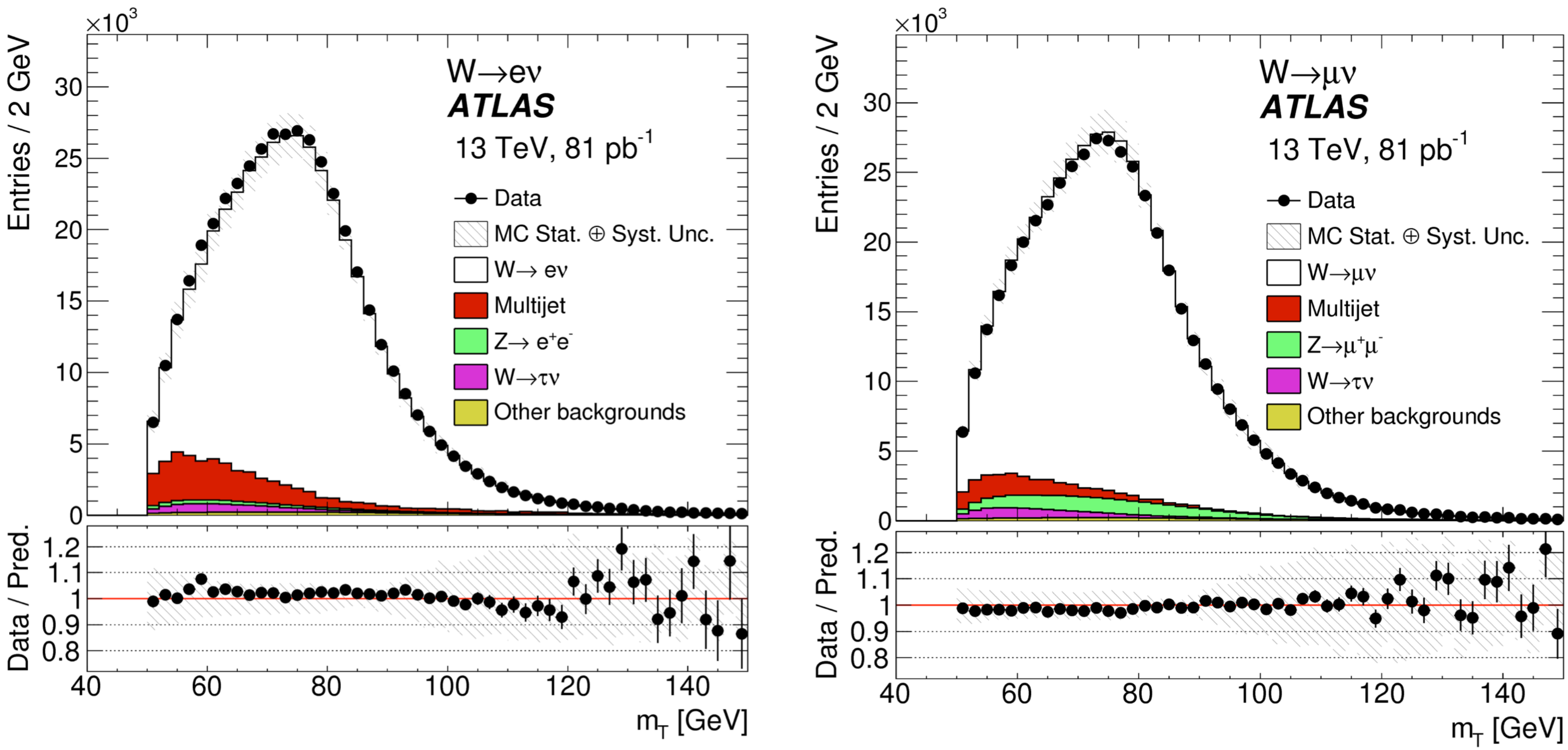

Experimental aspects

The Z to ll event samples are used to calibrate the detector response

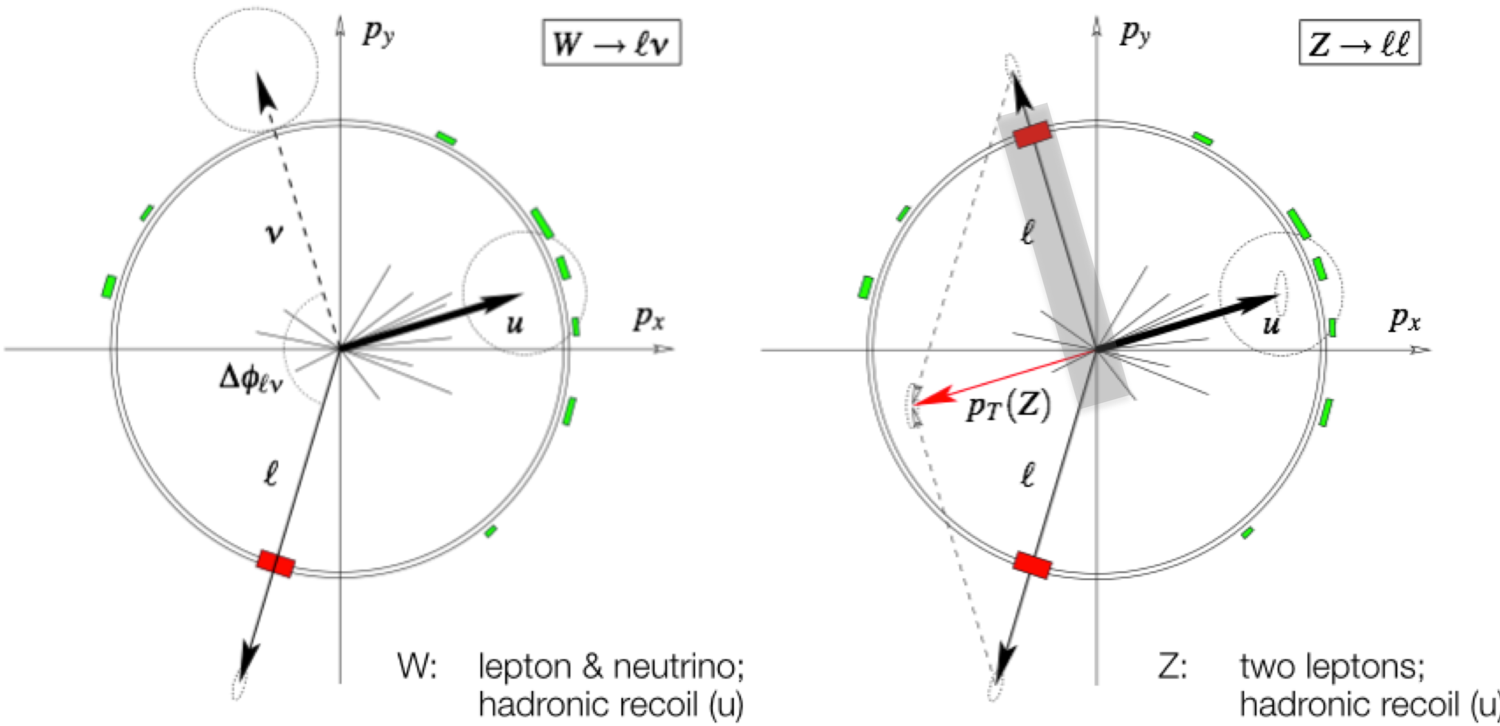

- One of the two leptons from Z decay is software-cancelled
- The topology is almost identical to the one of the $W \to l\nu$ decay (similar masses)
- The real Z direction and mass is known!
- Reconstruct m_T, use templates and compare with Z mass

m_Z distributions from the $Z \rightarrow l'\nu'$

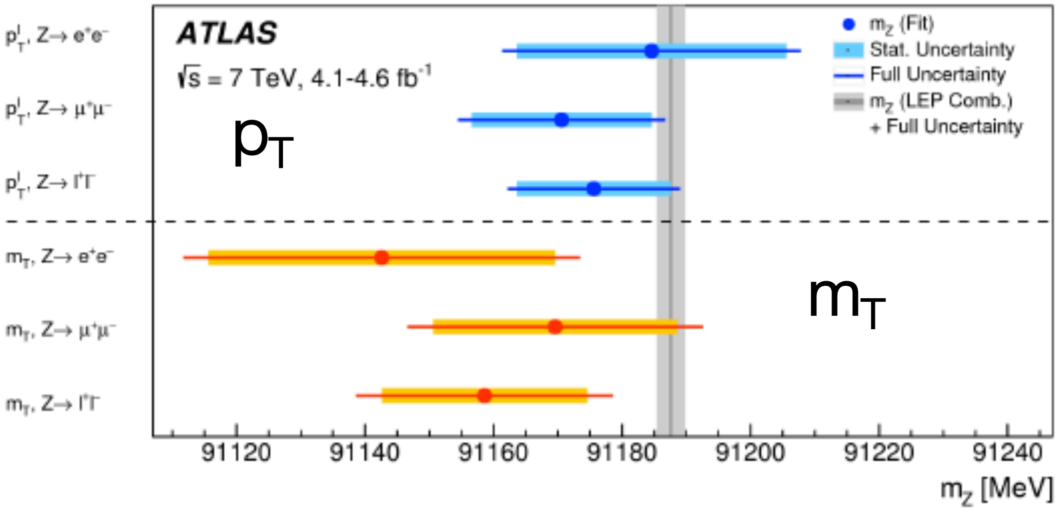

Lepton charge Distribution	Combined p_T^ℓ	m_T
Δm_Z [MeV]		
$Z \rightarrow ee$	$-3 \pm 21 \pm 10$	$-45 \pm 27 \pm 15$
$Z \rightarrow \mu\mu$	$-17 \pm 14 \pm 8$	$-18 \pm 19 \pm 13$
Combined	$-12 \pm 12 \pm 6$	$-29 \pm 16 \pm 12$

CMS PAS SMP-14-007

Sources of uncertainty	$M_Z^{\mathrm{W like}+}$ p_T	m_T	$\not{E}_T$	$M_Z^{\mathrm{W like}-}$ p_T	m_T	$\not{E}_T$
Lepton efficiencies	1	1	1	1	1	1
Lepton calibration	14	13	14	12	15	14
Recoil calibration	0	9	13	0	9	14
Total experimental syst. uncertainties	14	17	19	12	18	19
Statistics of the data sample	40	36	46	39	35	45

13

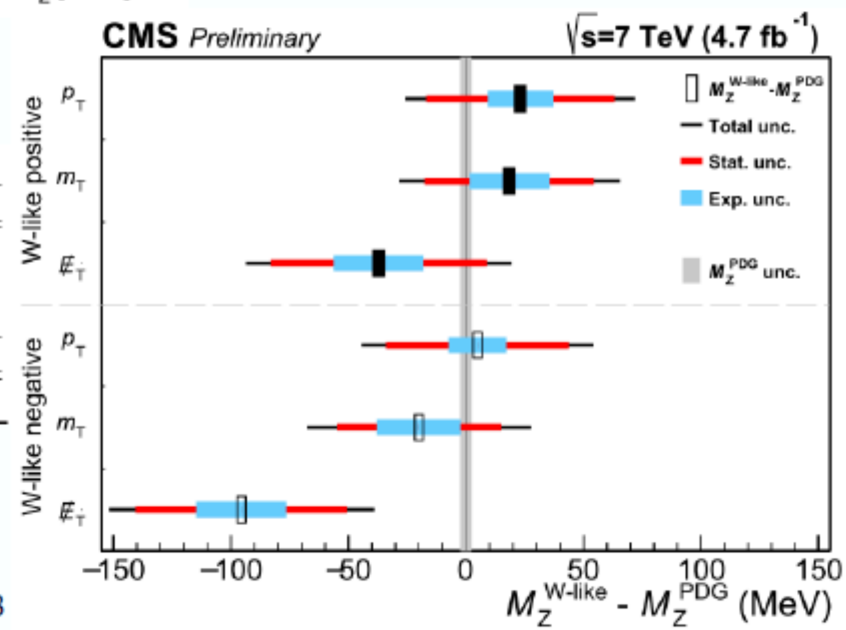

m_W measurement

Differential Z-boson cross section as a function of boson rapidity, and (b) differential W^+ and W^- cross sections as a function of charged decay-lepton pseudorapidity at $\sqrt{s}$=7 TeV. The measured cross sections are compared to the Powheg+Pythia 8 predictions, corrected to NNLO using DYNNLO with the CT10nnlo PDF set. The error bars show the total experimental uncertainties, including luminosity uncertainty, and the bands show the PDF uncertainties of the predictions.

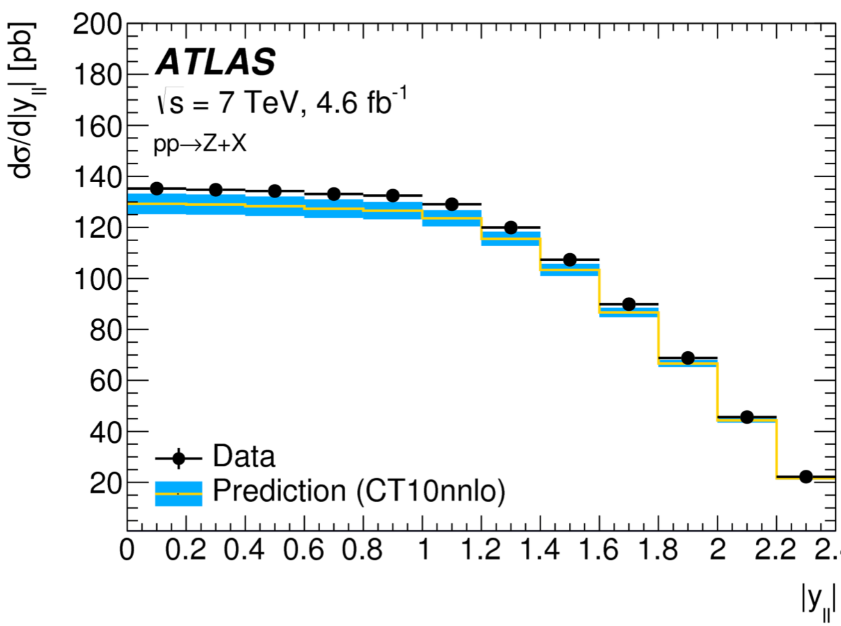

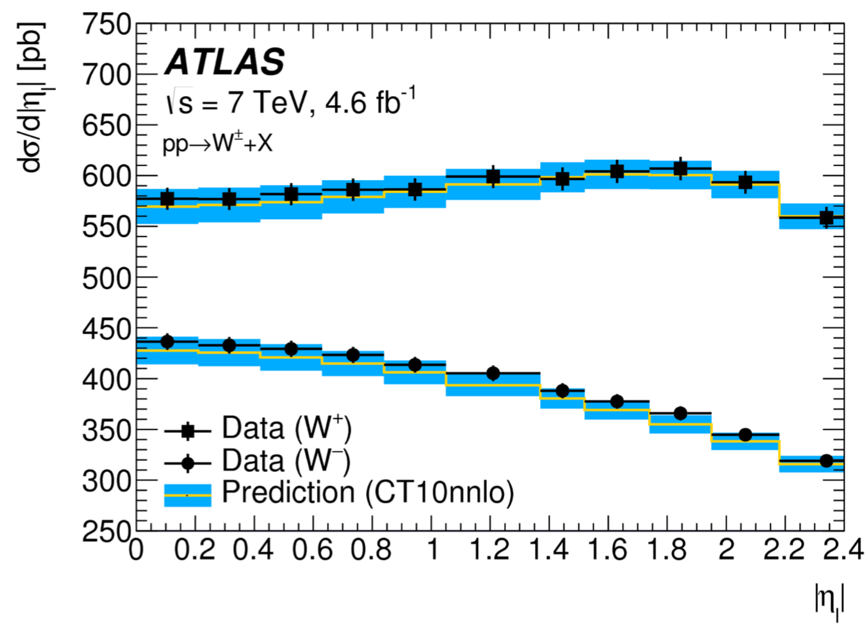

m_W: results

$$\begin{aligned} m_W &= 80369.5 \pm 6.8\ \text{MeV}(\text{stat.}) \pm 10.6\ \text{MeV}(\text{exp. syst.}) \pm 13.6\ \text{MeV}(\text{mod. syst.}) \\ &= 80369.5 \pm 18.5\ \text{MeV}, \end{aligned}$$

Combined categories	Value [MeV]	Stat. Unc.	Muon Unc.	Elec. Unc.	Recoil Unc.	Bckg. Unc.	QCD Unc.	EWK Unc.	PDF Unc.	Total Unc.	χ^2/dof of Comb.
m_T-p_T^ℓ, $W^\pm$, e-μ	80369.5	6.8	6.6	6.4	2.9	4.5	8.3	5.5	9.2	18.5	29/27

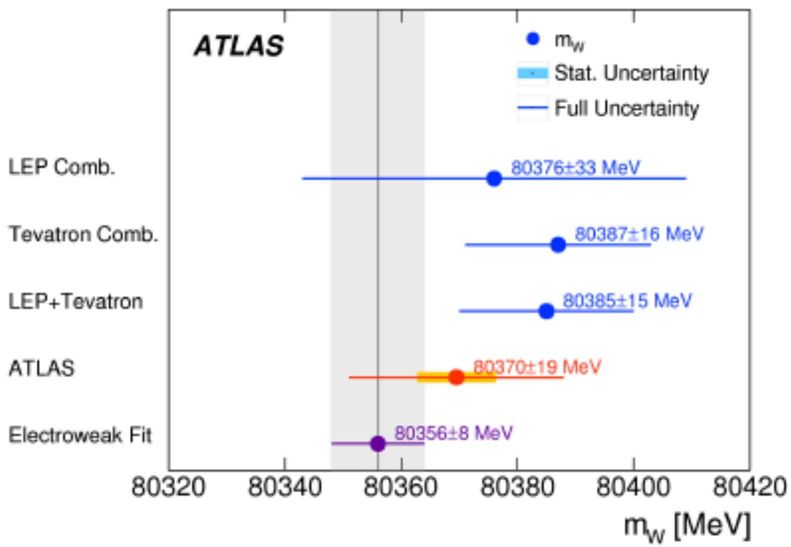

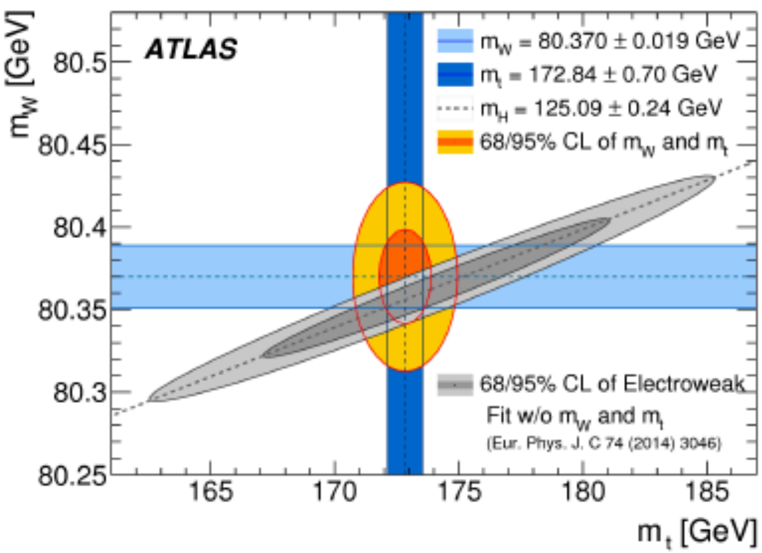

The result is consistent with the SM expectation, compatible with the world average and competitive in precision to the currently leading measurements by CDF and D0

m_W : Results

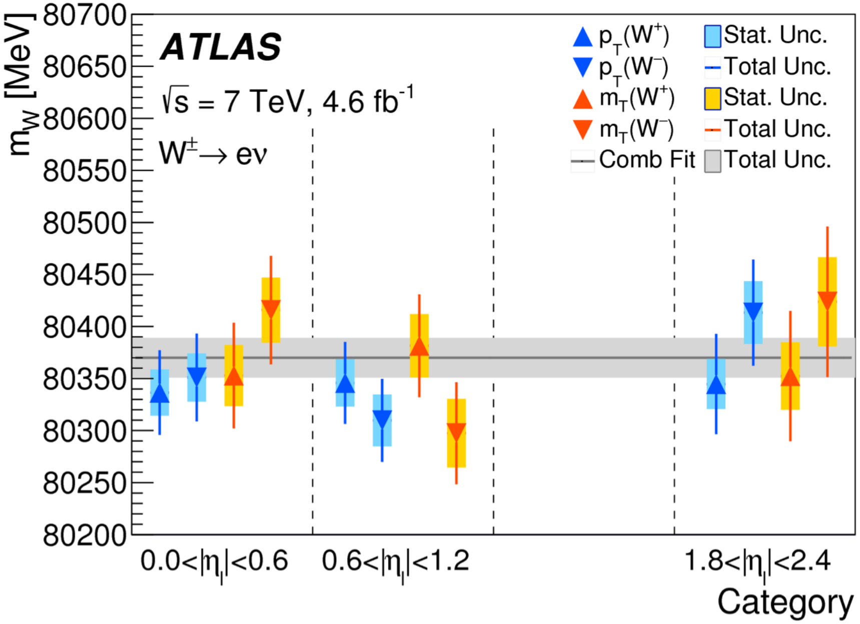
ATLAS
√s = 7 TeV, 4.6 fb⁻¹
W± → eν
pT(W+)
pT(W−)
mT(W+)
mT(W−)
Comb Fit
Stat. Unc.
Total Unc.
mW [MeV]
0.0<|ηl|<0.6
0.6<|ηl|<1.2
1.8<|ηl|<2.4
Category

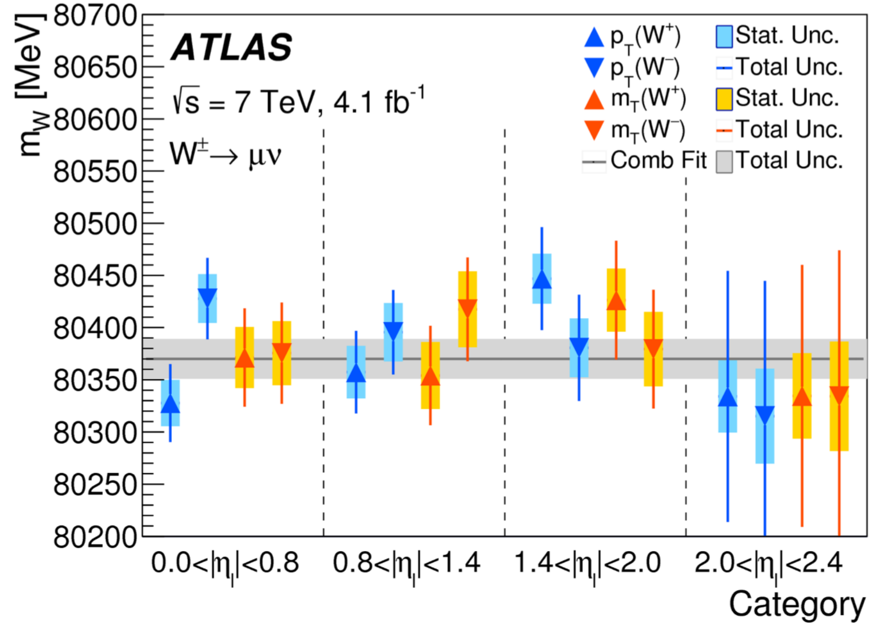
ATLAS
√s = 7 TeV, 4.1 fb⁻¹
W± → μν
pT(W+)
pT(W−)
mT(W+)
mT(W−)
Comb Fit
Stat. Unc.
Total Unc.
mW [MeV]
0.0<|ηl|<0.8
0.8<|ηl|<1.4
1.4<|ηl|<2.0
2.0<|ηl|<2.4
Category

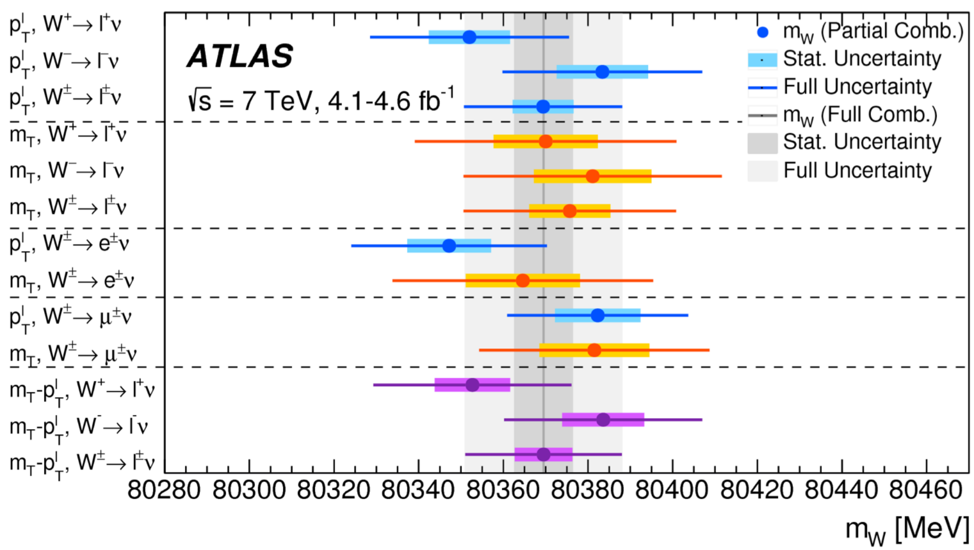
ATLAS
√s = 7 TeV, 4.1-4.6 fb⁻¹
mW (Partial Comb.)
Stat. Uncertainty
Full Uncertainty
mW (Full Comb.)
Stat. Uncertainty
Full Uncertainty
pT, W+ → l+ν
pT, W− → l−ν
pT, W± → l±ν
mT, W+ → l+ν
mT, W− → l−ν
mT, W± → l±ν
pT, W± → e±ν
mT, W± → e±ν
pT, W± → μ±ν
mT, W± → μ±ν
mT-pT, W+ → l+ν
mT-pT, W− → l−ν
mT-pT, W± → l±ν
mW [MeV]

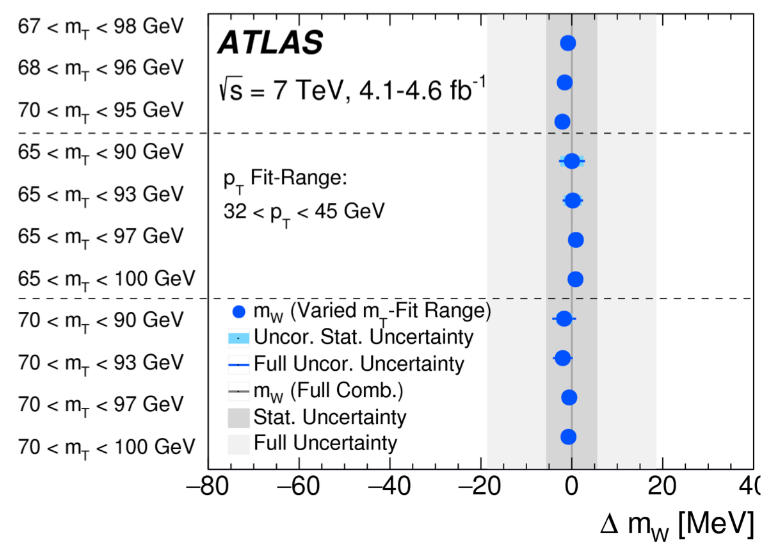
ATLAS
√s = 7 TeV, 4.1-4.6 fb⁻¹
pT Fit-Range:
32 < pT < 45 GeV
mW (Varied mT-Fit Range)
Uncor. Stat. Uncertainty
Full Uncor. Uncertainty
mW (Full Comb.)
Stat. Uncertainty
Full Uncertainty
67 < mT < 98 GeV
68 < mT < 96 GeV
70 < mT < 95 GeV
65 < mT < 90 GeV
65 < mT < 93 GeV
65 < mT < 97 GeV
65 < mT < 100 GeV
70 < mT < 90 GeV
70 < mT < 93 GeV
70 < mT < 97 GeV
70 < mT < 100 GeV
Δ mW [MeV]

Ratio of Cross Sections

Ratio of the electron- and muon-channel W and Z-boson production fiducial cross sections, compared to the expected values of the Standard Model of (1,1)and previous experimental verifications of lepton universality for on-shell W and Z bosons, shown as PDG average bands. The PDG average values and the result are shown with total uncertainties.

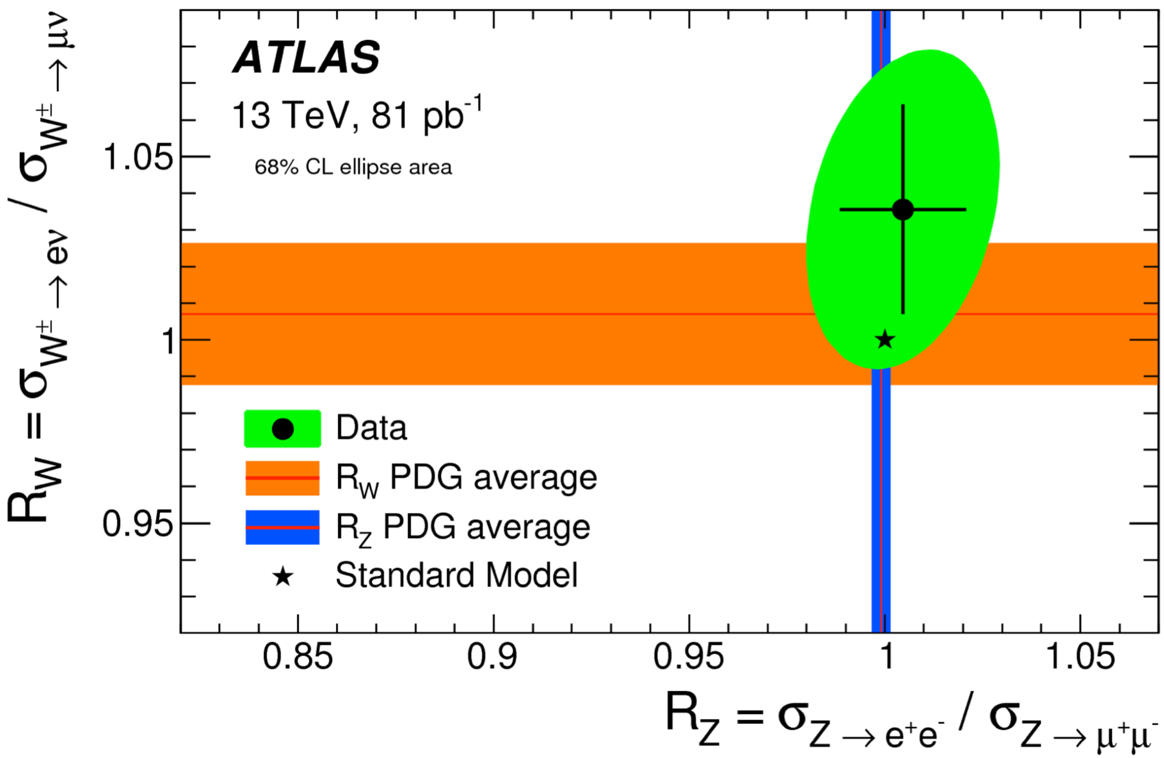

Results

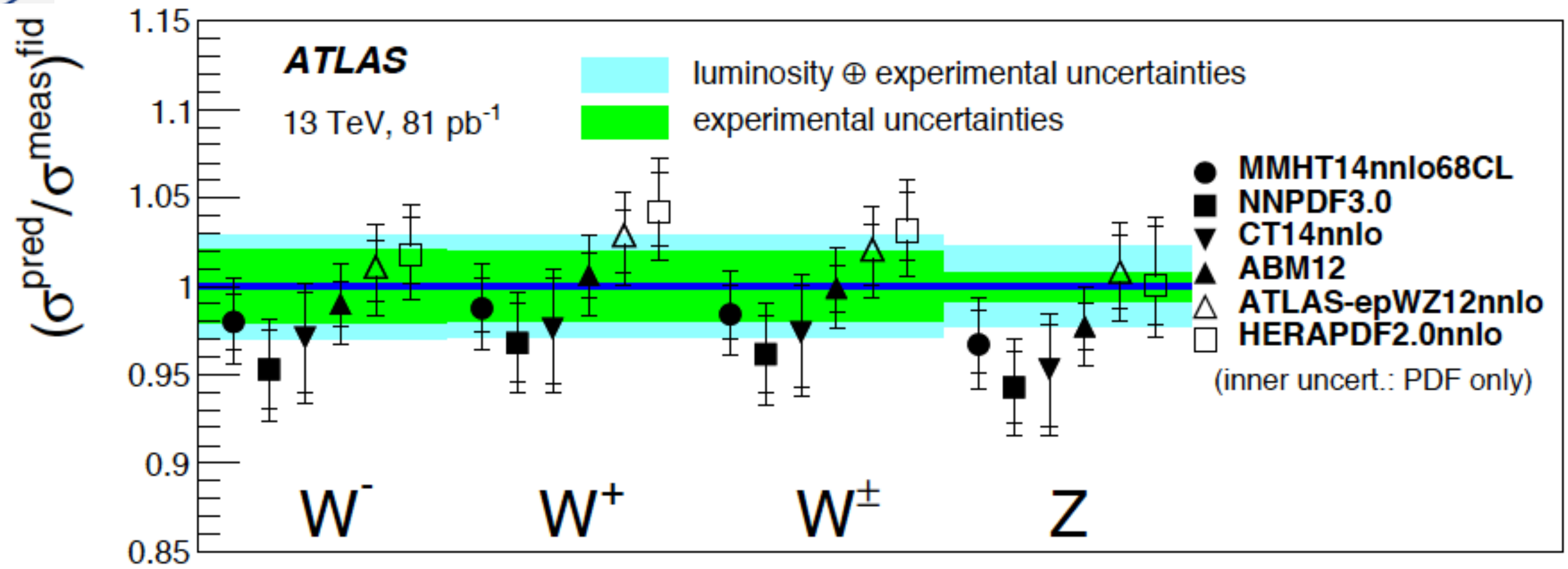

	W^+	W^-	Z
	Electron channel (value ± stat ± syst ± lumi)		
Signal events	228060 ± 510 ± 4920 ± 200	177890 ± 450 ± 6110 ± 180	34865 ± 187 ± 7 ± 3
Correction C	0.602 ± 0.012	0.614 ± 0.012	$0.552^{+0.006}_{-0.005}$
σ^{fid}[nb]	4.68 ± 0.01 ± 0.14 ± 0.10	3.58 ± 0.01 ± 0.14 ± 0.08	0.781 ± 0.004 ± 0.008 ± 0.016
Acceptance A	0.383 ± 0.007	0.398 ± 0.007	0.393 ± 0.007
σ^{tot}[nb]	12.23 ± 0.03 ± 0.42 ± 0.27	9.00 ± 0.02 ± 0.39 ± 0.20	1.987 ± 0.011 ± 0.041 ± 0.042
	Muon channel (value ± stat ± syst ± lumi)		
Signal events	237720 ± 520 ± 2210 ± 410	183180 ± 460 ± 2520 ± 360	44706 ± 212 ± 9 ± 4
Correction C	0.653 ± 0.012	0.650 ± 0.012	0.711±0.008
σ^{fid}[nb]	4.50 ± 0.01 ± 0.09 ± 0.10	3.48 ± 0.01 ± 0.08 ± 0.08	0.777 ± 0.004 ± 0.008 ± 0.016
Acceptance A	0.383 ± 0.007	0.398 ± 0.007	0.393 ± 0.007
σ^{tot}[nb]	11.75 ± 0.03 ± 0.33 ± 0.27	8.75 ± 0.02 ± 0.25 ± 0.20	1.977 ± 0.009 ± 0.041 ± 0.042

W mass compilation (pdg 2017)

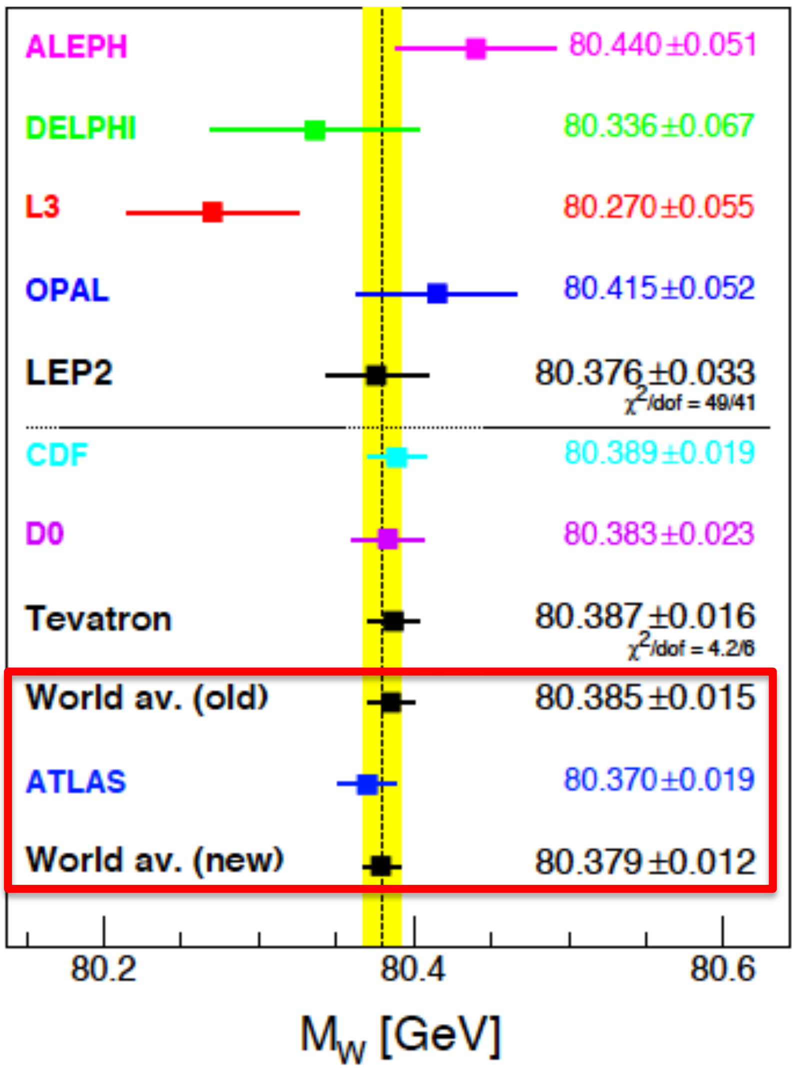

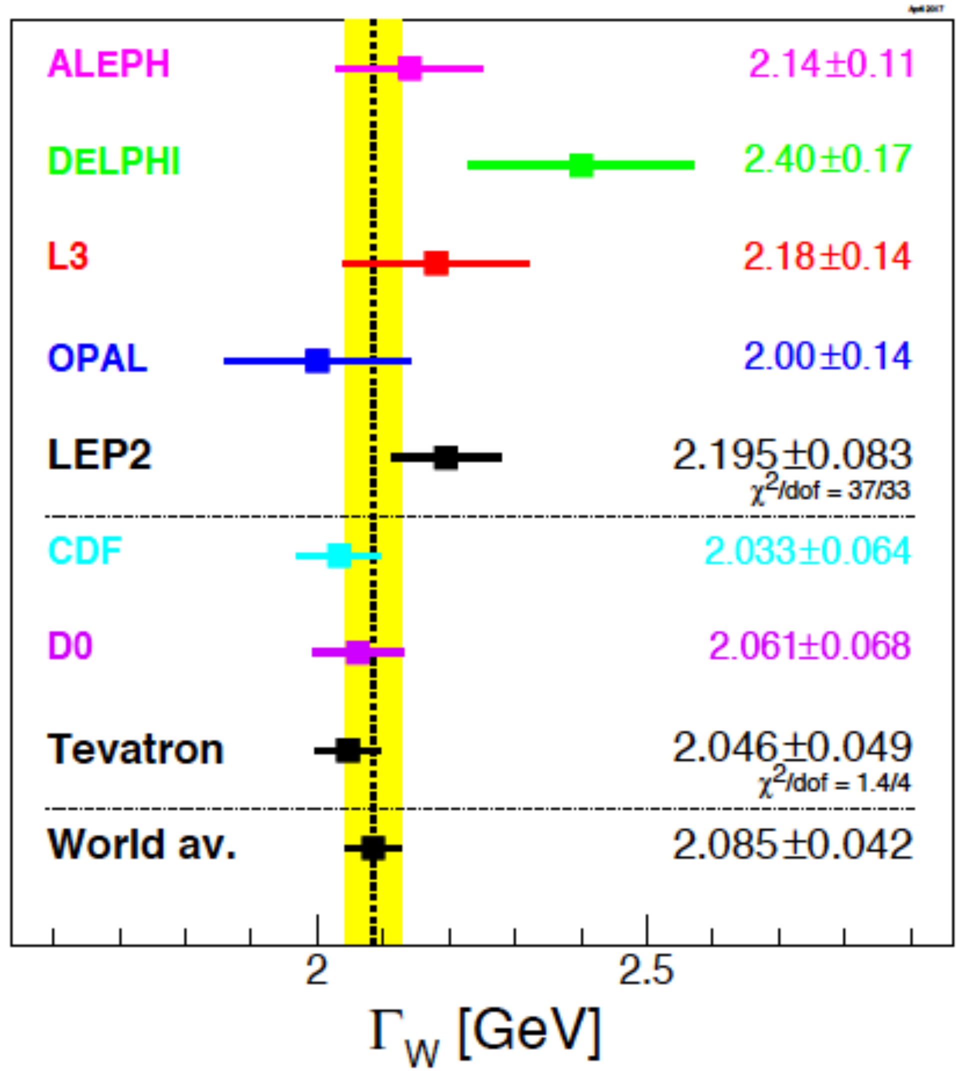

CMS EW Measurements

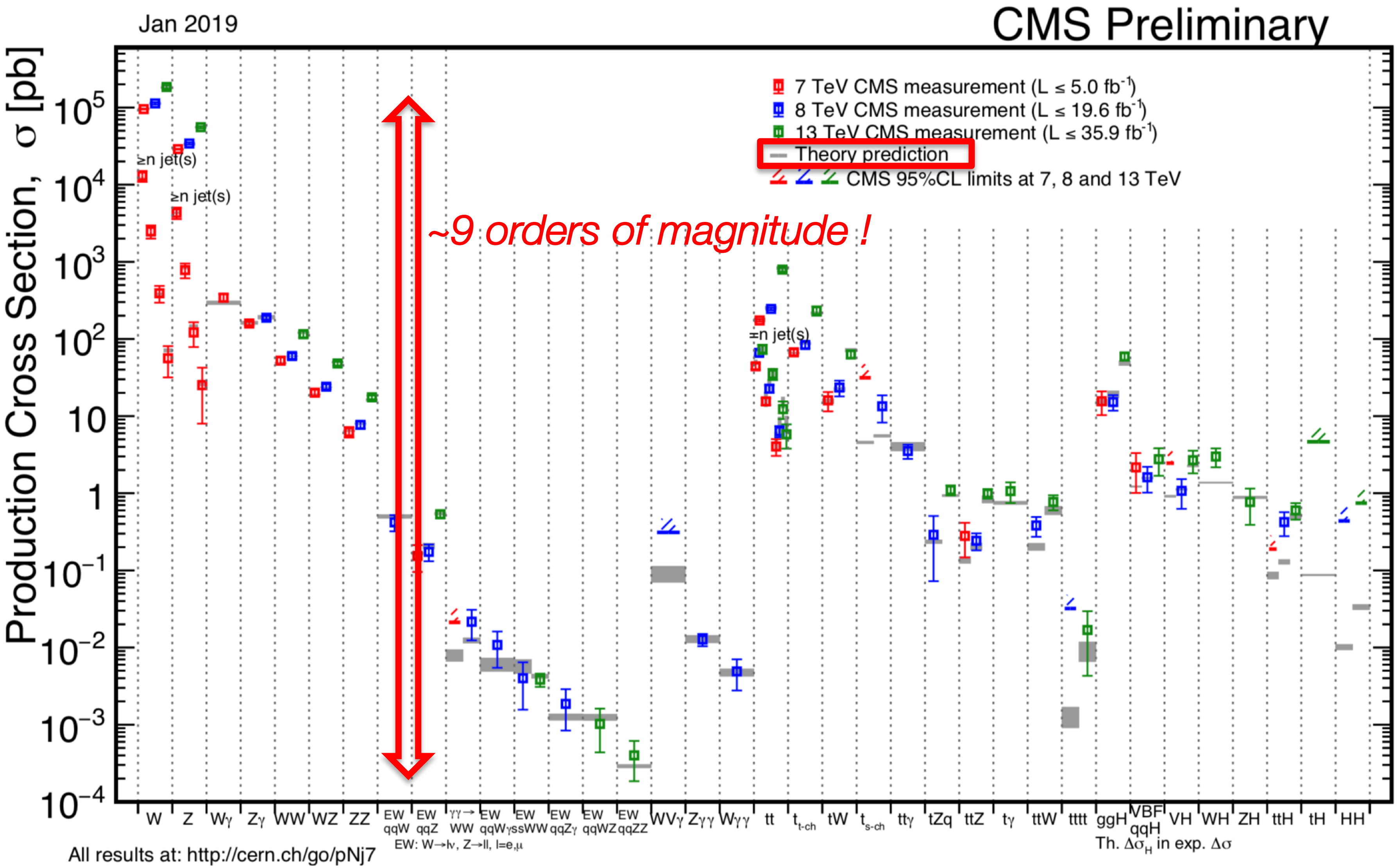

ATLAS EW Results

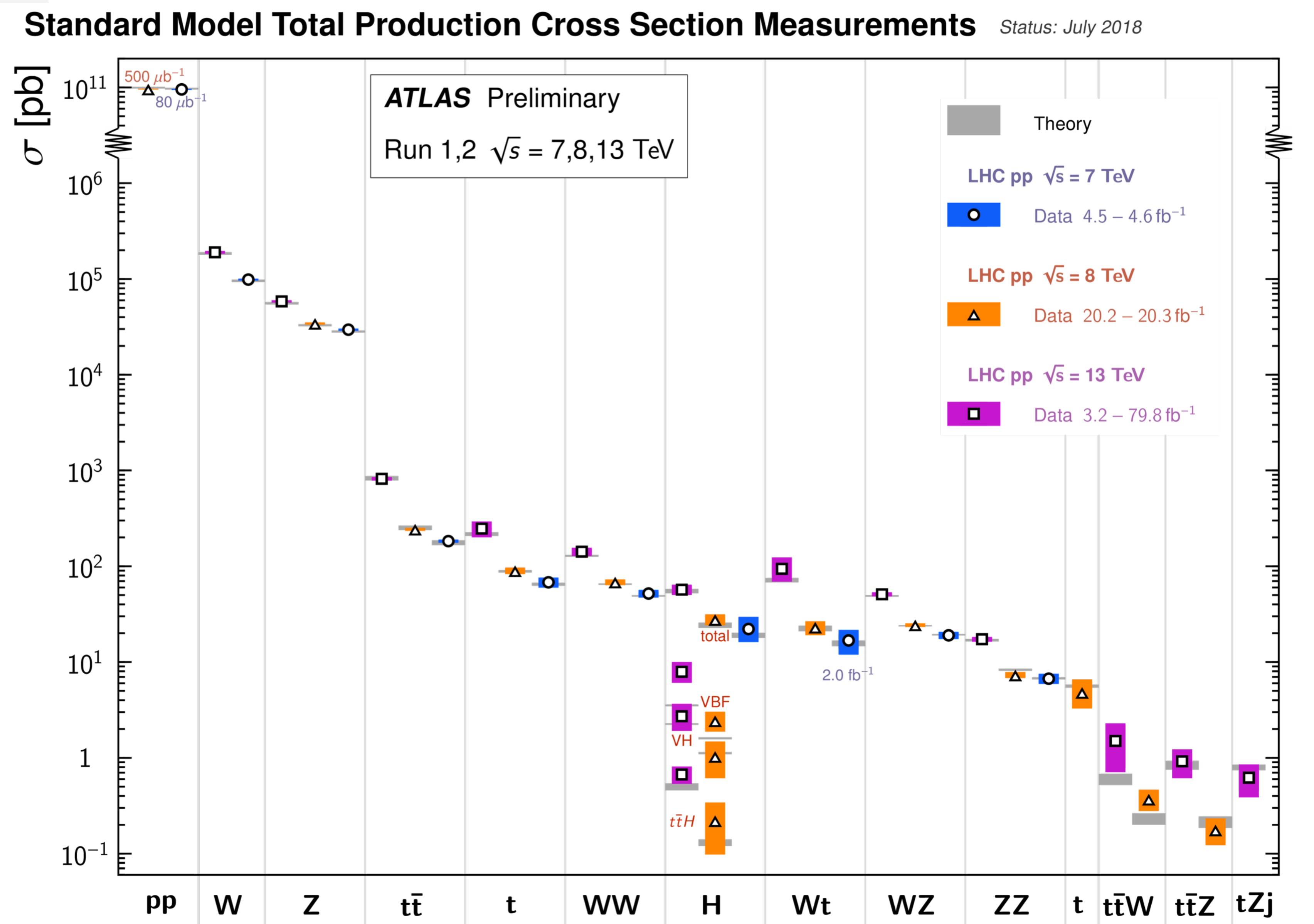

Global EW fits - 1

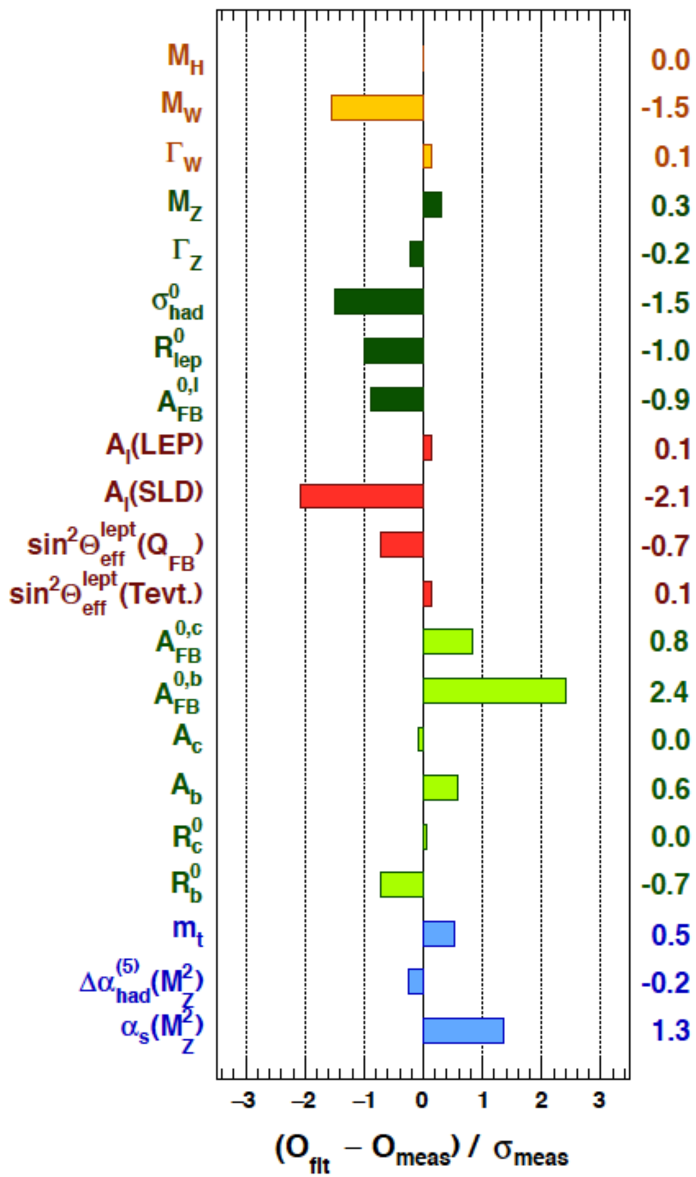

Comparison of the results with the indirect determination in units of the total uncertainty, defined as the uncertainty of the direct measurement and that of the indirect determination added in quadrature. The indirect determination of an observable corresponds to a fit without using the corresponding direct constraint from the measurement.

$$\frac{Result - Indirect\ Determination}{\sqrt{\sigma^2_{Result} + \sigma^2_{Ind.Det.}}}$$

In the context of global fits to the SM parameters, constraints on physics beyond the SM are currently limited by the measurement of the W-boson mass. Therefore improving the precision of the measurements of m_W is of high importance for testing the overall consistency of the SM.

Global EW fits – Input Parameters

Parameter	Input value	Free in fit	Fit Result	Fit w/o exp. input in line	Fit w/o exp. input in line, no theo. unc.
M_H [GeV]	125.1 ± 0.2	yes	125.1 ± 0.2	90^{+21}_{-18}	89^{+20}_{-17}
M_W [GeV]	80.379 ± 0.013	–	80.359 ± 0.006	80.354 ± 0.007	80.354 ± 0.005
Γ_W [GeV]	2.085 ± 0.042	–	2.091 ± 0.001	2.091 ± 0.001	2.091 ± 0.001
M_Z [GeV]	91.1875 ± 0.0021	yes	91.1882 ± 0.0020	91.2013 ± 0.0095	91.2017 ± 0.0089
Γ_Z [GeV]	2.4952 ± 0.0023	–	2.4947 ± 0.0014	2.4941 ± 0.0016	2.4940 ± 0.0016
$\sigma^0_{\rm had}$ [nb]	41.540 ± 0.037	–	41.484 ± 0.015	41.475 ± 0.016	41.475 ± 0.015
R^0_ℓ	20.767 ± 0.025	–	20.742 ± 0.017	20.721 ± 0.026	20.719 ± 0.025
$A^{0,\ell}_{\rm FB}$	0.0171 ± 0.0010	–	0.01620 ± 0.0001	0.01619 ± 0.0001	0.01619 ± 0.0001
A_ℓ $^{(\star)}$	0.1499 ± 0.0018	–	0.1470 ± 0.0005	0.1470 ± 0.0005	0.1469 ± 0.0003
$\sin^2\theta^\ell_{\rm eff}(Q_{\rm FB})$	0.2324 ± 0.0012	–	0.23153 ± 0.00006	0.23153 ± 0.00006	0.23153 ± 0.00004
$\sin^2\theta^\ell_{\rm eff}$(Tevt.)	0.23148 ± 0.00033	–	0.23153 ± 0.00006	0.23153 ± 0.00006	0.23153 ± 0.00004
A_c	0.670 ± 0.027	–	0.6679 ± 0.00021	0.6679 ± 0.00021	0.6679 ± 0.00014
A_b	0.923 ± 0.020	–	0.93475 ± 0.00004	0.93475 ± 0.00004	0.93475 ± 0.00002
$A^{0,c}_{\rm FB}$	0.0707 ± 0.0035	–	0.0736 ± 0.0003	0.0736 ± 0.0003	0.0736 ± 0.0002
$A^{0,b}_{\rm FB}$	0.0992 ± 0.0016	–	0.1030 ± 0.0003	0.1032 ± 0.0003	0.1031 ± 0.0002
R^0_c	0.1721 ± 0.0030	–	0.17224 ± 0.00008	0.17224 ± 0.00008	0.17224 ± 0.00006
R^0_b	0.21629 ± 0.00066	–	0.21582 ± 0.00011	0.21581 ± 0.00011	0.21581 ± 0.00004
$\overline{m}_c$ [GeV]	$1.27^{+0.07}_{-0.11}$	yes	$1.27^{+0.07}_{-0.11}$	–	–
$\overline{m}_b$ [GeV]	$4.20^{+0.17}_{-0.07}$	yes	$4.20^{+0.17}_{-0.07}$	–	–
m_t [GeV]$^{(\triangledown)}$	172.47 ± 0.68	yes	172.83 ± 0.65	176.4 ± 2.1	176.4 ± 2.0
$\Delta\alpha^{(5)}_{\rm had}(M_Z^2)$ $^{(\dagger\triangle)}$	2760 ± 9	yes	2758 ± 9	2716 ± 39	2715 ± 37
$\alpha_s(M_Z^2)$	–	yes	0.1194 ± 0.0029	0.1194 ± 0.0029	0.1194 ± 0.0028

$^{(\star)}$Average of LEP ($A_\ell = 0.1465 \pm 0.0033$) and SLD ($A_\ell = 0.1513 \pm 0.0021$) measurements, used as two measurements in the fit. The fit without the LEP (SLD) measurement gives $A_\ell = 0.1470 \pm 0.0005$ ($A_\ell = 0.1467 \pm 0.0005$). $^{(\triangledown)}$Combination of experimental (0.46 GeV) and theory uncertainty (0.5 GeV). $^{(\dagger)}$In units of 10^{-5}. $^{(\triangle)}$Rescaled due to α_s dependency.

Input values and fit results for the observables used in the global electroweak fit. The first and second columns list respectively the observables/parameters used in the fit, and their experimental values or phenomenological estimates (see text for references). The third column indicates whether a parameter is floating in the fit. The fourth column gives the results of the fit including all experimental data. In the fifth column, the fit results are given without using the corresponding experimental or phenomenological estimate in the given row (indirect determination). The last column shows for illustration the result using the same t setup as in the fifth column, but ignoring all theoretical uncertainties.

Di-bosons

Production mechanism

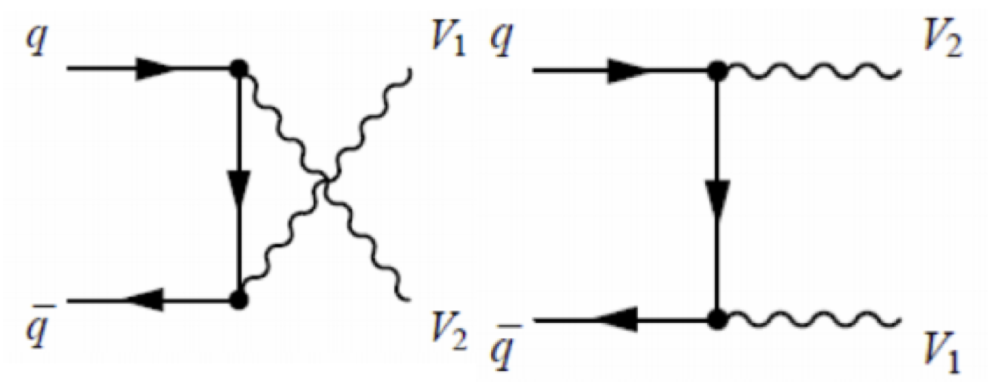

Why studying di-bosons?

- Stringent test of SM prediction in Electroweak sector and perturbative QCD at TeV scale
- background to many other channels, like Higgs Physics and exotic searches with leptons and large MET. In some cases may be irreducible

h to WW

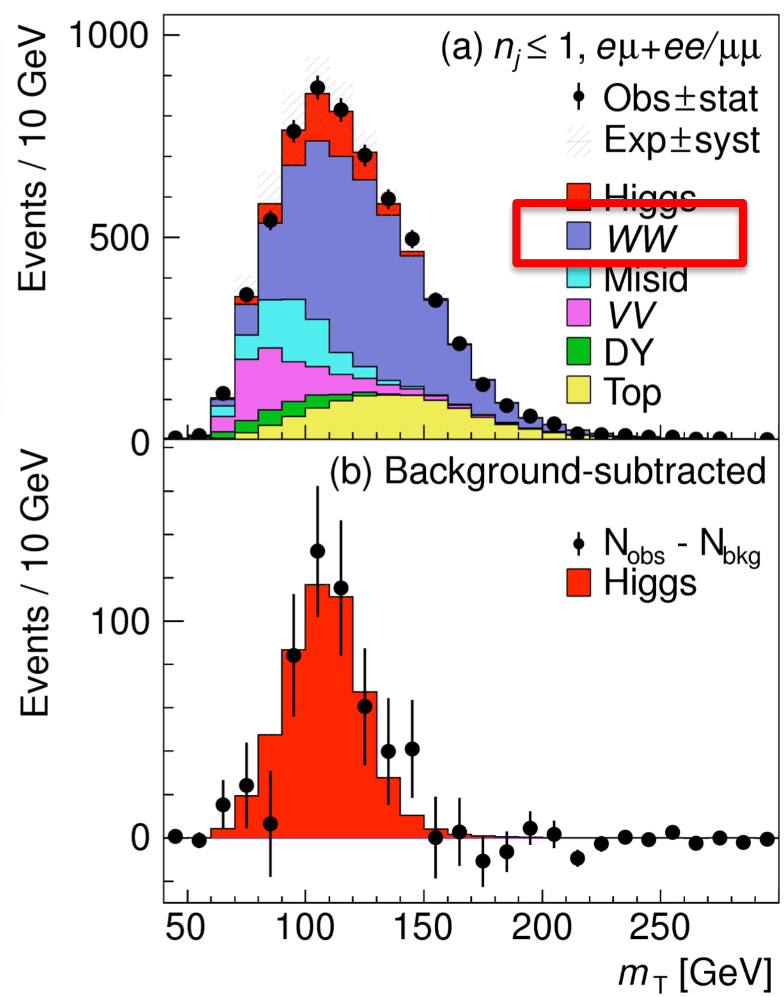

Di-bosons

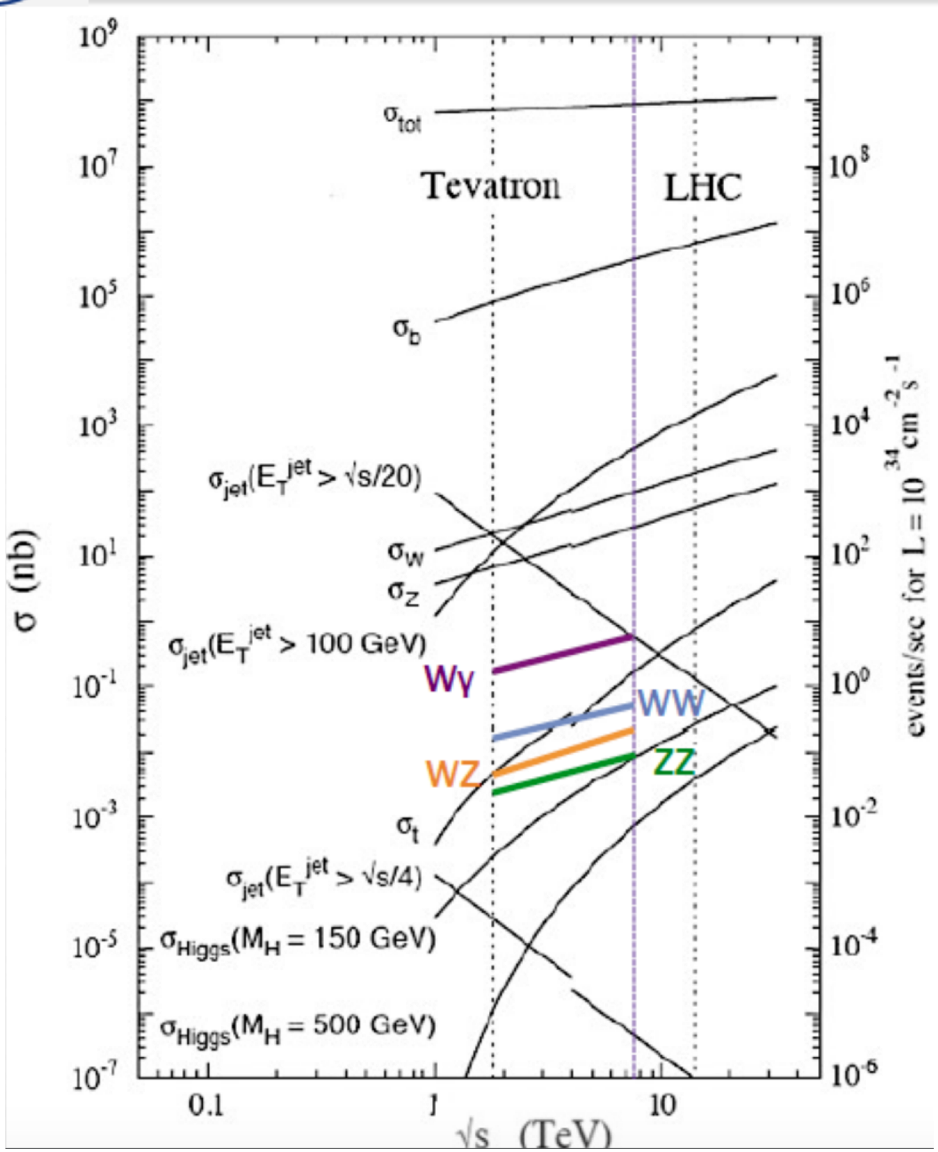

- Electroweak theory predicts triple and quartic gauge boson couplings (TGC, QGC).
- Due to new physics contribution TGC and QGC may deviate from SM prediction: anomalous couplings (neutral TGC's are forbidden at tree level).

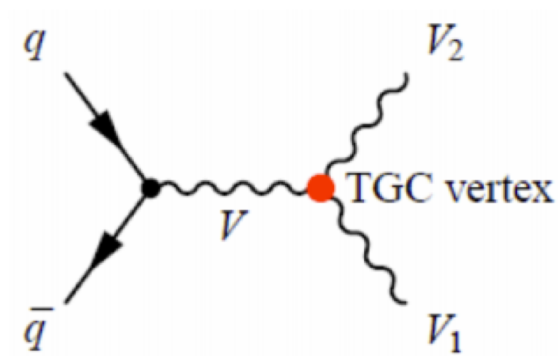

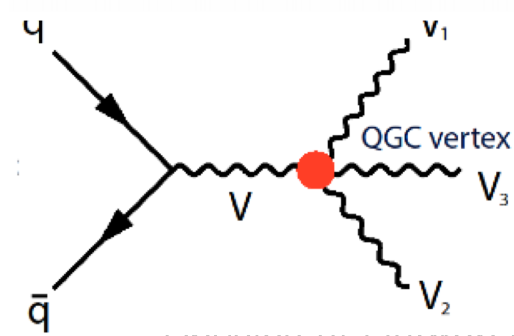

ATLAS compilation of di-bosons

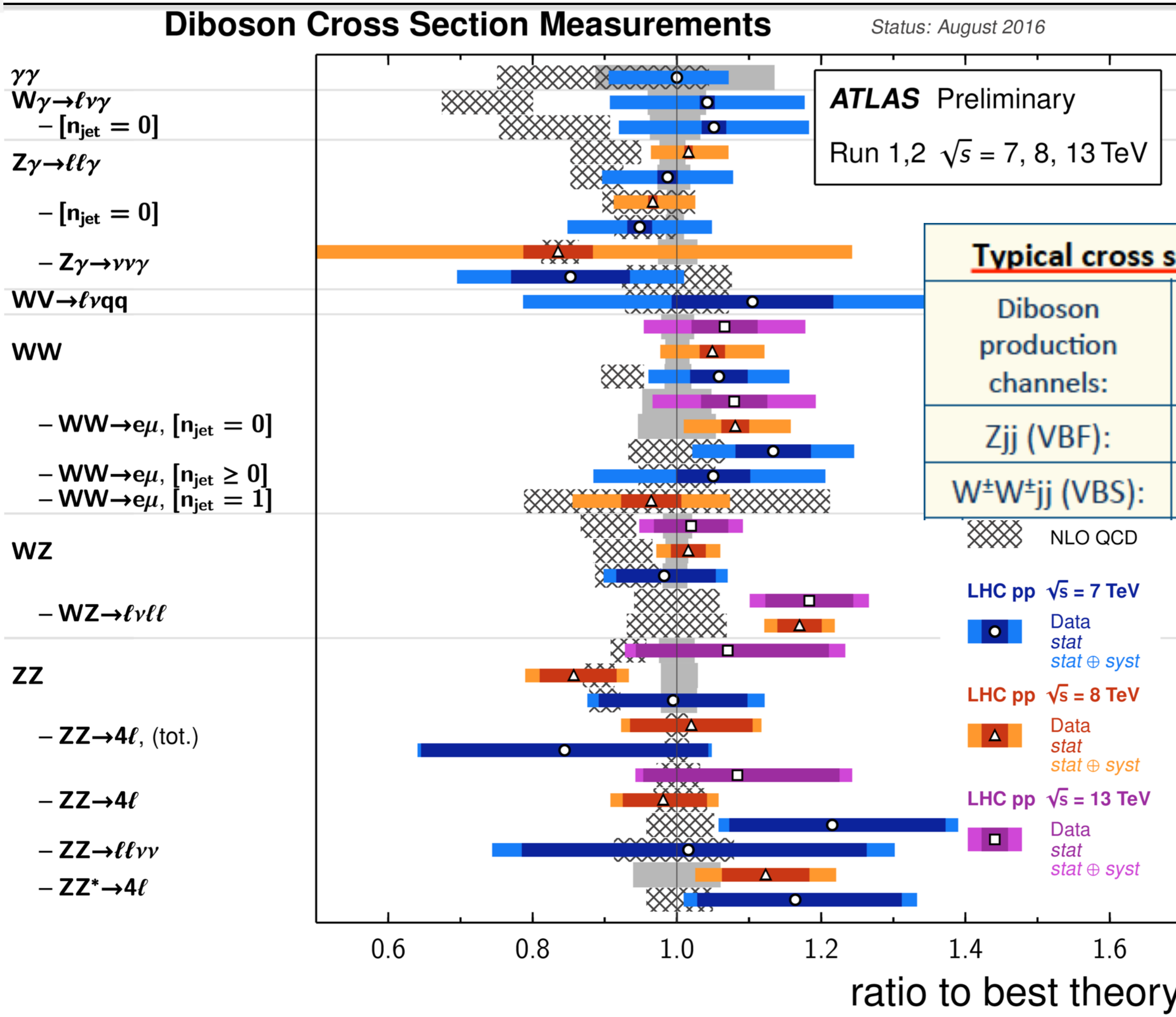

Typical cross section ranges

Diboson production channels:	between 1 and 100 pb
Zjj (VBF):	about 50 fb
$W^{\pm}W^{\pm}jj$ (VBS):	some fb

PRL **116,** 101801 (2016) PHYSICAL REVIEW LETTERS week ending 11 MARCH 2016

Measurement of the ZZ Production Cross Section in pp Collisions at $\sqrt{s} = 13$ TeV with the ATLAS Detector

G. Aad *et al.*[*]
(ATLAS Collaboration)

(Received 17 December 2015; published 10 March 2016)

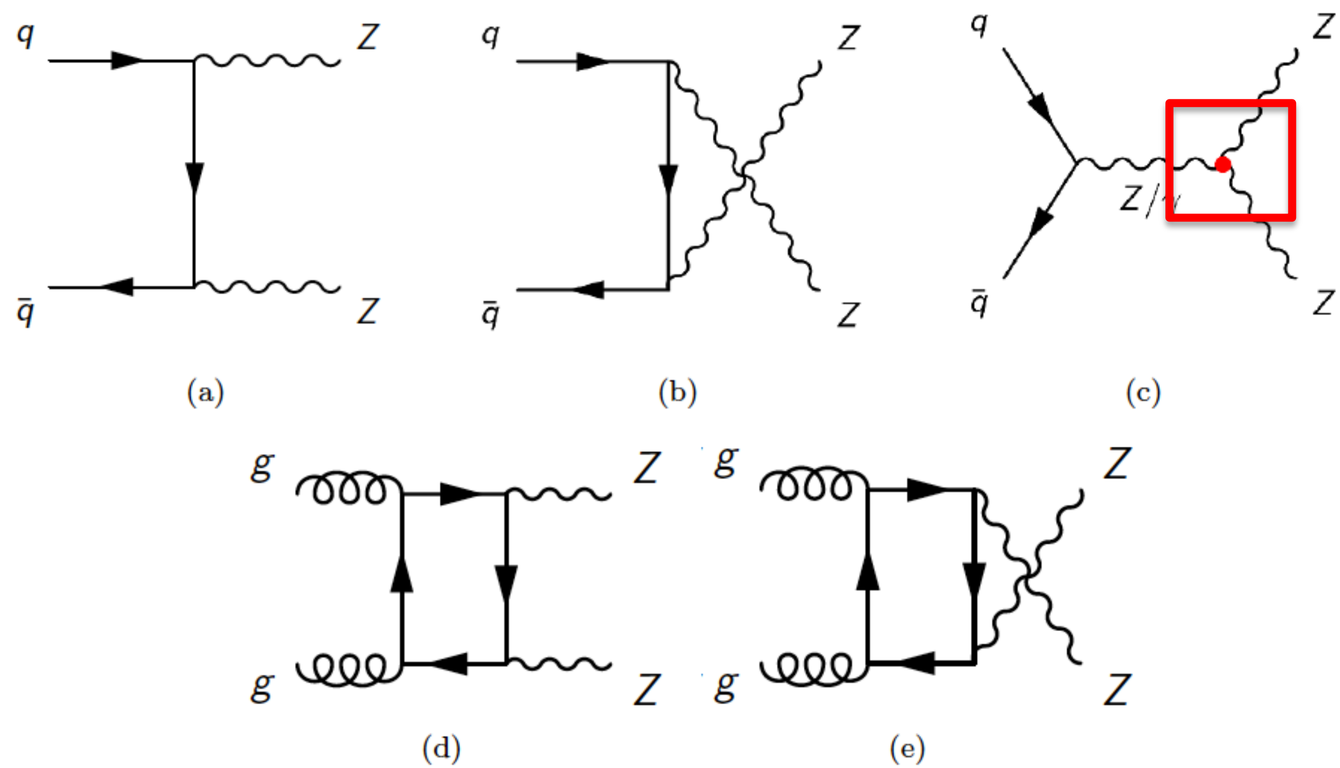

Figure 1. Leading order Feynman diagrams for ZZ production through the $q\bar{q}$ and gg initial state at hadron colliders. The s-channel diagram, (c) contains the ZZZ and $ZZ\gamma$ neutral TGC vertices which do not exist in the SM.

Selection of events

- Leptons: electrons & muons ; add γ close to *l* if $\sqrt{(\Delta\eta_{\ell,\gamma})^2 + (\Delta\phi_{\ell,\gamma})^2} < 0.1$
- Two pairs of leptons of same flavour and opposite charge; possible combinations : 2e2μ, 4e, 4μ. Mass of each pair between 66 and 116 GeV; in case of 4l of same flavour choose pairing which minimizes
$$|m_{ll,a} - m_Z| + |m_{ll,b} - m_Z|$$
- leptons well separated $\Delta R_{ll'} > 0.2$

A total of 63 events are observed in a sample of 3.2 0.2 fb^{-1} at $\sqrt{s}$ = 13 TeV, of which 15, 30, and 18 are in the 4e, 2e2μ, and 4μ channels, respectively.

MC simulation : scale factors are applied to the simulated events to correct for the small differences from data in the trigger, reconstruction, identification, isolation, and impact parameter efficiencies for electrons and muons . Furthermore, the lepton momentum scales and resolutions are adjusted to match the data.

Data-driven background estimation

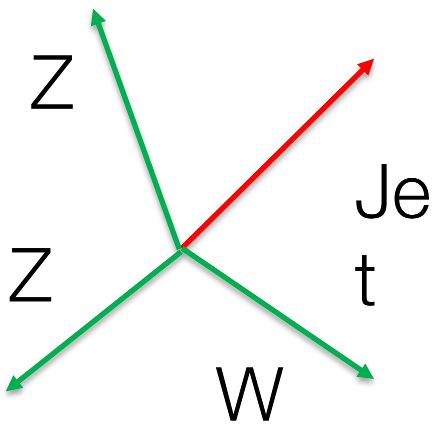

Background "normally" looks like 3xgreen +1red BUT 1red may be reconstructed as green

f = probability (red appears as green)

Assume you are able to select a sample of N events uniquely from ZW+jets then

$$N_{fakes} = \text{lllj (jets taken as lepton)} + \text{llll (HF decay)}$$

$$f = \text{llll} / N_{fakes}$$

BUT you have to subtract $N_{prompts}$ "llll" events NOT originating from ZW+jets (small correction).

$$N' = N_{fakes} + N_{prompts}$$

$$f = \text{llll} / (\text{Selected sample} - N_{prompts})$$

Data-driven background estimation

Background originates from Z or W decaying to leptons + jets: heavy flavour decays, mis-identified jets, decays in flight. Compute this background using the data-driven estimation described below

- define "good lepton" a lepton which is isolated and with a small impact parameter
- define "jet-like-lepton" a lepton which fails only one of these criteria
- select a sample of events with 3 "good leptons" + 1 "jet-like-lepton"
- define

"looks like"

$$f = \frac{probability(non-lepton = full-lepton)}{probability(non-lepton = jet-like-lepton)}$$

"Fakes"

- the number of background events N(BG) is then

$$N(BG) = lllj * f + lljj * f^2$$

- Number of signal events has also to be increased by number of real ZZ events N(ZZ) where one lepton is identified as "jet-like-lepton" . This term is computed as $N(ZZ)_{MC} * f$
- f is measured using a sample of single-lepton triggered events with a Z boson candidate + a 3rd lepton
  - f = # good-leptons / # jet-like-leptons

  after correcting, using MC, for real ZZ & ZW events

ZZ to llll : Acceptance

N(BG) = 0.62 +1.08−0.11 events

A factor **C_{ZZ} is applied to correct for detector inefficiencies and resolution effects**. It relates the background subtracted number of selected events to the number in the fiducial phase space, and is defined as the ratio of generated signal events passing the selection criteria using reconstructed objects to the number passing the fiducial criteria using generator-level objects. C_{ZZ} is determined with a combination of the POWHEG ZZ MC sample and the SHERPA loop-induced gg-initiated sample. The C_{ZZ} value and its total uncertainty is determined to be 0.55 ± 0.02, 0.63 ± 0.02, 0.81 ± 0.03 in the 4e, 2e2μ, 4μ channel.

The cross section measured in the fiducial phase space is also extrapolated to the total phase space, which includes a correction for QED final-state radiation effects. The extrapolation factor is obtained from the same combination of MC samples as used in the C_{ZZ} determination. The ratio of the fiducial to full phase-space cross section is 0.39±0.02, in all three channels.

ZZ to $llll$ and $ll\nu\nu$ in Run I

Measurement of the ZZ production cross section in proton-proton collisions at √s = 8 TeV using the ZZ ➔ $l^+l^-l'^+l'^-$ and ZZ➔ $l^+l^-\nu\nu$ decay channels with the ATLAS detector

JHEP01(2017)099

Fiducial Phase Space					
Selection	$e^-e^+e^-e^+$	$\mu^-\mu^+\mu^-\mu^+$	$e^-e^+\mu^-\mu^+$	$e^-e^+\nu\bar{\nu}$	$\mu^-\mu^+\nu\bar{\nu}$
Lepton p_T	> 7 GeV			> 25 GeV	
Lepton $\lvert\eta\rvert$	$\lvert\eta\rvert_{e_1,e_2,e_3} < 2.5$ $\lvert\eta\rvert_{e_4} < 4.9$	$\lvert\eta\rvert_\mu < 2.7$	$\lvert\eta\rvert_{e_1} < 2.5$, $\lvert\eta\rvert_{e_2} < 4.9$ $\lvert\eta\rvert_\mu < 2.7$	$\lvert\eta\rvert_e < 2.5$	$\lvert\eta\rvert_\mu < 2.5$
$\Delta R(\ell,\ell')$	> 0.2			> 0.3	
$m_{\ell^-\ell^+}$	$66 < m_{\ell^-\ell^+} < 116$ GeV			$76 < m_{\ell^-\ell^+} < 106$ GeV	
Axial-E_T^{miss}	–			> 90 GeV	
p_T-balance	–			< 0.4	
Jet veto	–			$p_{T\,jet} > 25$ GeV, $\lvert\eta\rvert_{jet} < 4.5$, and $\Delta R(e,\mathrm{jet}) > 0.3$	

$-E_T^{miss} \cdot \cos(\Delta\phi(\vec{E}_T^{miss}, \vec{p}_T^{\,Z}))$

$|E_T^{miss} - p_T^Z|/p_T^Z$

Table 1. Fiducial phase-space definitions for each of the five ZZ final states under study.

$$\sigma^{fid}_{ZZ\to e^-e^+e^-e^+} = 6.2\,^{+0.6}_{-0.5}\ \mathrm{fb}$$
$$\sigma^{fid}_{ZZ\to e^-e^+\mu^-\mu^+} = 10.8\,^{+1.1}_{-1.0}\ \mathrm{fb}$$
$$\sigma^{fid}_{ZZ\to \mu^-\mu^+\mu^-\mu^+} = 4.9\,^{+0.5}_{-0.4}\ \mathrm{fb}$$
$$\sigma^{fid}_{ZZ\to e^-e^+\nu\bar{\nu}} = 3.7 \pm 0.3\ \mathrm{fb}$$
$$\sigma^{fid}_{ZZ\to \mu^-\mu^+\nu\bar{\nu}} = 3.5 \pm 0.3\ \mathrm{fb}$$
$$\sigma^{total}_{pp\to ZZ} = 6.6\,^{+0.7}_{-0.6}\ \mathrm{pb}$$

- 20.3 fb-1 , √s = 8 TeV
- single lepton triggers+isolation+p_T>24 GeV
- choice of primary vertex
- pairing in 4-electrons channel

Background calculation

Irreducible background

Source	$e^-e^+e^-e^+$	$\mu^-\mu^+\mu^-\mu^+$	$e^-e^+\mu^-\mu^+$	$\ell^-\ell^+\ell'^-\ell'^+$
ZZZ^*/ZWW^*	0.12 ± 0.01	0.19 ± 0.01	0.28 ± 0.02	0.58 ± 0.02
DPI	0.13 ± 0.01	0.15 ± 0.01	0.29 ± 0.01	0.57 ± 0.02
$t\bar{t}\,Z$	0.15 ± 0.03	0.16 ± 0.03	0.35 ± 0.05	0.66 ± 0.07
Total irreducible background	0.40 ± 0.04	0.50 ± 0.04	0.93 ± 0.05	1.82 ± 0.08

DPI = double proton interaction

Table 3. Number of events from the irreducible background SM sources that can produce four true leptons scaled to 20.3 fb^{-1}. The full event selection is applied along with all corrections and scale factors. The errors shown are statistical only.

"fake-leptons" background

Ingredients in eq. (7.1)	$e^-e^+e^-e^+$	$\mu^-\mu^+\mu^-\mu^+$	$e^-e^+\mu^-\mu^+$	Combined ($\ell^-\ell^+\ell'^-\ell'^+$)
$(+)N_{\text{data}}(\ell\ell\ell j) \times f$	8.6 ± 0.7	4.8 ± 2.4	16.0 ± 3.5	29.3 ± 4.3
$(-)N_{ZZ}(\ell\ell\ell j) \times f$	0.58 ± 0.01	1.96 ± 0.02	2.82 ± 0.02	5.36 ± 0.03
$(-)N_{\text{data}}(\ell\ell jj) \times f^2$	3.6 ± 0.1	1.0 ± 0.4	4.1 ± 0.6	8.8 ± 0.8
$(+)N_{ZZ}(\ell\ell jj) \times f^2$	0.00 ± 0.01	0.02 ± 0.08	0.02 ± 0.02	0.04 ± 0.02
Background estimate, N(BG)	4.4 ± 0.7 (stat) ± 2.8 (syst)	1.8 ± 2.4 (stat) ± 0.9 (syst)	9.0 ± 3.6 (stat) ± 3.9 (syst)	15.2 ± 4.4 (stat) ± 7.1 (syst)

Table 4. The number of ZZ background events from sources with fake leptons estimated using the data-driven fake-factor method in 20.3 fb^{-1} of data. The uncertainties quoted are statistical only, unless otherwise indicated, and combine the statistical uncertainty in the number of observed events of each type and the statistical uncertainty in the associated fake factor. The systematic uncertainty is shown for the background estimate in each final state.

Yields

$ZZ \to \ell^-\ell^+\ell'^-\ell'^+$	$e^-e^+e^-e^+$	$\mu^-\mu^+\mu^-\mu^+$	$e^-e^+\mu^-\mu^+$	$\ell^-\ell^+\ell'^-\ell'^+$
Observed data	64	86	171	321
Expected signal	$62.2 \pm 0.3 \pm 2.6$	$83.7 \pm 0.4 \pm 3.2$	$141.6 \pm 0.6 \pm 4.0$	$287.0 \pm 0.8 \pm 8.1$
Expected background	$4.8 \pm 0.7 \pm 2.8$	$2.3 \pm 2.4 \pm 1.0$	$10.0 \pm 3.6 \pm 3.9$	$17.1 \pm 4.4 \pm 7.1$
$ZZ \to \ell^-\ell^+\nu\bar{\nu}$	$e^-e^+\nu\bar{\nu}$	$\mu^-\mu^+\nu\bar{\nu}$	$\ell^-\ell^+\nu\bar{\nu}$	
Observed data	102	106	208	
Expected signal	$51.1 \pm 0.9 \pm 2.6$	$55.1 \pm 1.0 \pm 2.9$	$106.2 \pm 1.3 \pm 3.9$	
Expected background	$32.4 \pm 5.5 \pm 3.3$	$33.2 \pm 6.0 \pm 3.4$	$65.6 \pm 8.1 \pm 4.7$	

Table 6. Summary of observed $ZZ \to \ell^-\ell^+\ell'^-\ell'^+$ and $ZZ \to \ell^-\ell^+\nu\bar{\nu}$ candidates in the data, total background estimates and expected signal for the individual decay modes and for their combination (last column). The first uncertainty quoted is statistical, while the second is systematic. The uncertainty in the integrated luminosity (1.9%) is not included.

Control region eμ

Source	$e^-e^+\nu\bar{\nu}$	$\mu^-\mu^+\nu\bar{\nu}$
WZ	$16.7 \pm 1.1 \pm 1.7$	$18.5 \pm 1.0 \pm 1.5$
$ZZ \to \ell^-\ell^+\ell'^-\ell'^+$	$0.6 \pm 0.1 \pm 0.1$	$0.6 \pm 0.1 \pm 0.1$
$t\bar{t}$, W^-W^+, Wt, $ZZ \to \tau\tau\nu\nu$, $Z \to \tau^-\tau^+$	$13.3 \pm 3.2 \pm 0.2$	$15.4 \pm 3.6 \pm 0.3$
W + jets — Matrix method	$2.6 \pm 1.1 \pm 0.5$	$-0.9 \pm 0.7 \pm 1.0$
Z + jets — Control region	$-0.7 \pm 3.5 \pm 2.7$	$-0.5 \pm 3.8 \pm 2.9$
Total background	$32.4 \pm 5.5 \pm 3.3$	$33.2 \pm 6.0 \pm 3.4$

Leptons not reconstructed, MC

Matrix Method

Definitions

- Prompt (P) and Fake (F) leptons TRUTH
- Signal (S) and Loose (L) regions RECONSTRUCTION
- Combinations N_{SS} .. N_{LL} … N_{PP}…N_{FF}

HP: the ratio of the number of signal leptons to the number of loose leptons is known separately for prompt and fake leptons

$$\begin{pmatrix} N_{SS} \\ N_{SL} \\ N_{LS} \\ N_{LL} \end{pmatrix} = \Lambda \cdot \begin{pmatrix} N_{PP} \\ N_{PF} \\ N_{FP} \\ N_{FF} \end{pmatrix}$$

$\text{lepton}_{1,2}$	signal/loose
fake	ε
prompt	ζ

$$\Lambda = \begin{pmatrix} \varepsilon_1\varepsilon_2 & \varepsilon_1\zeta_2 & \zeta_1\varepsilon_2 & \zeta_1\zeta_2 \\ \varepsilon_1(1-\varepsilon_2) & \varepsilon_1(1-\zeta_2) & \zeta_1(1-\varepsilon_2) & \zeta_1(1-\zeta_2) \\ (1-\varepsilon_1)\varepsilon_2 & (1-\varepsilon_1)\zeta_2 & (1-\zeta_1)\varepsilon_2 & (1-\zeta_1)\zeta_2 \\ (1-\varepsilon_1)(1-\varepsilon_2) & (1-\varepsilon_1)(1-\zeta_2) & (1-\zeta_1)(1-\varepsilon_2) & (1-\zeta_1)(1-\zeta_2) \end{pmatrix}$$

where ε_1 and ε_2 (ζ_1 and ζ_2) are the ratios of the number of signal and loose leptons for the leading and subleading prompt (fake) leptons, respectively.

Matrix method - 2

- prompt lepton efficiencies are determined from a data sample enriched with prompt leptons from $Z \longrightarrow l^+l^-$ decays, obtained by requiring $80 < m_{ll} < 100$ GeV;
- fake-lepton efficiencies are measured from a data set enriched with one prompt muon (by requiring it to pass the signal lepton selection and pT > 40 GeV) and an additional fake lepton (by requiring it to pass the loose selections)
- The fake-electron efficiency is determined from two samples of SS eμ events
- The fake-muon efficiency is determined from a sample of same-sign dimuon events

ZZ to llll : Results

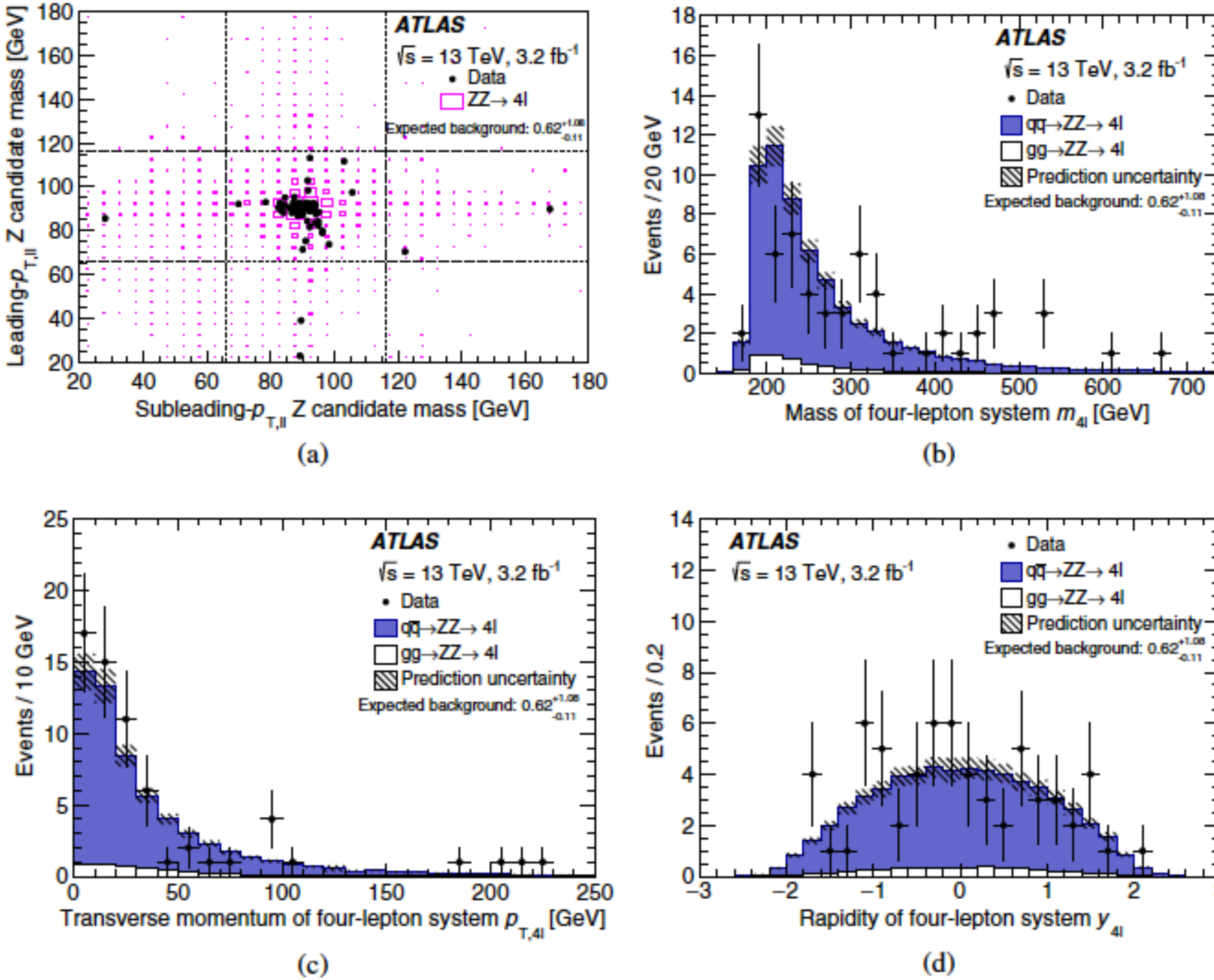

Results

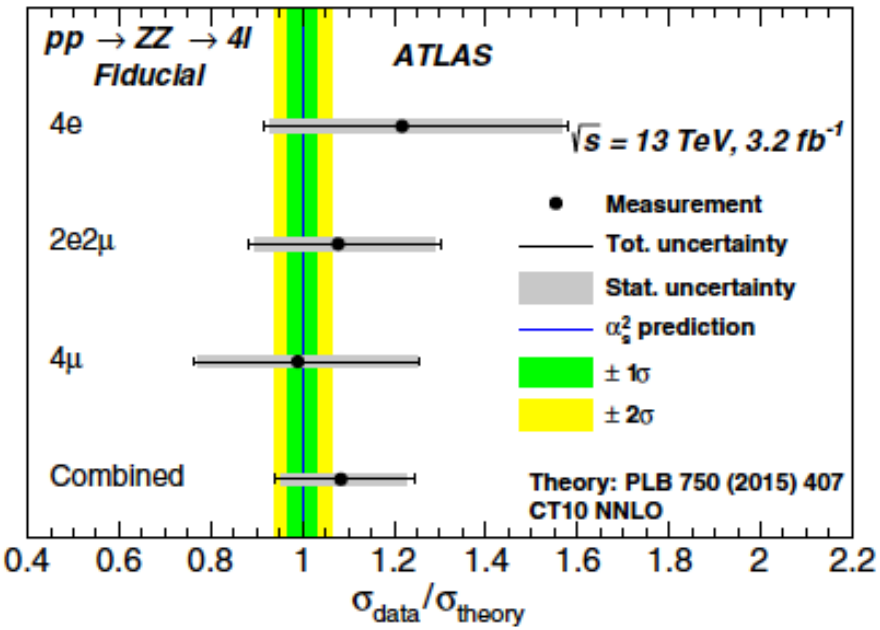

pp → ZZ → 4l
Fiducial
ATLAS
4e
2e2μ
4μ
Combined
√s = 13 TeV, 3.2 fb⁻¹
Measurement
Tot. uncertainty
Stat. uncertainty
α²s prediction
± 1σ
± 2σ
Theory: PLB 750 (2015) 407
CT10 NNLO
σdata/σtheory

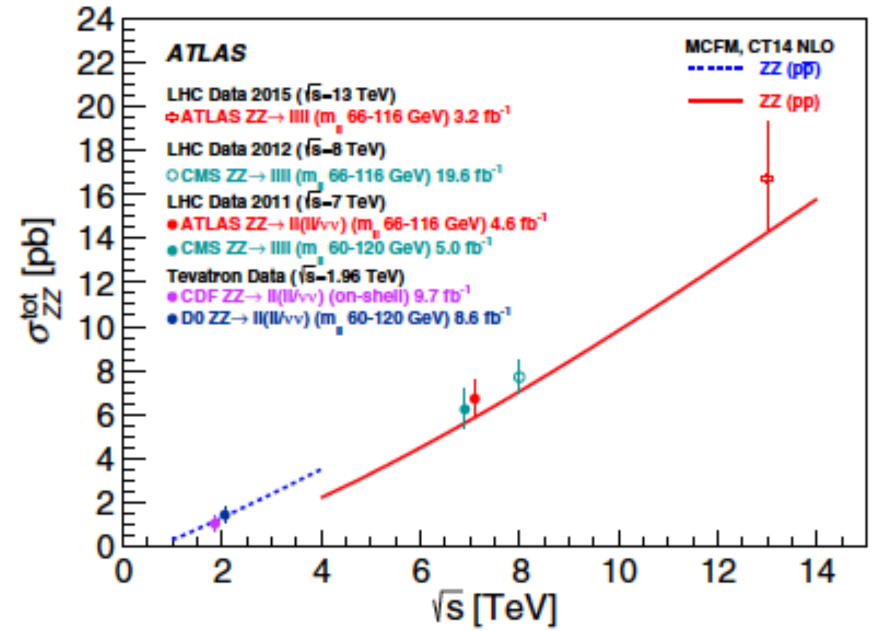

ATLAS
MCFM, CT14 NLO
ZZ (pp̄)
ZZ (pp)
LHC Data 2015 (√s=13 TeV)
ATLAS ZZ→ llll (mll 66-116 GeV) 3.2 fb⁻¹
LHC Data 2012 (√s=8 TeV)
CMS ZZ→ llll (mll 66-116 GeV) 19.6 fb⁻¹
LHC Data 2011 (√s=7 TeV)
ATLAS ZZ→ ll(ll/νν) (mll 66-116 GeV) 4.6 fb⁻¹
CMS ZZ→ llll (mll 60-120 GeV) 5.0 fb⁻¹
Tevatron Data (√s=1.96 TeV)
CDF ZZ→ ll(ll/νν) (on-shell) 9.7 fb⁻¹
D0 ZZ→ ll(ll/νν) (mll 60-120 GeV) 8.6 fb⁻¹
σ^tot_ZZ [pb]
√s [TeV]

WZ production in Run II

Measurement of the $W^{\pm}Z$ boson pair-production cross section in pp collisions at $\sqrt{s} = 13$ TeV with the ATLAS Detector

Phys. Lett. B 762 (2016) 1
DOI: 10.1016/j.physletb.2016.08.052

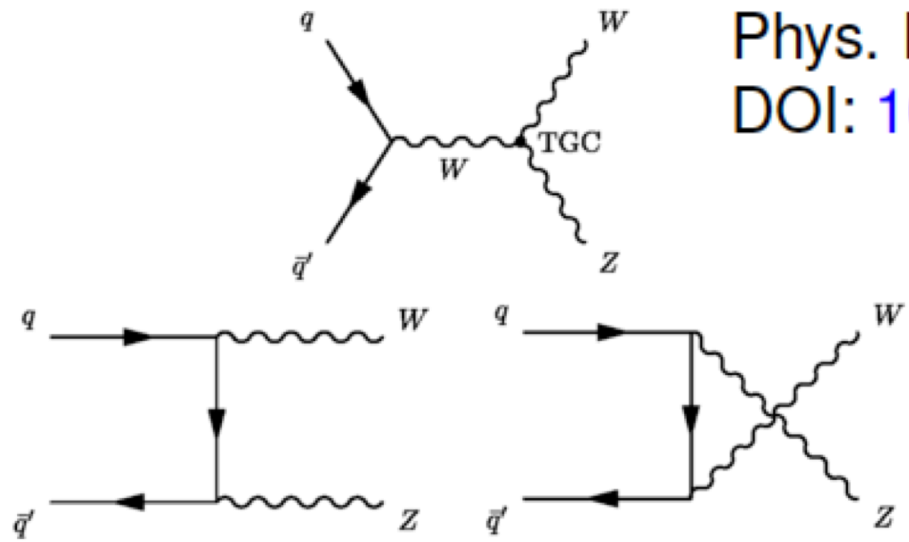

- Int. luminosity used = 3.2 fb^{-1}
- leptonic decays of Z & W (e+μ)
- $|\eta|$ leptons <2.5
- triggers, isolation, vertex
- exactly 3 leptons, pairing Z/W
- fiducial space defined by $p_T^l(Z) > 15$ GeV, $p_T^l(W) > 20$ GeV, $m_{ll}(Z)$ within 10 GeV from PDG value, $m_T^W > 30$ GeV, the angular distance ΔR between the charged leptons from the W and Z decay is larger than 0.3, and that ΔR between the two leptons from the Z decay is larger than 0.2

Extrapolate from fiducial volume to total cross section (take into account BR's)

yields

reducible background (data-driven) & irreducible background (MC)

Channel	eee	μee	$e\mu\mu$	$\mu\mu\mu$	All
Data	98	122	166	183	569
Total expected	102 ± 10	118 ± 9	126 ± 11	160 ± 12	506 ± 38
WZ	74 ± 6	96 ± 8	97 ± 8	129 ± 10	396 ± 32
$Z + j, Z\gamma$	16 ± 7	7 ± 5	14 ± 7	9 ± 5	45 ± 17
ZZ	6.7 ± 0.7	8.7 ± 1.0	8.5 ± 0.9	11.7 ± 1.2	36 ± 4
$t\bar{t} + V$	2.7 ± 0.4	3.2 ± 0.4	2.9 ± 0.4	3.4 ± 0.5	12.1 ± 1.6
$t\bar{t}, Wt, WW + j$	1.2 ± 0.8	2.0 ± 0.9	2.4 ± 0.9	3.6 ± 1.5	9.2 ± 3.1
tZ	1.28 ± 0.20	1.65 ± 0.26	1.63 ± 0.26	2.12 ± 0.34	6.7 ± 1.1
VVV	0.24 ± 0.04	0.29 ± 0.05	0.27 ± 0.04	0.34 ± 0.05	1.14 ± 0.18

Table 1: Observed and expected numbers of events after the $W^{\pm}Z$ inclusive selection described in Section 5 in each of the considered channels and for the sum of all channels. The expected number of $W^{\pm}Z$ events from POWHEG+PYTHIA and the estimated number of background events from other processes are detailed. The total uncertainties quoted include the statistical uncertainties, the theoretical uncertainties in the cross sections, the experimental uncertainties and the uncertainty in the integrated luminosity.

Results

$$\sigma^{\text{fid.}}_{W^\pm Z\to\ell'\nu\ell\ell} = \frac{N_{\text{data}} - N_{\text{bkg}}}{\mathcal{L}\cdot C_{WZ}} \times \left(1 - \frac{N_\tau}{N_{\text{all}}}\right)$$

MC correction factor to account for τ decays to e,μ

C_{WZ} accounts for detector effects, resolution, efficiency (efficiency$_l{}^3$! $.9^3 = .7$)

Channel	C_{W^-Z}	C_{W^+Z}	$C_{W^\pm Z}$	N_τ/N_{all}
eee	0.428 ± 0.005	0.417 ± 0.004	0.421 ± 0.003	0.040 ± 0.001
μee	0.556 ± 0.006	0.550 ± 0.005	0.553 ± 0.004	0.038 ± 0.001
$e\mu\mu$	0.550 ± 0.006	0.553 ± 0.005	0.552 ± 0.004	0.036 ± 0.001
$\mu\mu\mu$	0.729 ± 0.007	0.734 ± 0.006	0.732 ± 0.005	0.040 ± 0.001

$$\sigma^{\text{tot.}}_{W^\pm Z} = \frac{\sigma^{\text{fid.}}_{W^\pm Z\to\ell'\nu\ell\ell}}{\mathcal{B}_W\,\mathcal{B}_Z\,A_{WZ}}$$

B_W, B_Z branching fractions, A_{WZ} is the MC computed acceptance

$$\sigma^{\text{fid.}}_{W^\pm Z\to\ell'\nu\ell\ell} = 63.2\ \pm\ 3.2\,(\text{stat.})\ \pm\ 2.6\,(\text{sys.})\ \pm 1.5\,(\text{lumi.})\ \text{fb}.$$

$$\sigma^{\text{tot.}}_{W^\pm Z} = 50.6 \pm 2.6\,(\text{stat.}) \pm 2.0\,(\text{sys.}) \pm 0.9\,(\text{th.}) \pm 1.2\,(\text{lumi.})\,\text{pb}.$$

Anomalous Triple Gauge Coupling

Anomalous Triple Gauge Coupling

- Effect of aTGCs are modelled using an effective Lagrangian which depends on few parameters
- Increase of cross section at high invariant mass and high transverse momentum
- Neutral TGC are not allowed in the SM. In SM all parameters are 0, except g^V_1 and k^V which are 1
- Analysis on full 2011 dataset

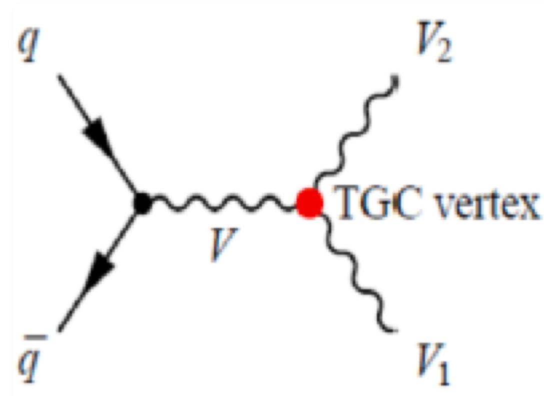

For practical purposes it is convenient to introduce deviations from the (tree-level) SM as

$$\Delta g_1^Z \equiv (g_1^Z - 1) \quad \equiv \tan\theta_W \delta_Z \ , \quad \Delta\kappa_\gamma \equiv (\kappa_\gamma - 1) \quad \equiv x_\gamma \ ,$$
$$\Delta\kappa_Z \equiv (\kappa_Z - 1) \quad \equiv \tan\theta_W (x_Z + \delta_Z) \ .$$
$$\lambda_\gamma \quad \equiv y_\gamma, \quad \lambda_Z \quad \equiv \tan\theta_W \, y_Z \ .$$

	Coupling	parameters	channel
Charged	WWγ	λ_γ, $\boxed{\Delta\kappa_\gamma}$	WW, Wγ
	WWZ	λ_Z, $\boxed{\Delta\kappa_Z}$, $\boxed{\Delta g^Z_1}$	WW, WZ
Neutral	ZZγ	h^Z_3, h^Z_4	Zγ
	Zγγ	h^γ_3, h^γ_4	Zγ
	ZZZ	f^Z_4, f^Z_5	ZZ
	ZγZ	f^γ_4, f^γ_5	ZZ

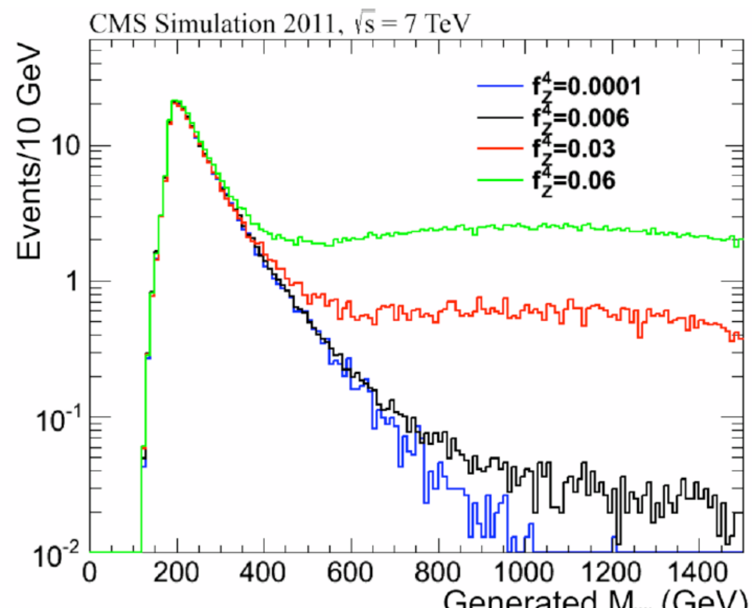

Anomalous TGC : WWZ and WWγ

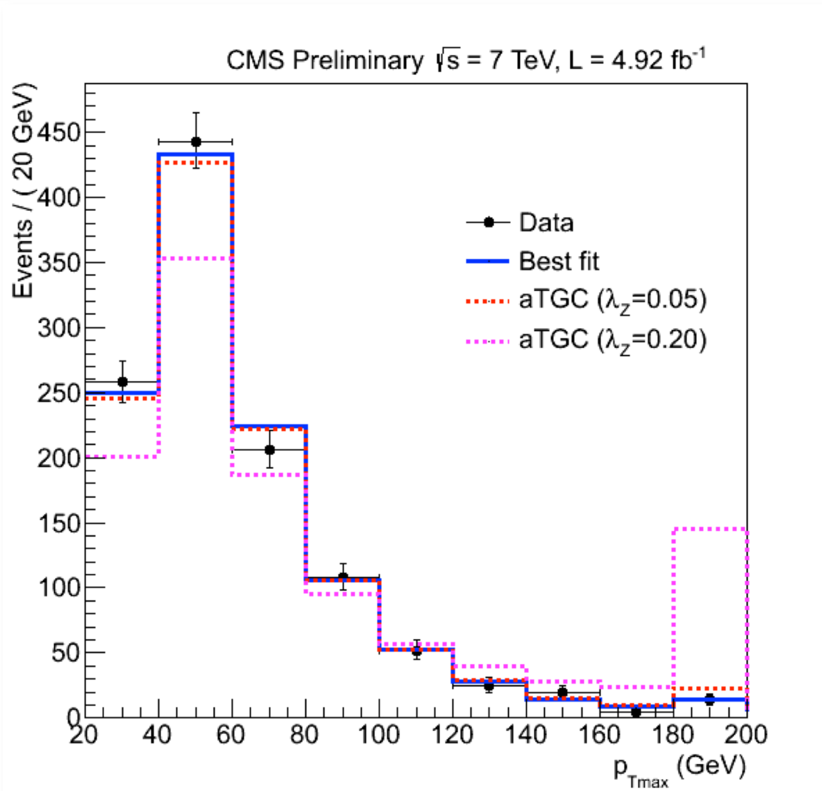

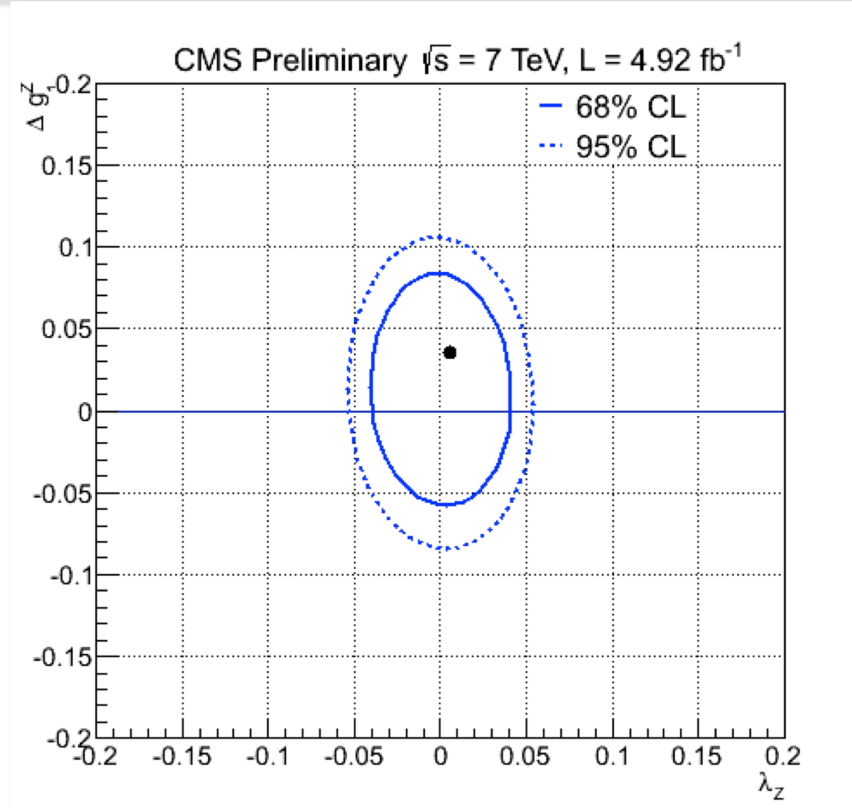

- Maximum likelihood fit performed for events in bin p_T^{lepton}
- **Statistics still limited** : so only one or two parameters left free during aTGC fits. The other ones are fixed to their SM value (=0)
- No sign of deviation from SM predictions

Charged Anomalous Triple Gauge Coupling Results

Limits on WWγ aTGC couplings

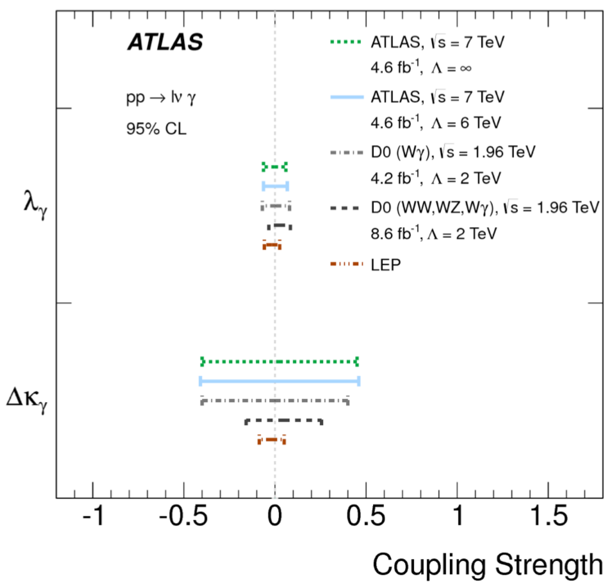

Limits on WWZ aTGC couplings

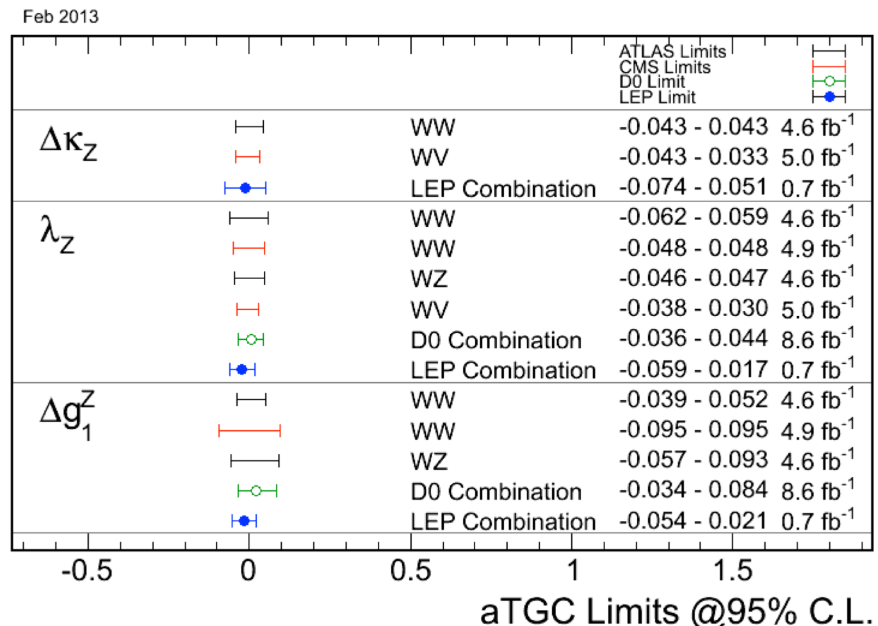

CMS Results

95% C.L.	$\Delta\kappa^{\gamma}$	λ	Δg_1^Z
$W\gamma \rightarrow l\nu\gamma$	[-0.38, 0.29]	[-0.05, 0.037]	-
$W^+W^- \rightarrow l\nu l\nu$	[-0.21, 0.22]	[-0.048, 0.048]	[-0.095, 0.095]
$W^+W^- + WZ \rightarrow l\nu jj$	[-0.111, 0.142]	[-0.038, 0.030]	-

- No sign of deviation from SM predictions

Neutral Anomalous Triple Gauge Coupling Results

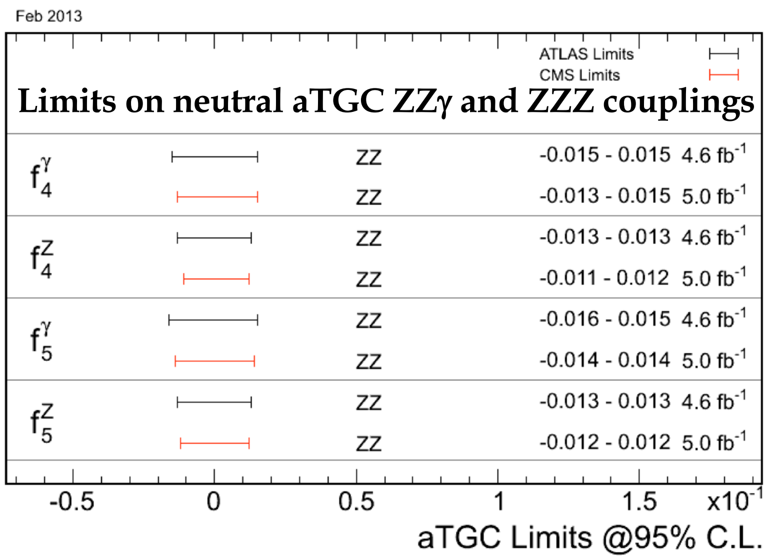

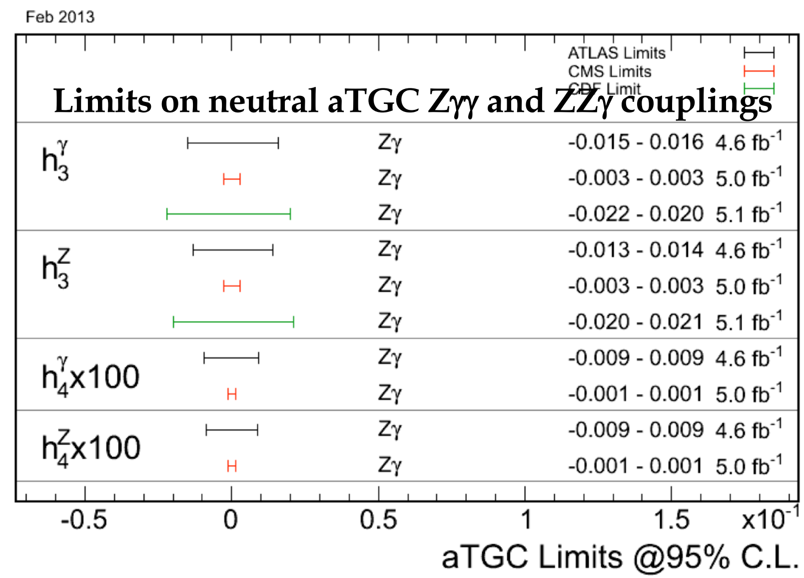

- **Limits surpassing Tevatron and LEP**
- Fully compatible with Standard Model
- Most stringent limits from CMS ννγ analysis
  - Last bin: $p_T(\gamma) > 400$ GeV
  - ATLAS use $p_T(\gamma) > 100$ GeV

Summary of TGC

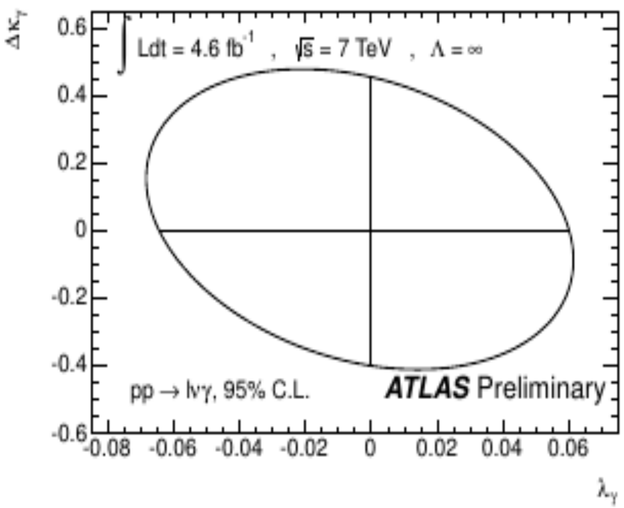

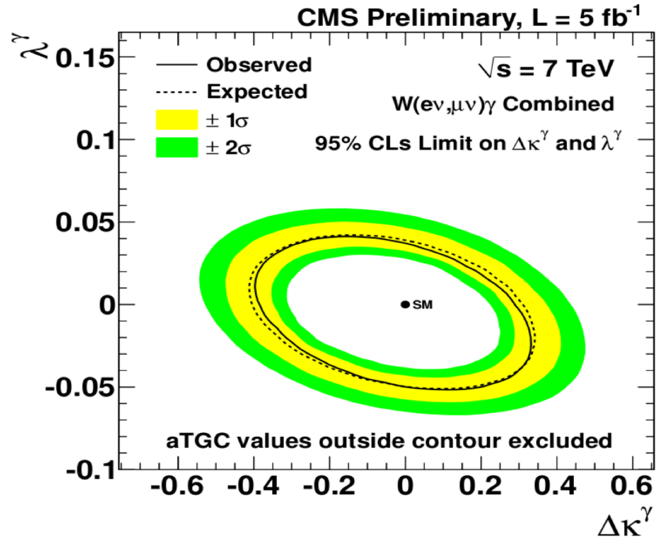

- All channels studied. No deviations from SM expectations
- But sensitivity still low :
  - Channel with highest statistics Wg give Dk_g < 0.4 and l_g < 0.05
  - while the « interesting » range is rather Dk_g ~ 0.01 and l_g ~ 0.001
- Expected improvements soon with the full 2012 stat to be analysed (23 fb-1) and combination of channels measuring the same couplings
- Need to run at 13 TeV (higher sensitivity with increasing s) and 100 fb-1 (2 to 3 years) to probe the « interesting » region

BACKUP

dilepton mass distributions from the Z → ll

Measurement of W± and Z-boson production cross sections in pp collisions at √s = 13 TeV with the ATLAS detector, *Phys. Lett. B 759 (2016) 601*

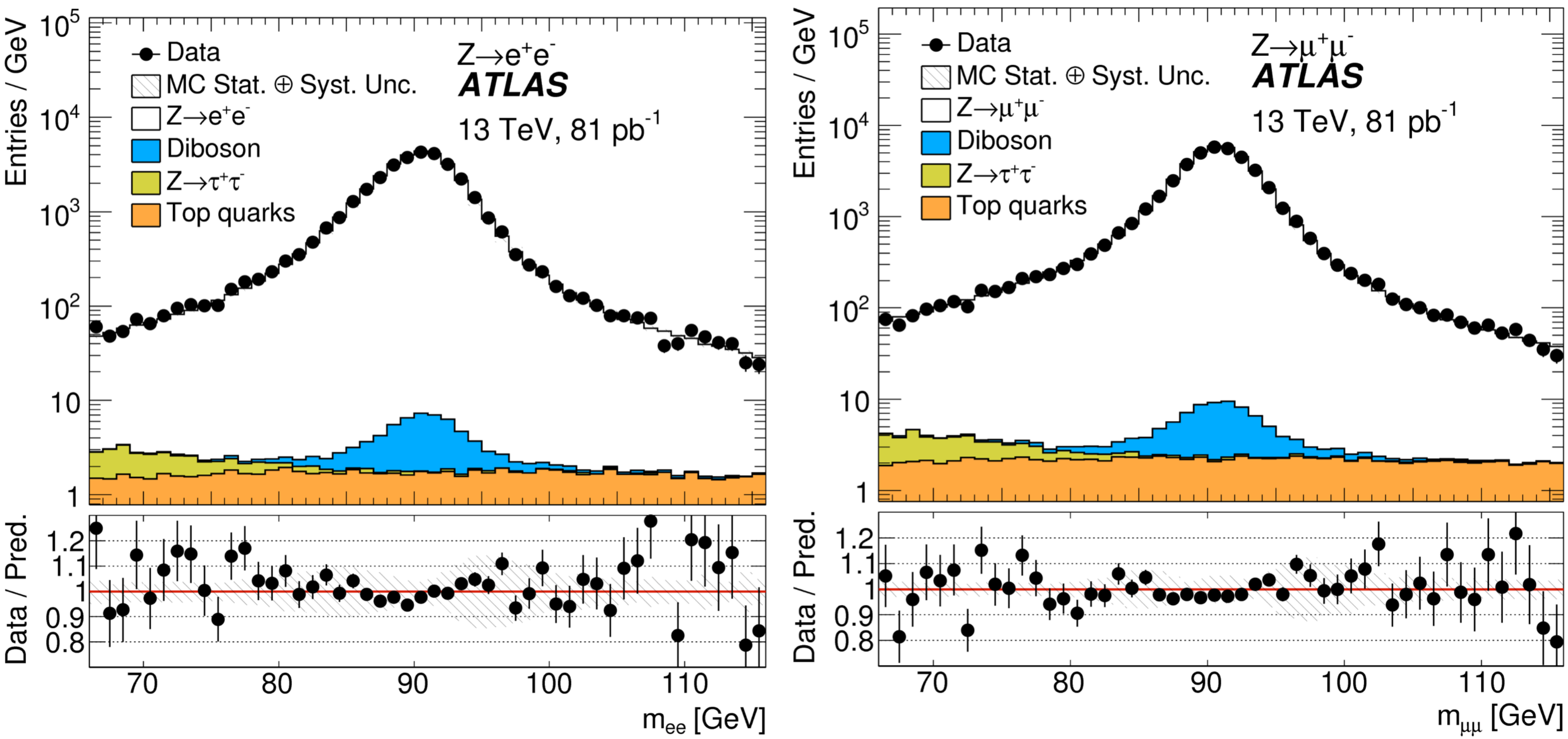

SR: Lepton quality & trigger match exactly two selected leptons of the same flavour but of opposite charge with invariant mass of

$$66 < m_{ll} < 116 \text{ GeV}.$$